REGULATORY MECHANISMS IN THE CHONDROGENESIS OF MESENCHYMAL PROGENITORS: THE ROLES OF CYCLIC TENSILE LOADING AND CELL-MATRIX INTERACTIONS

A Dissertation
Presented to
The Academic Faculty

by

John T. Connelly

In Partial Fulfillment
of the Requirements for the Degree
Doctor of Philosophy in the
Program of Bioengineering

Georgia Institute of Technology
August 2007

REGULATORY MECHANISMS IN THE CHONDROGENESIS OF MESENCHYMAL PROGENITORS: THE ROLES OF CYCLIC TENSILE LOADING AND CELL-MATRIX INTERACTIONS

Approved by:

Dr. Marc E. Levenston, Advisor
School of Mechanical Engineering
Georgia Institute of Technology

Dr. Andres J. Garcia
School of Mechanical Engineering
Georgia Institute of Technology

Dr. Ravi Bellamkonda
School of Biomedical Engineering
Georgia Institute of Technology

Dr. Joseph M. Le Doux
School of Biomedical Engineering
Georgia Institute of Technology

Dr. Barbara D. Boyan
School of Biomedical Engineering
Georgia Institute of Technology

Date Approved: May 29, 2007

ACKNOWLEDGEMENTS

I would first like to thank my advisor, Dr. Marc Levenston. His support and guidance through this project was essential to its success, and he has had a significant impact on my growth as a scientist. Marc gave me the freedom to pursue my own ideas, even some of the crazier ones, but he still kept me focused on the big picture and committed to doing good work. While this may not have been the most efficient way to get results, it definitely taught me a great deal about the scientific process and made me a stronger researcher. Marc has also been a great friend over the past few years. I have truly enjoyed working with him and look forward to future collaborations.

I would also like to acknowledge the contributions of my thesis committee members, Dr. Ravi Bellamkonda, Dr. Barbara Boyan, Dr. Andres Garcia, and Dr. Joseph Le Doux. In particular I would like to thank Dr. Garcia for his help and advice with many aspects of this work. Andres was always willing talk with me about my research or career and at times was like a second advisor. His directness and positive attitude provided continuous support, and things always seemed clearer after talking with Andres. I would also like to thank Dr. Boyan for challenging me and not letting me get off the hook too easily. She certainly made me think about cell biology and experimental design from a different perspective. In addition to my committee, others scientists and mentors have had a significant impact on this research. Dr. Johnna Temenoff has been a great friend and additional advisor over the past couple years. I would also like to thank my undergraduate research advisor, Dr. Marjolein van der Meulen, who got me started in the field of orthopaedics and inspired me to pursue my Ph.D. in bioengineering.

While at Georgia Tech, I have had the privilege of working with some of the smartest and most hard working people I could imagine. The other members of the Levenston lab have been incredible colleagues, helpful, enthusiastic, and fun to be around. I owe a huge debt of gratitude to the first generation of students, Janna, Stacy, and Eric, who established the lab and laid the groundwork for the rest of us. None of the work in this dissertation would have been possible without their years of hard work, developing techniques, protocols, and novel experimental systems. I would like to specifically acknowledge Dr. Eric Vanderploeg for helping me get started during my first year and providing a great example for how to be a good scientist. I would also like to thank Eric for developing the tensile loading system used in several of the studies presented here. Dr. Janna Mouw has also had a major impact on my research and personal development. Janna and I worked together for several years figuring out how to isolate and culture BMSCs and collaborated on several projects. She has been an amazing influence and challenged me scientifically more than anyone else. Janna has been a fantastic friend, and I think we have learned a lot from each other over the years.

In addition to the "older" students in the lab, Dr. Chris Wilson, Dr. Ashley Palmer, and Onyi Irrechukwu have been a part of the second generation with me and an integral part of my experiences in the Levenston lab. Chris started in the lab at the same time as I did, and we have shared a lot of experiences together from continuum mechanics to the craziness of trying to finish the dissertation. Chris is one of the most enthusiastic people I have ever met, and this attitude permeates everything he does. He loves his work and loves life, and he has been one of my best friends over the past few years. Likewise, Ashley has been an incredible friend to me while at Georgia Tech.

Together, the three of us have had a great time sharing an office, listening to Blues at the Northside Tavern, or even crammed into the back of a Peugot 106. In addition, I would also like to thank the other members of the Levenston lab, including Kathryn Brodkin for teaching me PCR and improving my swimming technique, Marine Amaroux for her friendship and hospitality, and Ed Phelps for all his help characterizing the chondrogenesis of BMSCs.

Beyond the Levenston lab, many people in the orthopaedics wing and biomedical engineering department have contributed to this work and provided an immense amount of help to me. I would like to thank Rhima Coleman for always being willing to lend me supplies and for fiery discussions about BMSC differentiation. I would also like thank Kelly Burns in the Garcia lab who is one of the most organized and generous people around. In addition, I would like to thank Timothy Petrie for his help producing the recombinant fibronectin fragments and *always* being available for me to ask questions. The members of the Temenoff lab have also been a huge help over the past year, especially Derek Doroski who let me borrow their loading rig when our rig unexpectedly stopped working during one of my final experiments. I would also like to acknowledge Dr. Mahesh Dodla for his help with the agarose conjugation protocols and Dr. Alex Peister for her advice and feedback.

In addition to those who have directly influenced my work in the lab, the love and support of many people outside of work has also been essential. I would first like to thank my parents who have been encouraging me as long as I can remember and were always willing to listen and offer advice (even if I did not want to hear it). I would like to thank them for being patient with this long process and with me being so far from home.

I could not have completed this project without their support. I would also like to thank other members of my family, Tim, Laura, and my grandmothers for their continued love and encouragement.

While in Atlanta, I have met many incredible people and developed some strong friendships. This network of friends has made these past several years fun and enjoyable, and I have no doubt that this fantastic group has had a significant positive impact on my work and research. One of the most important people in my life is Matt Haynes. Matt and I met after my second year at Georgia Tech, and we have had some amazing times together. Whether we were traveling across Europe, battling it out at Thursday night trivia, or just sitting on the beach, I have enjoyed every minute of it. Matt has provided unwavering support for me over the past few years and has always been willing to discuss things he knew little about at the time. As a result, he probably knows more about RGD, BMSCs, and chondrogenesis than any other IT manager in the world. Matt's help over the last few months of this dissertation has been incredible. He put up with my crankiness and stress and cooked dinner for me after particularly long days. I want to thank Matt for all of his help and love, and I look forward to our future adventures together.

TABLE OF CONTENTS

LIST OF TABLES

LIST OF FIGURES

SUMMARY

Cartilage tissue engineering represents an exciting potential therapy for providing permanent and functional regeneration of healthy cartilage tissues, but these treatment options have yet to be successfully implemented in a clinical setting. One of the primary obstacles for cartilage engineering is obtaining a sufficient supply of cells capable of regenerating a functional cartilage matrix. Mesenchymal progenitors can easily be isolated from multiple tissues, expanded in vitro, and possess a chondrogenic potential, but it remains unclear what types or combinations of signals are required for lineage-specific differentiation and tissue maturation. The overall goal of this dissertation was to investigate how the coordination of biochemical stimuli with cues from mechanical forces and the extracellular matrix regulate the chondrogenesis of bone marrow stromal cells (BMSCs).

These studies explored the potential for cyclic tensile loading and chondrogenic factors, TGF-β1 and dexamethsone, to promote fibrochondrocyte-specific differentiation of BMSCs. The application of cyclic tensile displacements to cell-seeded fibrin constructs promoted fibrochondrocyte patterns of gene expression and the development of a fibrocartilage-like matrix. These responses were influenced by the specific loading conditions examined and the differentiation state of the BMSCs. Additionally, the roles of integrin adhesion and cytoskeletal organization in BMSC differentiation were examined within engineered hydrogels presenting controlled densities of biomimetic ligands. Adhesion to the arginine-glycine-aspartic acid (RGD) motif inhibited chondrogenesis in a density-dependent manner and was influenced by interactions with the f-actin cytoskeleton. Together, this research provided fundamental insights into the regulatory mechanisms involved in the chondrogenesis of mesenchymal progenitor cells.

CHAPTER 1

INTRODUCTION

1.1 MOTIVATION

Cartilaginous tissues, including articular cartilage and fibrocartilage, perform essential mechanical functions in joints throughout the body. Traumatic injuries and degenerative diseases, such as osteoarthritis, are major sources of damage to these tissues and can impair their mechanical function. Unfortunately, the limited healing ability of cartilage and the lack of effective treatments create significant health problems with economic and social implications. Osteoarthritis alone affects over 21 million people in the U.S. and results in an estimated $86 billion in indirect costs. In addition, these conditions can be extremely painful and debilitating. Therefore, new technologies or therapies that promote cartilage regeneration have the potential to restore long term joint function and significantly improve the quality of life for many patients.

The engineering of tissue replacements through the combination of cells, scaffolding materials, or growth factors is one potential strategy for repairing damage to articular cartilage and fibrocartilage structures. However, there are major challenges for recreating cartilage tissues with the necessary material properties to function in the mechanically demanding, in vivo environment. Furthermore, the scarcity of autologous chondrocytes presents additional cell sourcing limitations. Mesenchymal progenitors, such as bone marrow stromal cells (BMSCs), are capable of undergoing chondrogenic differentiation and may be an alternative cell source for tissue engineering therapies, but it remains unclear how specific signals coordinate to promote the differentiation and maturation of these cells into articular chondrocytes and fibrochondrocytes. Therefore, a greater understanding of the regulatory mechanisms governing BMSC chondrogenesis

will significantly improve the potential application of these cells in tissue engineering therapies.

1.2 RESEARCH OBJECTIVES

The objective of the research presented in this dissertation was to investigate the roles of mechanical stimuli and cell-matrix interactions in regulating the chondrogenesis of bone marrow stromal cells. A model for the chondrogenesis of bovine BMSCs was established by characterizing the production and processing of extracellular matrix proteins and proteoglycans during long-term culture with TGF-β1. Given the significant physiologic levels of tension experienced by fibrocartilage tissues, the potential for tensile loading to guide fibrochondrocyte differentiation was examined by applying controlled tensile displacements to BMSCs during in vitro chondrogenesis. In addition, the roles of cell-matrix interactions in BMSC differentiation were investigated by engineering hydrogel constructs presenting cell adhesive ligands. Together, the goal of these studies was to elucidate some of the fundamental mechanisms that regulate the chondrogenesis of mesenchymal progenitors. The **central hypothesis** for this work was that interactions between biochemical stimuli and the physical environment modulate the chondrogenic differentiation and maturation of bone marrow stromal cells. This hypothesis was composed of three more specific hypotheses and research aims.

Hypothesis I: Long-term culture with TGF-β1 will promote BMSC chondrogenesis and the development of an ECM similar to the matrix produced by articular chondrocytes and characteristic of native articular cartilage.

Specific Aim I: Characterize the accumulation, organization, and turnover of various ECM components by BMSCs and articular chondrocytes (ACs) in agarose hydrogels during long-term culture with TGF-β1.

Previous studies in our laboratory and others have consistently demonstrated that members of the TGF-β superfamily stimulate chondrogenic gene expression and sulfated-glycosaminoglycan (sGAG) production in a variety of hydrogel systems. However, it remains unclear whether these conditions will ultimately promote chondrocyte maturation and the development of a functional cartilage matrix. The goal of this aim was to characterize the composition of the extracellular and pericellular matrices produced by BMSCs and ACs after 32 days of exposure to TGF-β1. The localization of various proteoglycans was examined by immunofluorescence and histological staining, and the presence of specific matrix proteins known to interact with these PGs was also determined by immunofluorescence and western blot analysis. The role of proteolytic enzymes in construct development was further investigated by examining the effects of aggrecanase and MMP inhibitors on PG accumulation, aggrecan processing, and construct mechanics.

Hypothesis II: Combinations of the chondrogenic factors, TGF-β1 and dexamethasone, with cyclic tensile loading will promote fibrochondrocyte-specific differentiation of BMSCs and the development of a fibrocartilage-like tissue.

Specific Aim II: Investigate the effects of cyclic tensile loading on BMSC chondrogenesis and tissue development within an engineered construct.

Since fibrocartilage tissues experience significant tensile forces in vivo, we hypothesized that tension plays an important role in fibrochondrocyte differentiation and may be a potential strategy for guiding the development of tissue engineered fibrocartilage by BMSCs. For these studies, BMSC chondrogenesis was first characterized within the fibrin matrices used in previous tensile loading experiments (Appendix A). Short periods of controlled tensile displacements (5% ± 5%, 1Hz) were applied to the fibrin constructs for varying durations and at specific stages of differentiation to investigate the effects of cyclic tension on early changes in gene expression and matrix synthesis rates. Intermittent tensile loading (1 hour load plus 3 hours recovery) was also applied to the constructs for up to two weeks in the presence of TGF-β1 and dexamethasone to explore the potential for extended loading periods to influence matrix production and turnover.

Hypothesis III: Interactions with extracellular matrix modulate BMSC chondrogenesis through integrin adhesion and cytoskeletal organization

Specific Aim III: Examine the effects of cell adhesion and cytoskeletal organization on BMSC differentiation in engineered hydrogels presenting synthetic RGD peptides.

Alginate and agarose hydrogels were modified with synthetic peptides containing the arginine-glycine-aspartic acid (RGD) motif known to bind multiple integrin receptors. These systems allowed for the controlled presentation of cell-adhesive ligands within a non-adhesive, hydrogel background. The effects of RGD interactions on gene expression and matrix synthesis were investigated during TGF-β1 and dexamethasone stimulation of BMSC chondrogenesis. The influences of RGD density and integrin specific adhesion in

regulating these responses were also determined. Finally, the role of cytoskeletal organization was examined within the modified agarose gels using inhibitors of f-actin polymerization and rho-associated kinase (ROCK).

1.3 SIGNIFICANCE AND SCIENTIFIC CONTRIBUTION

The studies presented in this dissertation provide significant insights into the mechanisms regulating BMSC chondrogenesis. Investigations into the influence of cyclic tensile loading on fibrochondrocyte differentiation identified several key parameters involved in the response of BMSCs to mechanical stimuli. Furthermore, these experiments explored the ability of physiologically relevant forces to guide differentiation along a fibrochondrocyte-like lineage. The use of RGD-modified hydrogels allowed for a careful examination of specific cell-matrix interactions involved in BMSC chondrogenesis. These studies also provided fundamental insights into the interactions between biochemical stimuli, integrin adhesion, and cytoskeletal organization that regulate lineage selection within a three-dimensional environment.

In addition to advancing the current understanding of progenitor cell differentiation, the findings of these studies have important implications for tissue engineering and regenerative medicine. Specific Aim I evaluated the ability of BMSCs to produce a functional cartilage matrix within a tissue engineered construct and provided a more thorough examination of matrix composition than has been previously reported. In addition, the tensile loading studies demonstrated the potential application of BMSCs for fibrocartilage engineering, and the effects of RGD interactions on BMSC chondrogenesis highlight the importance selecting appropriate biomaterials for tissue

engineering applications. Together, these findings provide a framework for future investigations into the use of BMSCs for fibrocartilage and articular cartilage engineering.

CHAPTER 2

BACKGROUND

2.1 CARTILAGE COMPOSITION AND FUNCTION

Cartilaginous tissues are found throughout the body and perform a wide range of mechanical and structural functions. In diarthroidal joints such as the knee, articular cartilage and fibrocartilage play important roles in the motion and load bearing capabilities of the joint. Normal activities subject these tissues to high levels and complex combinations of compressive, tensile, and shear forces. As a result, the unique compositions and structures of the extracellular matrix (ECM) in articular cartilage and fibrocartilage are essential for their biomechanical functions.

2.1.1 Articular Cartilage

Articular cartilage covers the ends of long bones and serves as a low friction surface for smooth joint motion. In addition to joint lubrication, articular cartilage must withstand and distribute significant compressive and shear forces, often several times body weight[1]. The tissue's ECM is composed of water (68-85%), collagen (10-20%), and proteoglycans (5-10%)[2], and the interactions between these components give rise to its load bearing capabilities[3,4]. Furthermore, the organization of the matrix molecules within the three zones of the tissue (superficial, middle, and deep) results in a depth-dependent variation in material properties that reflect the complex loading environment within the joint[5-7].

Type II collagen is the most abundant type of collagen in articular cartilage and is responsible for the tissue's ability to bear shear and tensile forces[2]. Collagen II is organized into long fibers and is supported by several fibril-associated collagens, such as

collagen VI and IX [2]. The collagen II content is highest in the superficial zone, and the fibrils are organized tangentially to the articulating surface in order to withstand the higher levels of shear and tension in this region[5,7-10]. The collagen fibers are oriented randomly within the middle zone and perpendicular to the surface within the deep zone where they are anchored to the subchondral bone[5,7-10].

The major structural proteoglycan in articular cartilage is aggrecan, which consists of numerous sulfated-glycosaminoglycan (sGAG) chains attached to a protein core[11]. The aggrecan molecule is linked to a hyaluronic acid backbone forming a large macromolecule. The highly negatively charged sGAGs confer a fixed charge to the tissue[12,13], and interactions between the mobile ions in the interstitial fluid and proteoglycans create an osmotic swelling pressure that is resisted by the collagen network[3,4,14]. This resulting osmotic pressure and low hydraulic permeability allows articular cartilage to bear the large compressive forces that develop during normal activity. The proteoglycan and water contents are highest in the middle and deep zones which experience primarily compressive forces[2,15]. Taken together, the zonal organization of collagen and proteoglycans within articular cartilage highlights key structure-function relationships between matrix organization and tissue mechanics.

Articular chondrocytes are the resident cells within articular cartilage and are responsible for the maintenance of the extracellular matrix. Articular chondrocytes express and synthesize the major ECM components, collagen II and aggrecan. In addition, the cells produce proteolytic enzymes that breakdown the matrix and contribute to the homeostatic turnover of the tissue[16,17]. Articular chondrocytes are fully differentiated cells and are normally non-proliferative in vivo. Although generally considered a single cell type, there are regional variations in the expression levels of the matrix proteins that reflect the differences in matrix composition[18,19]. In vivo, chondrocytes have primarily round morphologies, but rapidly adhere and spread in monolayer culture. These changes in morphology are accompanied by a steady loss of

collagen II and aggrecan expression and reduced proteoglycan (PG) synthesis[20,21]. However, chondrocytes cultured in three-dimensional environments, such as hydrogels or cell aggregates, can maintain their differentiated phenotype for multiple weeks in vitro[22].

2.1.2 Fibrocartilage

Fibrocartilage tissues are found in the meniscus of the knee, the temporomandibular joint disk (TMJ), and the annulus fibrosous of the intervertebral disc. In the knee, the menisci help to stabilize the joint and distribute forces between the femur and the tibial plateau[23]. Similar to articular cartilage, the fibrocartilage ECM is composed of water (60-70%), collagen (15-25%), and proteoglycans (1-2%) [2]; however, the relative amounts and specific components of the matrix molecules are distinctly different. The predominant collagen in fibrocartilage is collagen type I with lesser amounts of collagens II and VI[24]. Compared to articular cartilage, the total proteoglycan and water contents are lower in fibrocartilage, and the proteoglycans have a lower percentage of aggrecan and a higher percentage of the small PGs decorin and biglycan[25,26].

The overall differences in matrix composition reflect the significantly higher levels of tensile forces experienced by fibrocartilages in vivo[23,27]. In the meniscus, zonal variations in matrix composition and organization also reflect local differences in the loading environment[2,23]. The inner one third of the semi-lunar shaped structure experiences the highest levels of compression during joint loading and therefore, has the highest PG and water content, as well as randomly oriented collagen fibers[2]. In contrast, the outer one third of the meniscus has a lower PG content but a higher amount of collagen. The collagen I fibers in this region are organized into large (100μm),

circumferentially organized fibers that bear tensile hoop stresses[23]. Similar relationships between mechanics and matrix composition and organization can be found in the fibrocartilage of ligament insertion points[28] and intervertebral discs[29]. This close connection between composition and function within fibrocartilage tissues suggests a potential role for mechanical regulation of tissue development and maintenance.

In addition to differences in the ECM, there are significant differences in the cell types between articular cartilage and fibrocartilage. Typically referred to as fibrochondrocytes, fibrocartilage cells have a more "fibroblastic" morphology than articular chondrocytes and express higher levels of collagen I and less collagen II and aggrecan[30,31]. Recent findings also indicate that fibrochondrocytes produce higher levels of active aggrecanases responsible for aggrecan catabolism[32]. These results suggest that high levels of aggrecanase generated cleavage fragments may be a unique marker for fibrocartilage and the fibrochondrocyte phenotype. Consistent with the zonal variations in matrix composition of the meniscus, the cells in the inner region also express significantly higher levels of collagen II, aggrecan, and biglycan genes and less decorin[24,33,34]. Interestingly, high collagen I expression is fairly constant throughout the tissue. The limited body of knowledge regarding fibrochondrocytes presents challenges for defining and understanding their phenotype. However, recent studies comparing the differential responses of articular chondrocytes and fibrochondrocytes to exogenous growth factors and mechanical stimuli provide key insights into the fundamental differences between these cell types[35,36].

2.2 CARTILAGE INJURY AND REPAIR

2.2.1 Osteoarthritis and Injury

Damage to articular cartilage and fibrocartilage represents a significant health problem in the U.S. and can arise from a traumatic injury or chronic degradation, such as osteoarthritis. Acute injuries, including focal defects and cracks in the cartilage, often result in impaired movement, pain, and inflammation[37]. The persistence of these injuries can lead to further degeneration of the tissue and the development of severe osteoarthritis[37]. Osteoarthritis is typically considered a chronic disease due to "wear and tear" of the articular cartilage. The condition tends to increase with age and is most common in adults over the age of 40[38]. The symptoms range from mild pain and impaired motion to severe pain and complete debilitation.

Progression of osteoarthritis is characterized by a loss of proteoglycans and water from the tissue, followed by degradation of the collagen network[39,40]. Over time, the loss of ECM components results in impaired mechanical function. Specifically, the lower PG content reduces the osmotic swelling and compressive stiffness of the cartilage[39]. In addition, damage to the collagen network decreases the tissue's tensile stiffness and ability to resist deformation[41]. The low cellularity of articular cartilage and limited vascular supply significantly inhibit its intrinsic ability to repair damage. In addition, chondrocytes from older patients have a lower biosynthetic activity[42,43], further hindering the ability to regenerate a cartilage matrix.

Damage to fibrocartilage tissues, particularly the meniscus, is most commonly due to acute injuries. Approximately one third of meniscal injuries are sports related[44] and associated with overloading or twisting of the joint[44,45]. Partial and full-thickness tears are the most common type of damage to the menisci and develop in several forms. Lesions in the vascularized, outer region of the meniscus can naturally heal, while those in the inner region rarely heal[45]. Within the past 20 years it has become clear that the

menisci are critical for joint stability and load distribution[46,47]. Removing the damaged tissue by total menisectomy increases the contact stresses on the underlying cartilage and almost always leads to osteoarthritis[45,48]. Unrepaired tears can also disrupt the joint's biomechanics and increase the risk of further injury. Therefore, successful treatment of meniscal damage is important for protecting against future injuries and maintaining healthy joint function.

2.2.2 Current Treatments

There are limited options for treating injuries or degeneration of cartilaginous tissues. Less severe cases of osteoarthritis can be managed by treating the pain with non-steroidal anti-inflammatory drugs, while in the most severe cases of arthritis, total joint replacement is a highly successful treatment for restoring joint function. Unfortunately, a major drawback with joint replacement is the limited lifespan of the implant. Artificial joints last an average of 10-15 years before requiring a second surgery and are only realistic options for patients over 60 years old[49]. Like many types of surgery, joint replacement also includes risks of infection, blood clotting, and other complications.

Alternative treatments, such as microfracture and subchondral drilling, attempt to exploit the body's own healing response by exposing the cartilage defect to the vascular supply in the subchondral bone and stimulating new tissue formation[37]. This strategy has had some success in promoting cartilage growth[50], but the new tissue often has a disorganized, fibrous matrix and is mechanically inferior to native articular cartilage[51]. Although these techniques have been shown to provide short term pain relief and improvements in joint function, they do not ultimately protect the cartilage from future degeneration[37]. Autograft and allograft transplants of osteochondral tissue have had similar short term successes[52], but studies in animal models indicate that the implanted cartilage fails to integrate with the surrounding tissue[53]. Clearly, the current strategies for

repairing articular cartilage are insufficient, and there is a significant need to develop new therapies or devices that promote normal tissue regeneration and restore long term joint function.

The primary goal of treating meniscal injuries is to preserve the load distribution function of the menisci and biomechanics of the knee[54]. Therefore, strategies that encourage healing or regeneration of the fibrocartilage are preferred to total or even partial menisectomy. While some minor tears can heal naturally[55], most injuries require some type of surgery. Common surgical techniques for repairing meniscal lesions involve improving the vascular supply to the damage site and the use of closure devices, such as sutures, arrows, or fibrin glue[54]. Together these treatments stabilize the tear, while enhancing the healing process. Surgical intervention is most successful in the outer one-third of the meniscus[54]; however, repairing damage to the inner region is still a major challenge requiring additional investigation.

2.2.3 Tissue Engineering

The development of engineered tissues and cell-based therapies has the potential to significantly improve the repair of damaged cartilage. The general strategy for tissue engineering is to promote the regeneration of normal, healthy tissue using cells from the body. For articular cartilage, the ultimate goal is to permanently restore smooth joint motion and the tissue's load bearing capability. However, recreating the native matrix composition and structure, which are essential for the tissue's mechanical function, is a major challenge. In recent years, much work has focused on the development of scaffold materials, culture conditions, and cell sources that promote regeneration of functional articular cartilage. Hydrogels, such as agarose[22], alginate[56], and poly- (ethylene glycol) (PEG)[57], that encapsulate cells within a 3D environment all support a rounded

morphology and the chondrocytic phenotype. Although many materials allow for accumulation of a cartilaginous matrix, subtle differences in the stiffness, pore size, and degradation rate can all influence cell activity and matrix deposition[58,59].

Exogenous growth factors have been extensively investigated for their ability to enhance matrix synthesis within a tissue engineered construct. Members of the transforming growth factor (TGF) superfamily, including TGF-β1 and the bone morphogenetic proteins (BMPs), are potent stimulators of chondrocyte matrix synthesis[60-62] and have been shown to enhance the mechanical properties of tissue engineered cartilage[63]. Despite advances in scaffolding materials and culture conditions, cartilage constructs developed in the laboratory can still only achieve a fraction of the strength and stiffness of native articular cartilage[64]. Complete replication of the tissue's mechanical properties prior to implantation may not be necessary for successful repair, but the demanding mechanical environment within the joint likely requires the construct to have some minimum level of mechanical function.

The availability of an appropriate cell supply is another major hurdle facing cartilage tissue engineering. The limited number of autologous chondrocytes, combined with their dedifferentiation during monolayer expansion, suggests a need for an alternative cell source. Mesenchymal stem cells can be isolated from various tissues throughout the body including adipose[65], bone marrow[66], and skeletal muscle[67], and have the ability to differentiate along chondrogenic lineages. In addition, monolayer-expanded chondrocytes have the potential to re-differentiate under the appropriate conditions[68,69]. Although these strategies are promising, much work is still needed to identify the

mechanisms regulating chondrogenesis, as well as the utility of these cell types for tissue engineering applications.

Tissue engineering is also an attractive therapy for repairing fibrocartilage damage. Similar to articular cartilage, a challenge for fibrocartilage is developing a tissue substitute with a matrix composition and organization that provides the appropriate mechanical function. Scaffolds with controlled fiber alignment[70] and heterogeneous material properties[71] have been employed to recreate the native matrix composition and organization of fibrocartilage tissues, while growth factor supplementation has been used to stimulate matrix synthesis[35]. Cell source limitations are also a significant problem for fibrocartilage engineering given the limited availability of native fibrochondrocytes and their low biosynthetic activity[36]. Articular chondrocytes and mesenchymal progenitors could be used for fibrocartilage repair; however, an improved understanding of the fibrochondrocyte phenotype and differentiation pathways is required for the use of these cell types in tissue engineering applications.

2.3 MESENCHYMAL PROGENITORS AND CHONDROGENESIS

2.3.1 Bone Marrow Stromal Cells

Bone marrow is a heterogeneous mixture of many cell types including blood cells, hematopoeitic stem cells, macrophages, and stromal cells. Bone marrow stromal cells (BMSCs) are an attractive cell source for tissue regeneration and repair due to their pluripotency, availability, and expandability. In addition, they provide an interesting model system for studying the differentiation of mesenchymal lineages. BMSCs are most often isolated by their ability to adhere to tissue-culture plastic and proliferate in

monolayer[72-76]. Cells obtained in this manner are capable of differentiating into multiple mesenchymal cell types, including osteogenic, myogenic, chondrogenic, and adipogenic lineages[77-79].

Transforming growth factor beta-1 (TGF-β1) is highly expressed in pre-cartilage condensations during development[80] and in chondrogenic cells within the growth plate[81]. TGF-β1 has also been shown to induce chondrogenic differentiation in vitro for a variety of cell types and culture systems. Treatment of rabbit BMSCs with TGF-β1 in pellet culture increased collagen II gene expression and matrix synthesis[82], and similar results have been found with other animal models in pellet culture[83,84]. In addition to pellet culture, three-dimensional scaffolds such fibrin, alginate, agarose, and PEG have all been shown to support TGF-β1 stimulation of chondrogenesis[85-89]. Together, these studies consistently demonstrated increased expression of chondrogenic genes, increased collagen II and PG synthesis, and a rounded morphology in response to TGF-β1.

While much work has been devoted to studying chondrogenesis of BMSCs for articular cartilage repair, few studies have explored the use of progenitors for repairing fibrocartilage damage. In one study, autologous BMSCs from a rabbit were seeded into a collagen sponge and implanted into a partial meniscal defect[90]. Although the newly formed tissue was "histologically similar" to normal fibrocartilage, the implant failed to restore mechanical function of the meniscus and ultimately resulted in osteoarthritis of the joint. In a separate study, caprine BMSCs were injected into the knee joint following medial meniscectomy and appeared to enhance regeneration of a meniscus-like tissue[91]. These preliminary findings indicate that BMSCs could be a potential cell source for fibrocartilage repair, but exogenous stimuli may be required to develop a mechanically

functional tissue substitute. Further understanding of the key signals involved in fibrochondrocyte differentiation would greatly improve the therapeutic potential of BMSCs for fibrocartilage repair.

2.3.2 Mechanical Stimuli

Mechanical forces are important regulators of primary cell function and differentiation of progenitors. Numerous studies have investigated the effects of dynamic compression, hydrostatic pressure, and shearing forces on articular chondrocyte metabolism in explant and gel culture[64,92-95]. In general, each of these physiologically relevant types of loading enhance matrix biosynthesis and can even increase the strength and stiffness of tissue engineered constructs[64]. Some studies have also begun to examine the role of compression and hydrostatic pressure in the differentiation of BMSCs. Dynamic compressive loading of BMSC-seeded hydrogels increased collagen II and aggrecan gene expression as well as collagen and PG synthesis[85,96,97]. Similarly, the application of cyclic, hydrostatic pressure on BMSC aggregates increased collagen and PG production over a two week culture period[98]. Taken together, these studies provide strong evidence that physiologically relevant loading can stimulate matrix synthesis of primary chondrocytes and enhance the chondrogenesis of BMSCs.

Compared to dynamic compression, the influence of tensile forces on chondrocytes and fibrochondrocytes is less clear. In several studies, cyclic tensile loading inhibited PG synthesis in both chondrocytes and fibrochondrocytes in fibrin gel culture[36,99]. In addition, this response was dependent on the magnitude of loading[99]. One of the most striking results of these studies was the effect of cyclic tension on

chondrocyte morphology. After 48 hours, tensile loading induced formation of cytoskeletal projections and a stellate morphology, similar to fibrochondrocytes[36]. Similar inhibition of chondrocyte matrix synthesis has also been reported for cells stretched on a silicone membrane[100]. Overall, the effects of cyclic tension on matrix metabolism and cell morphology suggest that tension may promote a more fibrochondrocyte-like phenotype.

In addition to primary chondrocytes and fibrochondrocytes, tensile loading has the potential to influence the differentiation of several types of progenitors. Chick limb bud cells stretched on a silicone membrane displayed lower collagen II and aggrecan gene expression[101], and this effect could be blocked by a soluble RGD peptide and anti-α2, α5, and β1 integrin antibodies, suggesting that the inhibition of chondrogenesis by tensile loading is mediated by cell-matrix adhesion. Tensile loading in combination with torsion also promoted collagen I, collagen III, and tenascin-C expression by bovine BMSCs in collagen gels[102], while uniaxial stretching of human mesenchymal stem cells increased collagen I and smooth muscle α-actin expression[103]. Taken together, these studies indicate that tensile loading inhibits chondrogenic gene expression and promotes collagen I expression, characteristic of more fibrous tissues such as tendon, ligament, and fibrocartilage. Therefore, tensile forces may provide important cues for guiding fibrochondrocyte-specific differentiation of mesenchymal progenitors.

2.3.3 Cell-Matrix Interactions

Interactions with the extracellular matrix provide important signals for directing cell growth, migration, survival, and differentiation. Integrins are a class of hetero-

dimeric receptors consisting of an alpha and beta subunit and anchor the cell to its surrounding matrix. Integrins are also involved in cell signaling in which binding to a specific ligand promotes further integrin activation, ligand binding, and receptor clustering[104]. Proteins such as vinculin and talin associate with the intracellular domain of clustered integrins to form a focal complex and connect with the f-actin cytoskeleton[105,106]. This process of focal adhesion formation is essential for strong adhesion to the extracellular matrix and linkage to the cell's cytoskeleton[107]. In addition, kinases and other signaling molecules can associate with focal complexes and provide a mechanism for transducing signals from the cell's environment[105,106]. Integrin adhesion and signaling regulate a wide variety of cell functions, and the specificity of these responses involves both the particular pair of subunits and the bound ligand[108].

Integrin specific adhesion to matrix proteins, such as collagen and fibronectin, plays an important role in the differentiation of osteogenic[108,109] and myogenic lineages[110], but the influence of cell matrix interactions during chondrogenesis is less well understood. During skeletal development, adhesion to fibronectin has been shown to be necessary for pre-cartilage condensation of the mesenchyme[111], and the specific isoform of fibronectin can influence the extent of chondrogenic differentiation[112]. Cell-matrix interactions also have the potential to regulate in vitro differentiation of stem cells. In one report, type II collagen hydrogels enhanced TGF-β1 induced chondrogenesis of bovine BMSCs over type I collagen and alginate gels[113]. These findings highlight the significance of cell-biomaterial interactions for tissue engineering applications. Presentation of specific matrix proteins or biomimetic ligands may be a useful strategy for directing cell differentiation and matrix production. Therefore, an improved

understanding of cell-matrix interactions during chondrogenesis would provide key insights for the development of new scaffold materials and cell-based therapies in cartilage tissue engineering.

CHAPTER 3

CHARACTERIZATION OF PROTEOGLYCAN PRODUCTION AND PROCESSING BY CHONDROCYTES AND BMSCS IN TISSUE ENGINEERED CONSTRUCTS

3.1 INTRODUCTION

Tissue engineering and regenerative therapies have the potential to repair damage to articular cartilage and restore long-term joint function. However, there are significant challenges for recreating a tissue with the appropriate matrix composition and mechanical function[2]. The limited availability of autologous chondrocytes, combined with their rapid dedifferentiation during monolayer expansion[114], present additional obstacles for cartilage engineering. Stem cells and other progenitors are possible alternatives to articular chondrocytes, but it has yet to be established whether these cells can develop into mature chondrocytes and produce a cartilaginous matrix with the necessary mechanical properties.

Bone marrow stromal cells (BMSCs) are mesenchymal progenitors that can easily be isolated from the bone marrow and expanded in vitro[79,115], making them particularly attractive for tissue engineering applications. In addition, BMSCs have the potential to differentiate along chondrogenic, osteogenic, and adipogenic lineages[78,115]. When cultured in three-dimensional environments, the addition of exogenous transforming growth factor beta-1 (TGF-β1) promotes expression of chondrocyte-specific genes and proteoglycan (PG) synthesis[83,86]. Although BMSC-seeded constructs accumulate a

cartilage-like matrix consisting of type II collagen and sulfated-glycosaminoglycans (sGAG)[116], the total amount of matrix and material properties are inferior to constructs developed with articular chondrocytes[117]. Furthermore, it is unclear if the PG composition and organization produced by differentiating BMSCs is characteristic of native articular cartilage.

Proteoglycans play an essential role in the load-bearing function of articular cartilage. The main structural PG within cartilage is aggrecan, which consists of a protein core with numerous sGAG side chains[16]. The aggrecan molecules are linked to a hyaluronic acid backbone, forming a large macromolecule. Interactions between the negatively charged sGAG chains and ions in the interstitial fluid produce an osmotic swelling pressure that is resisted by the collagen II network and allows articular cartilage to bear high compressive forces[3,4]. While aggrecan is the most abundant PG within the tissue, small amounts of other PGs, including perlecan, decorin and biglycan, are found within the pericellular matrix[118,119]. These small PGs are known to interact with growth factors and matrix proteins, such as collagen VI and fibronectin and may play a more direct role in regulating cell function[120]. Additionally, the large PG versican is highly expressed in pre-cartilage condensations[121] and developing limb cartilage but is replaced by aggrecan during maturation[122]. The temporal changes in the PG expression profile that occur during development raise interesting questions about the composition of the matrix produced by progenitor cells undergoing in vitro chondrogenesis.

Synthesis and turnover of the extracellular matrix is critical for the homeostasis of healthy articular cartilage. Aggrecan catabolism is tightly regulated by the activity of multiple, including matrix-metalloproteinases (MMPs)[17] and aggrecanases[16]. These

enzymes cleave the aggrecan core protein at specific locations and release various sized fragments from the PG macromolecule[123]. Aggrecan cleavage is responsible for the loss of sGAGs from the tissue, and it is therefore closely linked to the tissue's compressive properties[124]. Upregulation of MMP and aggrecanase activity occurs during osteoarthritis and in response to inflammatory cytokines[125]. In addition, TGF-β1 has been shown to stimulate both cartilage matrix synthesis and degradation[126,127]. Differences in aggrecan processing have been observed between articular chondrocytes and meniscal fibrochondrocytes, which have higher endogenous levels of aggrecanase activity and produce a matrix with more degraded aggrecan[32]. Growth factor regulation and cell type differences in proteolytic activity may be important considerations for developing tissue engineered cartilage with the appropriate composition and function.

Although TGF-β1 has been shown to promote aggrecan gene expression and sGAG accumulation by BMSCs, it remains unclear whether the actual matrix composition is similar to that produced by mature chondrocytes. Therefore, the goal of this study was to characterize the proteoglycan production and processing by BMSCs within a tissue engineered construct. Bovine BMSCs and articular chondrocytes (ACs) were seeded into agarose gels and cultured up to 32 days in the presence of TGF-β1. The localization of various proteoglycans was examined by immunofluorescence and histological staining, and the presence of specific matrix proteins known to interact with these PGs was also determined by immunofluorescence and western blot analysis. The role of proteolytic enzymes in construct development was further investigated by examining the effects of aggrecanase and MMP inhibitors on PG accumulation, aggrecan processing, and construct mechanics. The results of this study illustrate key differences

in matrix synthesis and turnover between BMSCs and ACs. These findings provide new insights into the chondrogenesis of BMSCs and their potential use for articular cartilage regeneration.

3.2 MATERIALS AND METHODS

3.2.1 Materials

Immature bovine hind limbs were from Research 87 (Marlborough, MA). Recombinant human TGF-β1 was from R&D Systems (Minneapolis, MN), and basic-fibroblast growth factor (bFGF) was from Peprotech (Rocky Hill, NJ). Type VIII agarose, agarase, bovine serum albumin (BSA), protease-free chondroitinase ABC, 1,9 dimethyl methylene blue (DMMB), and Hoechst dye 33258 were from Sigma Aldrich (St. Louis, MO). The ITS+ premix and ProteinaseK were from BD Biosciences (San Jose, CA). Fetal bovine serum was from Hyclone (Logan, UT), and cell culture reagents, including Dulbecco's Modified Eagles Medium (DMEM), antibiotic/antimycotic, trypsin, non-essential amino acids (NEAA), and phosphate buffered saline (PBS), were from Invitrogen (Carlsbad, CA). 4-12% gradient polyacrylamide gels and prestained standards were also from Invitrogen. The ECF substrate was from GE Healthcare (Piskataway, NJ), and the Protease Inhibitor Cocktail I was from Calbiochem (San Diego, CA). The WST-1 assay kit was from BioVision (Mountain View, CA). The aggrecanase inhibitor (RO3310769) and the MMP inhibitor (RO1136222) were kind gifts from Roche Palo Alto (Palo Alto, CA).

The collagen type II and collagen type VI antibodies were from Abcam (Cambridge, MA). The anti-aggrecan G1 and anti-aggrecan G3 antibodies were provided

by John Sandy, Ph.D. (Rush University, Chicago, IL) and the anti-decorin and anti-biglycan antibodies were from Larry Fisher, Ph.D. (NIDCR, Bethesda, MD). Alexafluor 488 anti-rabbit IgG and Alexafluor 594 anti-mouse IgG were from Molecular Probes (Carlsbad, CA). The anti-fibronectin was from Sigma Aldrich (St. Louis, MO), and the anti-versican was from the University of Iowa Developmental Studies Hybridoma Bank (Iowa City, IA).

3.2.2 Cell Isolation

Bone marrow was harvested from the tibiae and femora of an immature calf and physically disrupted by passage through 50ml and 10ml serological pipettes, followed by 16, 18, and 20 gage needles. The marrow was then separated by centrifugation, and the fatty layer was removed. The remaining heterogeneous mixture was rinsed with PBS and pre-plated for 30 min to remove the rapidly adherent cells. The remaining cells were then re-plated at approximately 250,000 cells/cm^2 on tissue culture plastic and cultured in low-glucose DMEM, 1% antibiotic/antimycotic, 10% FBS, and 1ng/ml basic-FGF. After 3 days, the non-adherent cells were removed during the first media change. The remaining adherent BMSCs were expanded until nearly confluent, at which time they were trypsinized and replated at 6,000 cells/cm^2. Cells were expanded twice more to near-confluence before seeding in agarose. Consistent with previous reports[128], BMSCs isolated in this manner were positive for the cell surface markers CD29 and CD44 and negative for CD45 as determined by flow cytometry.

Articular chondrocytes (ACs) were isolated from the cartilage of the femoral-patellar groove and femoral condyles of an immature calf. The cartilage tissue was

minced and digested overnight in 0.2% collagenase with agitation. Cells were filtered through a 70μm mesh, followed by sequential centrifugation and rinsing to remove the collagenase. The number of viable cells was counted by trypan blue exclusion.

3.2.3 Construct Seeding and Culture

BMSCs and ACs were seeded into 1.5% agarose gels at a density of $10x10^6$ cells/ml. A 3% agarose solution in PBS was melted and cooled to 42ºC. The agarose was mixed 1:1 with a suspension of $20x10^6$ cells/ml in PBS. The agarose-cell suspension was mixed thoroughly and pipetted between glass plates with 3mm spacing. The gels were cooled at 4ºC for 20min and cylindrical punches were made with a 6mm biopsy punch. The gel constructs were moved to 24-well plates, and fresh media were added. BMSC- and AC-seeded gels were cultured up to 32 days in serum-free medium (DMEM, ITS+, antibiotic/antimycotic, NEAA, HEPES, ascorbate) plus 10ng/ml TGF-β1. Media was further supplemented with 1μM aggrecanase inhibitor, 1μM MMP inhibitor, or the carrier, 0.01% DMSO. As previously reported, the aggrecanse inhibitor specifically targets ADAMTS-4/5 (A Disintegrin And Metalloproteinase with Thrombospondin Motifs - 4/5), while the MMP inhibitor acts on a broad range of collagenases, gelatinases, and membrane type MMPs[124]. The doses used in this study were based on previous work with bovine articular cartilage[124] and a preliminary dose response study with BMSCs. Media were collected and changed every 2 days.

3.2.4 Immunofluorescence staining and histology

Gel constructs were fixed in 10% neutral buffered formalin for 4h, rinsed in PBS, and dehydrated in 70% ethanol. Samples were subsequently embedded in paraffin and sectioned at 5μm onto superfrost plus slides. Sections were deparaffinized and rehydrated in water. Sulfated-glycosaminoglycans were stained with Safranin-O, and cell nuclei were counter-stained with hemotoxylin. For immunoflurescence staining, sections were de-glycosylated with 0.1U/ml chondroitinase ABC for 1h at room temperature and blocked with 5% BSA for 30min. Sections were then stained with primary antibodies against aggrecan-G1 (1:100), aggrecan-G3, or collagen II (1:100) and a secondary solution with AlexaFluor 488 anti-rabbit IgG (1:100) and Hoechst dye (1:5000). Costaining was performed via sequential staining using primary antibodies against decorin or biglycan, and a secondary antibody, AlexaFluor 488 anti-rabbit IgG (or non-immune rabbit IgG), followed by a biotinylated primary antibody to collagen VI and detection with avidin-AlexaFluor 594 (or non-immune). Immunofluorescent slides were preserved with aqueous gel mount and imaged using a Zeiss Axiovert 200 fluorescence microscope (Heidelberg, Germany).

3.2.5 Western Blot Analysis

Proteins and proteoglycans for western blot analysis were extracted from the agarose gel constructs in 4M guanidine-HCl plus the protease inhibitor cocktail I overnight at 4ºC. Equal portions of the extracts or day 32 media samples were pooled (N=6/group) and precipitated in 100% ethanol plus 5mM sodium acetate overnight at -20ºC. The precipitated material was deglycosylated with chondroitinase ABC, keratinase

I, and keratinase II for 4 hours at 37ºC in the presence of protease inhibitors. The extract material was then dried and resuspended in a reducing loading buffer. Equal portions of the extract or media samples (approximately 5μg) were separated by eletrophoresis on 4-12% tris-glycine gradient gels and transferred to nitrocellulose membranes. The membranes were blocked overnight with 1% non-fat dry milk at 4ºC. The membranes were probed for one hour at room temperature with primary antibodies against collagen VI, decorin, biglycan, fibronectin, aggrecan-G1, aggrecan-G3, and the DLS neoepitope. Secondary detection was performed with an anti-rabbit, alkaline phosphatase antibody. The membranes were developed with a fluorescent ECF substrate and imaged using a Fuji FLA3000 phospho-imager.

3.2.6 sGAG and Viability Quantification

Following protein extraction, the gel constructs were lyophilized and sequentially digested with ProteinaseK (1mg/80mg tissue) at 60ºC overnight and agarase (4U/construct) at 45ºC for 4h. Construct digests, protein extracts, and media samples were analyzed for sGAG content using the 1,9 dimethylmethylene blue assay[129]. The total sGAG content in the gel constructs was reported as the sum of the extract and digest contents. In addition, day 32 media samples were analyzed for mitochondrial activity, indicative of cell viability, using the WST-1 assay according to the manufacturer's instructions. WST-1 and sGAG data were analyzed by one-way ANOVA and Tukey's test for post-hoc analysis. Significance was determined by $p<0.05$.

3.2.7 Mechanical Testing

Constructs were stored in PBS supplemented with the protease inhibitor cocktail at 4ºC until they underwent mechanical testing. Immediately prior to testing, each construct was weighed wet, and the diameter and thickness were measured at 3 distinct locations on the construct. Each construct was then placed in a custom, unconfined compression chamber fixtured to an ELF 3100 uniaxial testing frame (Bose, Minnetonka, MN) and a 250g button-type load cell (Honeywell Sensotec, Columbus, OH). The construct was immersed in PBS with protease inhibitors, positioned between smooth, impermeable platens, and preloaded to 10-20mN. Using Wintest software and the Dynamic Mechanical Analysis (DMA) package, the constructs were compressed to 10% strain at 100μm/min, and allowed to equilibrate to the new strain state for 30min. Following relaxation, the constructs underwent sinusoidal compression at 0.1 and 1Hz with an amplitude of 1.5% strain. Dynamic moduli were calculated and exported from the DMA software. The mechanical testing data were analyzed by one-way ANOVA and Tukey's test for post-hoc analysis. Significance was determined by $p<0.05$.

3.3 RESULTS

3.3.1 Extracellular matrix accumulation and localization

The accumulation and localization of cartilage matrix molecules by chondrocytes and BMSCs was examined by immunofluorescence and Safranin-O staining. After 32 days in TGF-β1 supplemented medium, Safranin-O staining of the tissue constructs demonstrated that ACs and BMSCs produced a proteoglycan-rich matrix (Fig 3.1A).

There was more intense staining in the AC-seeded gels, particularly in the interterritorial regions, than in the BMSC-seeded gels. In addition, there were clear differences in the distribution of sGAG throughout the constructs. AC samples had high levels of sGAG throughout the construct, while BMSC samples had primarily pericellular sGAG and less amounts at the periphery of the construct (Fig 3.1A, top). There also appeared to be more heterogeneity within the BMSC constructs, where many cells could be observed lacking a dense pericellular matrix.

The specific species of proteoglycans within the agarose gel constructs were further examined by immunofluorescence staining of the aggrecan (G1 and G3) and versican core proteins. AC and BMSC constructs stained intensely for the aggrecan G1 globular domain, with more aggrecan in the AC samples (3.1B). The distribution of G1 was similar to the pattern of sGAG seen with the Safranin-O staining, suggesting that the major proteoglycan within the constructs is aggrecan. Positive staining for the G3 domain in both groups indicated the presence of full length aggrecan (3.1C). There also appeared to be higher levels of pericellular G3 in the BMSC constructs. Low levels of versican could be detected with anti-sera raised against the hyaluronan binding region for the BMSC constructs only (3.1D).

The patterns of type II collagen accumulation were similar to those of aggrecan. Collagen II deposition was highest in the pericellular region, and the AC constructs had overall greater amounts of collagen II than the BMSC constructs (3.1E). Combined with the proteoglycan staining, these results demonstrate that both ACs and BMSCs produce a cartilage-like extracellular matrix composed of aggrecan and collagen II when cultured

with TGF-β1. However, the AC constructs accumulated more matrix than the BMSC constructs and with a more uniform distribution.

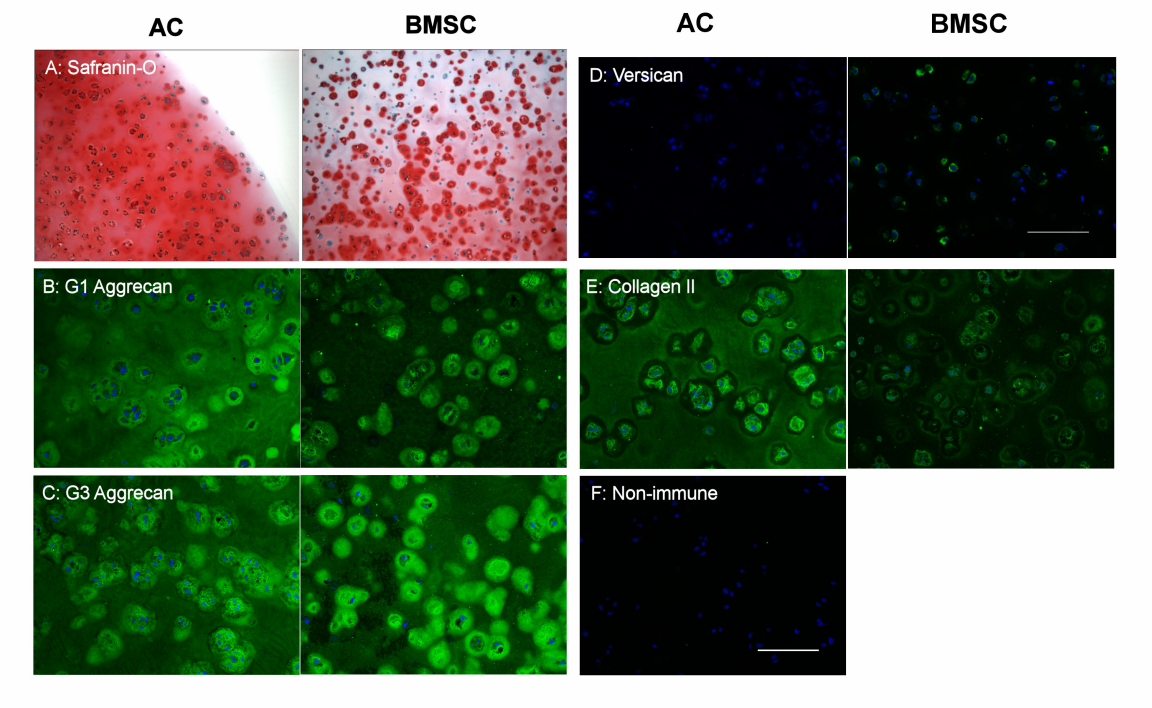

Figure 3.1: Safranin-O and immunofluorescence images of day 32 constructs. (A) Safranin-O. (B) Aggrecan G1 globular domain, green. (C) Aggrecan G3 globular domain, green. (D) Versican hyaluronan binding domain, green. (E) Type II collagen, green. (F) Non-immune control. DNA is blue in all images. Scale bar = 100μm.

3.3.2 Pericellular matrix composition

The composition of the pericellular microenvironment within the chondrocyte and BMSC constructs was investigated by immunofluorescence staining and western blot analysis. Intense pericellular staining for collagen VI was observed around ACs throughout the construct, while the BMSC constructs displayed little collagen VI staining (Fig 3.2A-B). In contrast, high levels of the small PGs, decorin and bigycan, were present in the BMSC samples, but not in the AC samples (Fig 3.2A-B). BMSC constructs also displayed greater amounts of pericellular fibronectin, as well as diffuse

accumulation in the interterriteorial region (Fig 3.2C). The fibronectin distribution varied considerably in the BMSC constructs, with the highest levels observed at the periphery of the gel. The differential production of collagen VI, decorin, biglycan, and fibronectin between the ACs and BMSCs was verified by western blot analysis of protein extracts from the tissue engineered constructs (Fig 3.2D-G). These results demonstrate distinct differences in the composition of the pericellular matrix produced by ACs and BMSCs.

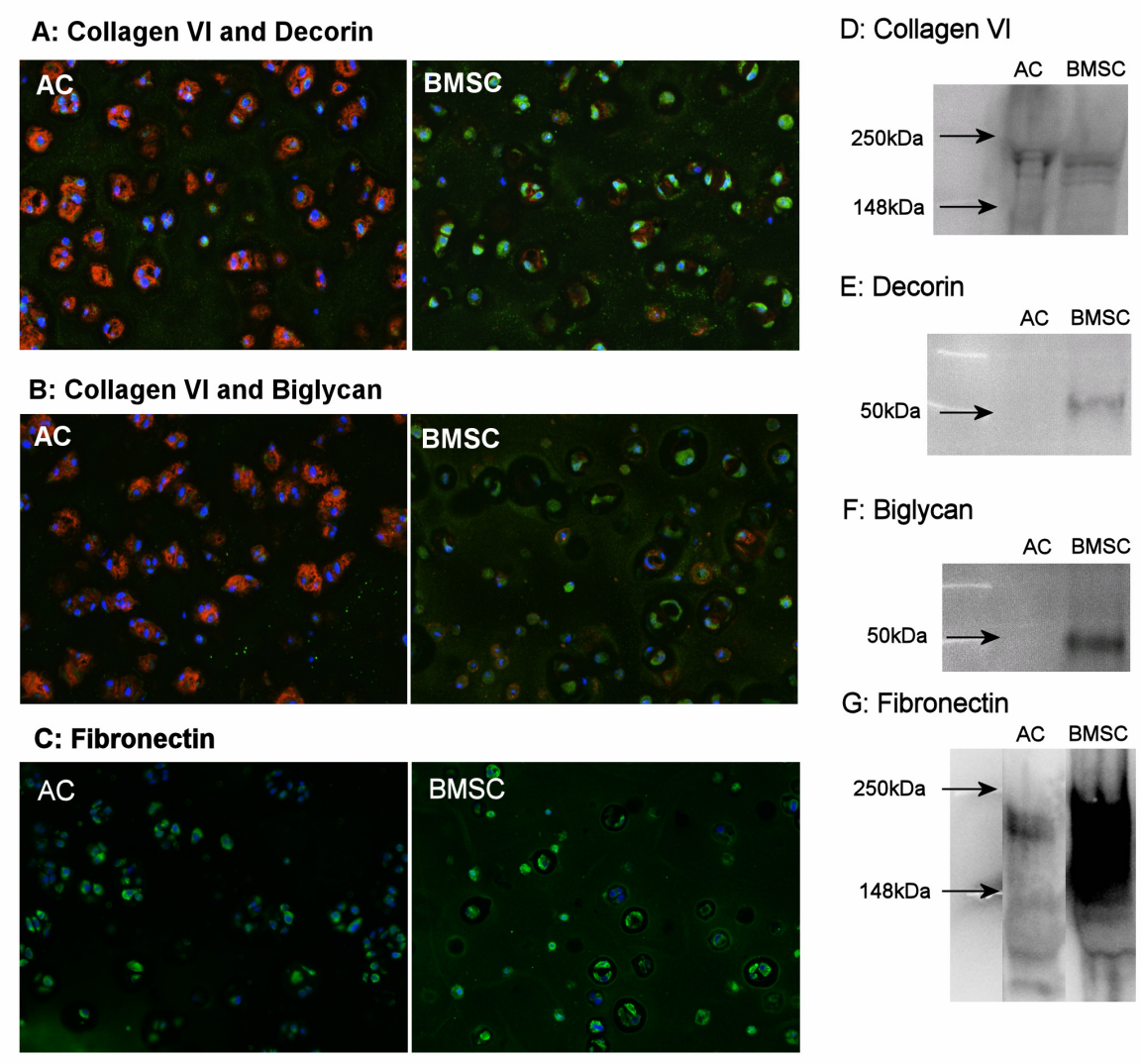

Figure 3.2: Immunofluorescence and western blot analysis of the pericellular matrix composition in day 32 constructs. (A) Co-staining for collagen VI, red, and decorin, green. (B) Co-staining for collagen VI, red, and biglycan, green. (C) Fibronectin, green. DNA is blue in all images. Western blots of construct extracts for (D) collagen VI, (E) decorin, (F) biglycan, and (G) fibronectin.

3.3.3 Effects of Aggrecanse and MMP inhibitors on matrix accumulation

To investigate the role of proteolytic enzymes in ECM production, additional BMSC-seeded constructs were cultured in the presence an aggrecanse inhibitor and an MMP inhibitor. Analysis of the day 32 constructs with the WST-1 mitochondrial activity assay indicated that there were no toxic effects of the inhibitors on the BMSCs during long term culture (Fig 3.3A). The inhibitors had no effect on the cumulative amount of sGAG released to the media (3.3B). However, addition of the MMP inhibitor significantly decreased sGAG accumulation (Fig 3.3C). These differences were relatively small compared to the amount of sGAG produced by ACs. Consistent with the Safranin-O staining, AC constructs contained approximately twice as much sGAG as the BMSC constructs. Immunofluorescence staining for collagen II indicated higher levels of pericellular collagen with both inhibitor treatments (Fig 3.3D).

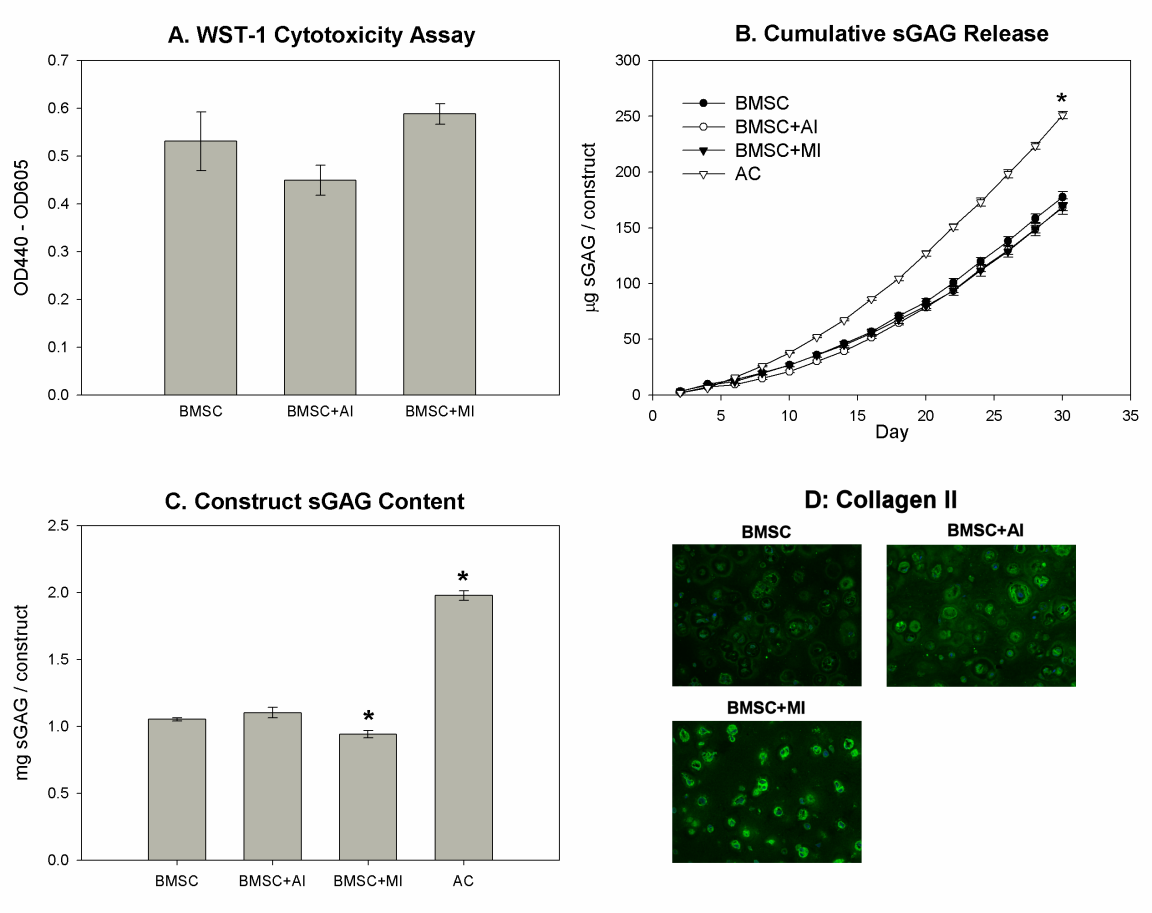

Figure 3.3: Influence of the aggrecanase inhibitor (AI) and MMP inhibitor (MI) on extracellular matrix production by BMSCs. (A) WST-1 analysis of day 32 mitochondrial activity, N=4/group. (B) Cumulative sGAG released to the media, N=6/group, *P<0.05 with BMSC group. (C) Total sGAG accumulation within the construct, N=6/group, *P<0.05 with BMSC. (D) Immunofluroescence images of collagen II accumulation, green, and DNA, blue.

3.3.4 Aggrecan processing by BMSCs

The effects of the aggrecanse and MMP inhibitors on aggrecan processing were examined by western blot analysis of the construct extracts and conditioned media. Detection of the aggrecan core protein with the anti-G1 antibody indicated that the aggrecan retained within the construct was primarily full-length (450kDa). Lower levels of processed aggrecan could be detected at approximately 50kDa, 120kDa, and just

below 250kDa (Fig 3.4A). The proteolytic inhibitors did not appear to have an effect on the detection of the full length or processed forms of G1 aggrecan. Similar analysis of the day 32 media samples indicated that the aggrecan released to the media was also full-length (Fig 3.4A). The DLS neoepitope, generated by m-calpain, could be observed in the extracts of BMSC constructs. Interestingly, the aggrecanase inhibitor appeared to reduce the amount of this form of aggrecan, but the MMP inhibitor appeared to have no effect on DLS generation (Fig 3.4B). Analysis of the G1 aggrecan distribution in native articular cartilage revealed characteristic patterns of ADAMTS-4/5 (70kDa) and MMP (60kDa) mediated cleavage. Together, these results indicate that the aggrecan within the BMSC constructs is primarily full-length and that low levels of proteases, including m-calpain, are active under the conditions examined.

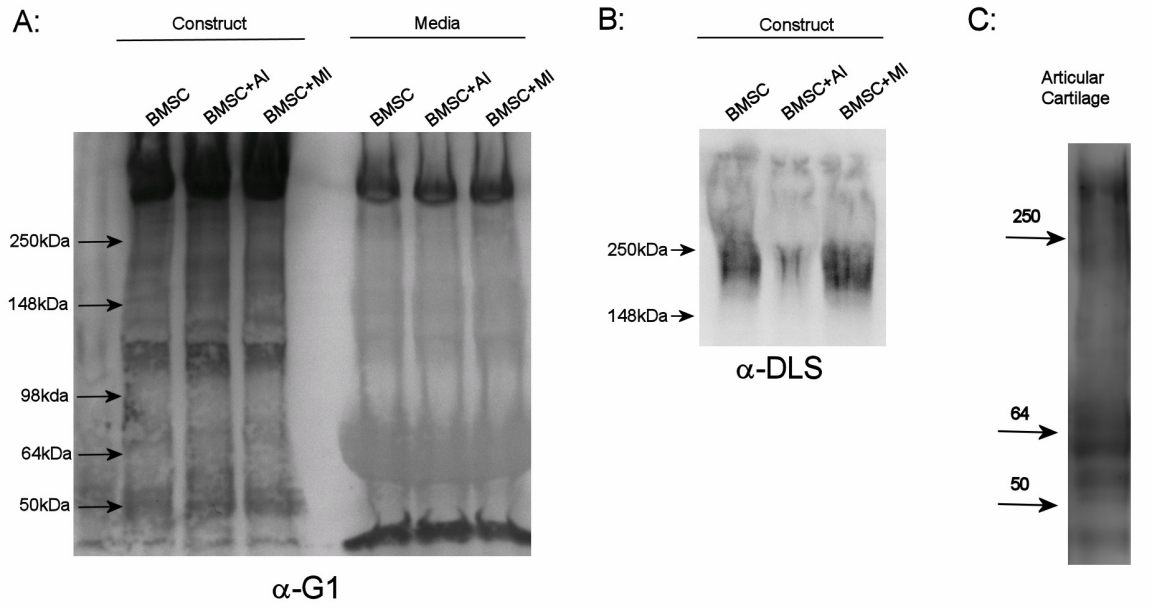

Figure 3.4: Western blot analysis of aggrecan processing. (A) Detection of aggrecan G1 domain in construct extracts and day 32 media samples from control, aggrecanase inhibitor (AI), or MMP inhibitor (MI) treatments. (B) Detection of the m-calpain generated neoepitope in construct extracts. (C) Detection of G1 aggrecan in native articular cartilage.

3.3.5 Construct mechanics

The functional implications of matrix accumulation and processing were evaluated by measuring the dynamic compressive moduli at 0.1Hz and 1.0Hz (Fig 3.5). By day 32, BMSC constructs had significantly higher (6.7X) compressive moduli than day 0 samples. The aggrecanase inhibitor slightly, but significantly, increased (1.1X) the modulus at 1.0Hz, and the MMP inhibitor slightly decreased (0.8X) the moduli at both frequencies. Consistent with the greater amount of matrix accumulation, the AC constructs had dynamic compressive moduli of approximately 1MPa, significantly higher (3.3X) than the moduli of all the BMSC constructs.

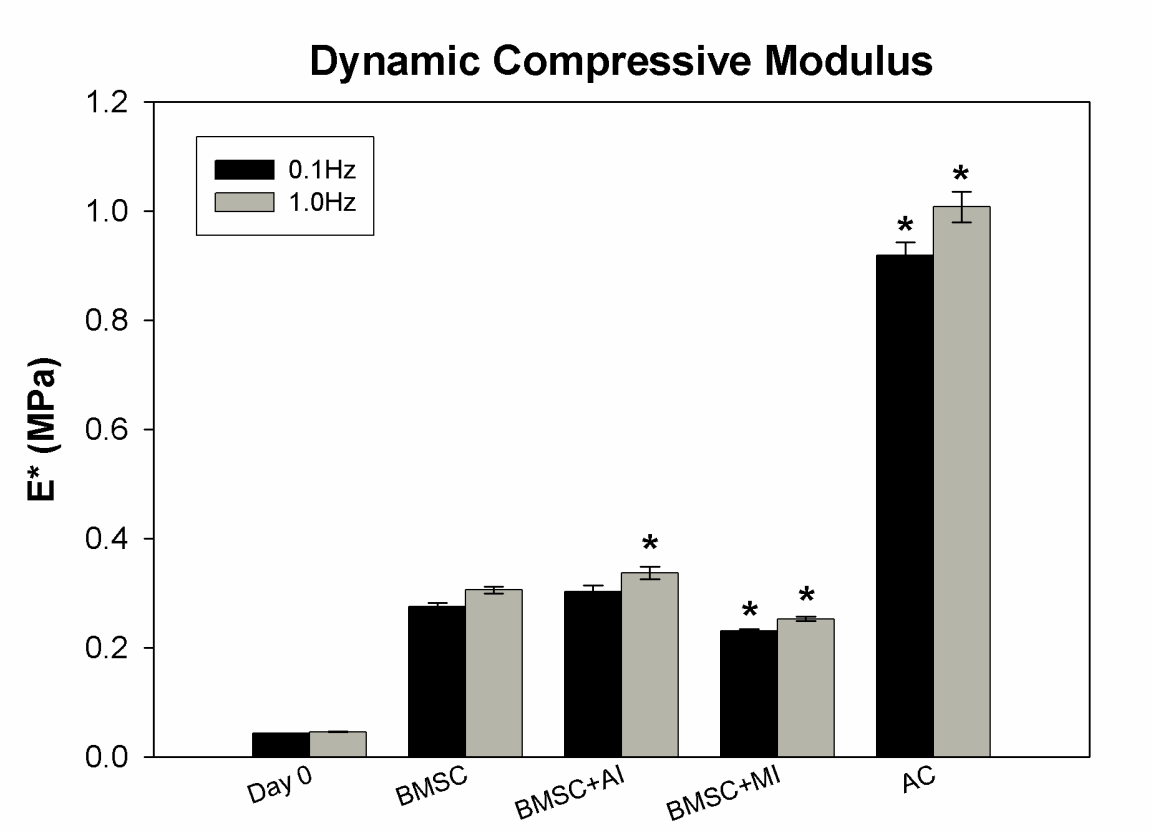

Figure 3.5: Construct mechanics. The dynamic compressive moduli of day 0 and day 32 constructs measured at 0.1Hz and 1.0Hz. *P<0.05 with BMSC, N=6/group.

3.4 DISCUSSION

The objective of the present study was to examine the composition, organization, and processing of proteoglycans by BMSCs within a tissue engineered construct. Bovine BMSCs were cultured in agarose hydrogels and in the presence of TGF-β1, conditions known to promote chondrocytic differentiation. Under these conditions, the major proteoglycan produced by BMSCs was aggrecan, and the strong G3 staining and western blot analysis indicated that the aggrecan was primarily full length. In addition, there were large amounts of collagen II present within the pericellular matrix. Despite synthesizing an extracellular matrix characteristic of articular cartilage, BMSCs produced far less total matrix than chondrocytes under the same culture conditions. Furthermore, there were distinct differences in matrix organization and composition of the pericellular environment between the two cell types. These findings provide new insights into the chondrogenic potential of BMSCs and the character of their extracellular matrix.

Consistent with previous findings[117], AC constructs had a 3-fold higher dynamic compressive modulus than BMSC constructs, and this difference in mechanical function was most likely due to the higher levels of matrix accumulation by ACs. Analysis of the sGAG released to the media indicated that by day 32 both cell types were releasing sGAG at a constant rate, and ACs were releasing sGAG at a higher rate than BMSCs. Previous reports have also shown that after longer culture periods (up to 10 weeks), bovine BMSCs still produced less sGAG than articular chondrocytes[117], suggesting that there are fundamental differences in the phenotypes of these cells, rather than a lag in matrix synthesis during the initial stages of differentiation. The regional variations in matrix accumulation within the BMSC constructs revealed that for a given sample there

was significant heterogeneity in the level of chondrogenesis. Interestingly, there appeared to be higher levels of sGAG in the interior of the gel, where hypoxic conditions may have enhanced differentiation and sGAG synthesis[130]. In addition, the presence of cells completely lacking a proteoglycan-rich pericellular matrix indicates that not all of the cells were undergoing chondrogenesis and that the initial population of BMSCs may not have been a homogeneous population of mesenchymal progenitors.

The distinct differences in the pericellular matrices between ACs and BMSCs provide additional insights into the differentiation state of these cells and potential mechanisms for regulating cell activity. The AC pericellular environment had high levels of collagen VI, similar to native cartilage[131], while the BMSC pericellular matrix contained little collagen VI and higher fibronectin, decorin and biglycan. These results indicate that the BMSCs were not yet mature chondrocytes. The high fibronectin expression at the periphery of the construct had the inverse distribution of sGAG and may represent a marker of less differentiated cells. A similar expression pattern has been observed during limb development, where fibronectin is upregulated in pre-cartilage condensations of the mesenchyme but decreases in mature cartilage[111]. Other constituents of the pericellular matrix are also known to regulate cell activity. In vivo, collagen VI interacts with decorin and biglycan[132] and may aid in collagen II and aggrecan matrix assembly[133]. In addition, the small PGs can bind TGF-β1 and influence its availability to cells[134]. Given that chondrogenesis is a dynamic process, where ECM production and turnover are constantly changing, different cell-matrix interactions may be required at specific stages of development, and the unique composition of the BMSC pericellular matrix may actually be necessary for differentiation. The complex

interactions between cells, ECM, and growth factors have the potential to regulate differentiation and tissue development through multiple mechanisms, and additional studies are clearly required to more completely understand their role in chondrogenesis.

Matrix catabolism is a critical component of tissue development and homeostasis, and perturbations in the balance between synthesis and degradation can significantly alter cartilage composition and function[124]. In this study, aggrecanase and MMP inhibitors were employed to examine the effects of proteolytic degradation in construct development. In general, catabolic enzymes appeared to play a minor role in matrix accumulation by BMSCs. Western blots for the aggrecan G1 domain indicated that an abundant amount of full-length aggrecan was present in the constructs, and compared to native tissue, the patterns of G1 aggrecan seen in the BMSC samples contained little or no ADAMTS-4/5 or MMP generated fragments[16,135], suggesting that the activity of these enzymes is low within this system. Nevertheless, the aggrecanase inhibitor did appear to reduce m-calpain activity and provided a small but significant improvement in construct stiffness. Interestingly, the MMP inhibitor significantly decreased the total sGAG content and dynamic moduli of the tissue constructs. This effect may have been a result of inhibited autocrine growth factor signaling. In growth plate cartilage, MMP-3 is known to activate latent TGF-β[136], and MMP-7 is responsible for degrading the binding proteins of insulin-like growth factor[137]. Based on the WST-1 activity and previous studies with these inhibitors it does not appear that the lower sGAG production was due to cytotoxic effects. Taken together, these results demonstrate that proteolytic enzymes can both positively and negatively affect construct development.

Overall, the findings of this study have important implications for future directions in cartilage tissue engineering. BMSC production of a proteoglycan-rich matrix consisting of primarily intact aggrecan is a promising development for the use of these cells in articular cartilage repair. Furthermore, the low proteolytic activity of differentiating BMSCs may be advantageous if they are eventually implanted into a cartilage defect. Despite these advances, BMSCs cultured in TGF-β1 supplemented medium do not differentiate into mature chondrocytes after 32 days in agarose gel culture. Additional biochemical stimuli, such as growth factors[138,139] or glucocorticoids[140], have been shown to enhance chondrogenesis, and optimization of the specific culture conditions may be necessary for chondrocyte maturation. Mechanical stimuli[96] and low-oxygen tension[130], are also potential strategies for improving in vitro differentiation and construct development. Finally, the distinct pericellular matrices produced by ACs and BMSCs suggest that cell-matrix interactions play an important role in chondrogenesis, and the design of scaffolds presenting specific matrix proteins may be another approach for guiding differentiation and ECM production.

CHAPTER 4

CYCLIC TENSILE LOADING ALTERS GENE EXPRESSION AND MATRIX SYNTHESIS OF BMSCS IN FIBRIN CONSTRUCTS

4.1 INTRODUCTION

Fibrocartilage is a specialized type of cartilage found in the menisci of the knee, the tempromandibular joint disks (TMJ), and the insertion sites of tendons. The tissue consists of approximately 60% water, and the extracellular matrix (ECM) is composed of primarily type I collagen and sulfated proteoglycans[27]. Damage to fibrocartilage tissues such as the meniscus can disrupt the normal joint biomechanics and lead to the early onset of osteoarthritis in the articular cartilage of the knee[23]. Unfortunately, fibrocartilage has a limited ability for regeneration, particularly in avascular regions[23], and the development of successful treatments for repair is essential for restoring joint function and preventing future degeneration.

Tissue engineering therapies that combine cells, scaffolding, or other biologic factors are potential strategies for repairing damaged fibrocartilage. However, a major limitation with cartilage tissue engineering is the availability of an appropriate cell source. Few primary chondrocytes and fibrochondrocytes can be obtained from a single patient, and these cells have a limited expansion potential in vitro. Mesenchymal progenitor cells are an alternative cell source that can easily be isolated from autologous tissues and expanded in monolayer cultures[115]. In addition, these cells have the potential to differentiate into multiple mesenchymal lineages[77,115]. It is well established that bone

marrow stromal cells (BMSCs) contain multipotent progenitors capable of chondrogenic differentiation[82-84,87,89]. Transforming growth factor β1 (TGF-β1) and the glucocorticoid dexamethasone promote chondrogenesis within a variety of three-dimensional culture systems, such as pellet culture[82,83] or hydrogel constructs[87,89,141].

While much work has been devoted to studying the chondrogenesis of BMSCs for articular cartilage repair, few studies have explored the use of progenitors for repairing fibrocartilage damage. In one report, autologous BMSCs from a rabbit were seeded into a collagen sponge and implanted into a partial meniscal defect[90]. Although the newly formed tissue was "histologically similar to normal fibrocartilage," the implant failed to restore mechanical function of the meniscus and resulted in osteoarthritic degradation in the joint. In another study, caprine BMSCs were injected into the knee joint following medial meniscectomy and resulted in regeneration of meniscus-like tissue[91]. These studies suggest that BMSCs may be a potential cell source for fibrocartilage repair, but additional stimuli may be required to develop a mechanically functional tissue substitute. Furthermore, there has been little work to identify key factors involved in fibrochondrocyte-specific differentiation.

Mechanical stimuli are important regulators of cell function in primary cells and differentiation in progenitors. Numerous studies have demonstrated that physiologically relevant types of loading, such as dynamic compression, hydrostatic pressure, and shearing forces, can enhance matrix biosynthesis[64,92-95] and even increase the strength and stiffness of tissue engineered constructs[64]. Recently, several reports also indicated that dynamic compression of BMSC-seeded hydrogels stimulated collagen II and aggrecan gene expression as well as collagen and proteoglycan (PG) synthesis[85,142]. Similarly,

cyclic hydrostatic pressure on BMSC aggregates resulted in increased collagen and PG production after two weeks in culture[98]. Taken together, these studies indicate that physiologically relevant loading can stimulate matrix synthesis of primary chondrocytes and enhance chondrogenesis of BMSCs.

Since fibrocartilage tissues experience significant tensile forces during normal physiologic loading, tension may be a key regulator of the fibrochondrocyte phenotype. Cyclic tension has been shown to down-regulate PG and protein synthesis of both chondrocytes and fibrochondrocytes in fibrin gel culture[36]. Interestingly, tensile loading of articular chondrocytes also induced formation of cytoskeletal projections and a stellate morphology, similar to fibrochondrocytes [36]. In addition to primary chondrocytes and fibrochondrocytes, tensile loading can also influence BMSC differentiation. Cyclic tension in combination with torsional loading promoted collagen I, collagen III, and tenascin-C expression by bovine BMSCs in collagen gels[102]. Similarly, uniaxial stretching of human mesnchymal stem cells increased collagen I and smooth muscle α-actin expression[103]. These findings provide additional evidence that physiologically relevant forces may be an important factor in differentiation and development of fibrocartilage. Furthermore, cyclic tensile loading of BMSCs could be a potential strategy for promoting fibrochondrocyte-specific differentiation for tissue engineering therapies.

The objective of the current study was to examine the initial effects of cyclic tensile loading on bovine BMSCs during in vitro chondrogenesis. A time course for the chondrogenesis of bovine BMSCs in fibrin gels was first established in free-swelling culture. Short periods of cyclic tensile loading were then introduced at various stages of

differentiation, and the initial effects of loading were examined by measuring changes in gene expression, cell morphology, and matrix synthesis rates. The results of this study provide new insights into the effects of mechanical stimuli on chondrogenesis and examine the potential of tensile loading to promote fibrochondrocyte differentiation.

4.2 MATERIALS AND METHODS

4.2.1 Materials

Immature bovine hind limbs were from Research 87 (Marlborough, MA). Recombinant human TGF-β1 and basic-fibroblast growth factor (bFGF) were from Peprotech (Rocky Hill, NJ). Bovine fibrinogen, dexamethasone, aprotinin, 1,9 dimethyl methylene blue (DMMB), and Hoechst dye 33258 were from Sigma Aldrich (St. Louis, MO). ^{35}S-sodium sulfate and bovine thrombin were from MP Biomedicals (Solon, OH), and the ITS+ premix and ProteinaseK were from BD Biosciences (San Jose, CA). Fetal bovine serum was from Hyclone (Logan, UT), and cell culture reagents, including Dulbecco's Modified Eagles Medium (DMEM), antibiotic/antimycotic, trypsin, non-essential amino acids (NEAA), and phosphate buffered saline (PBS), were from Invitrogen (Carlsbad, CA). The RNeasy mini kit was from Qiagen (Valencia, CA), and the AMV reverse transcriptase kit was from Promega (Madison, WI). The SybrGreen master mix was from Applied Biosystems (Forest City, CA). Alexafluor 594-conjugated phalloidin was from Molecular Probes (Eugene, OR).

4.2.2 BMSC Isolation and Expansion

Bone marrow was harvested from the tibiae and femora of an immature calf and physically disrupted by passage through 50ml and 10ml serological pipettes, followed by 16, 18, and 20 gage needles. The marrow was then separated by centrifugation, and the fatty layer was removed. The remaining heterogeneous mixture was rinsed with PBS and pre-plated for 30 minutes to remove the rapidly adherent cells. The remaining cells were then re-plated at approximately 250,000 cells/cm^2 on tissue culture plastic and cultured in low-glucose DMEM, 1% antibiotic/antimycotic, 10% FBS, and 1ng/ml basic-FGF. After 3 days, the non-adherent cells were removed during the first media change. The remaining adherent BMSCs were expanded until nearly confluent, at which time they were trypsinized and replated at 6,000 cells/cm^2. Cells were expanded twice more to near-confluence before seeding into fibrin.

4.2.3 Fibrin gel seeding and culture

BMSCs were seeded into fibrin gels (50mg/ml) at a density of $10x10^6$ cells/ml by combining a fibrinogen/cell suspension in DMEM with bovine thombin (50U/ml final concentration) and casting the gel in custom polycarbonate molds. The fibrin gels also contained 1TIU/ml of aprotinin to prevent fibrinolysis and degradation of the construct. For the unloaded time course, fibrin gels were cast in cylindrical molds (11mmØ x 3mm). For the loading studies, the gels were cast in rectangular molds between porous polyethylene end-blocks (Fig. 4.1 inset). Infiltration of the fibrinogen/cell suspension into the polyethylene prior to gelation fixed the gels to the endblocks and provided a rigid support for applying controlled tensile strains to the gels. Fibrin gel constructs were

cultured in a basal medium consisting of high-glucose DMEM, ITS+ premix, NEAA, antibiotic/antimycotic, ascorbate, and 2mg/ml tranexamic acid or in a chondrogenic medium, consisting of basal medium plus 10ng/ml TGF-β1 and 100nM dexamethasone. For the intermittent loading experiment, tranexamic acid was replaced with 0.1TIU/ml aprotinin to prevent fibrinolysis. Media were changed every 2 days.

4.2.4 Cyclic Tensile Loading

The cylindrical fibrin constructs were first cultured under free-swelling conditions to establish a time-course for chondrogenic differentiation of bovine BMSCs within a fibrin matrix. Gene expression, sGAG accumulation, and DNA contents were measured at days 0, 2, 4, 7, and 12 following seeding.

For the cyclic tensile loading experiments, the effects of loading duration were first examined after pre-culturing the constructs for 4 days in basal or TGF-β1 supplemented media. Sinusoidal tensile displacements of 10% (peak-peak) were applied to the constructs at 1Hz using a custom loading device (Fig 4.1) while unloaded controls remained in free-swelling culture. Constructs were loaded for 3 or 12 hours and immediately analyzed for gene expression and cell morphology.

To investigate the effects of pre-culture on the response to loading, fibrin constructs were cultured in basal or chondrogenic medium for 1, 4, or 12 days prior to loading. Following pre-culture, the constructs were loaded at 10% displacement and 1Hz and examined for gene expression after 3 hours of loading. In addition, the influences of intermittent tensile loading on matrix synthesis rates were investigated after 4 or 12 days of pre-culture. For this experiment, the constructs were loaded for 3 hours at 10%

displacement and 1Hz frequency, followed by 3 hours recovery at 0% displacement, with the load/recovery cycle repeated four times for 24 hours.

4.2.5 Real Time RT-PCR

Total RNA was isolated from the fibrin gel constructs using the Tri-spin method[143]. Gels were immediately dissociated in lysis buffer plus 2-mercaptoethanol. RNA was extracted from the fibrin using the Trizol reagent and chloroform and precipitated with 100% isoproponol. The RNA was further purified using the Qiagen RNeasy kit according to the manufacturer's protocol. Total RNA (1μg) was reverse transcribed to cDNA using the AMV reverse transcriptase kit. Gene expression was measured by real-time RT-PCR using the SybrGreen master mix and custom primers for collagen II (X02420), aggrecan core protein (NM_173906), Sox-9 transcription factor (AF278703), and collagen I (AB008683). The PCR reactions and detection were performed with an ABI Prism 7700 (Applied Biosystems, Forest City, CA).

4.2.6 Matrix Synthesis and DNA Content

During the 24 hour intermittent loading period, 5μCi/ml ^{35}S-sodium sulfate and 10μCi/ml 3H-proline were included in the culture media to measure sGAG and protein synthesis, respectively. Following loading, radiolabel incorporation was quenched with 4 sequential 30 minute washes in PBS plus 0.8mM sodium sulfate and 1.0mM L-proline at 4°C. The gels were weighed, lyophilized, reweighed and digested with Proteinase K at 60°C. Radiolabel contents were measured using a liquid scintillation counter. The total

sGAG contents were measured using the DMMB assay[144], and the DNA contents were measured using the Hoechst dye assay[145].

4.2.7 F-actin Staining

Portions of the fibrin gels were fixed in 10% neutral buffered formalin for 20 minutes and stored in PBS at 4°C. The gels were blocked with 5% FBS and 1% Triton-X100 for 30 minutes and labeled with Hoechst dye and AlexaFluor 594-phalloidin for 90 minutes at 37°C. The gels were rinsed thoroughly and imaged using a laser scanning confocal microscope (LSM 510, Zeiss, Heidelberg, Germany).

4.2.8 Data Analysis

All data are presented as the mean ± SEM. Gene expression levels were transformed by a Box-Cox transformation for normality. Data were analyzed by a general linear model with time point, loading condition, and media formulation as factors. All pairwise comparisons were performed with Tukey's test. Significance was at $P < 0.05$.

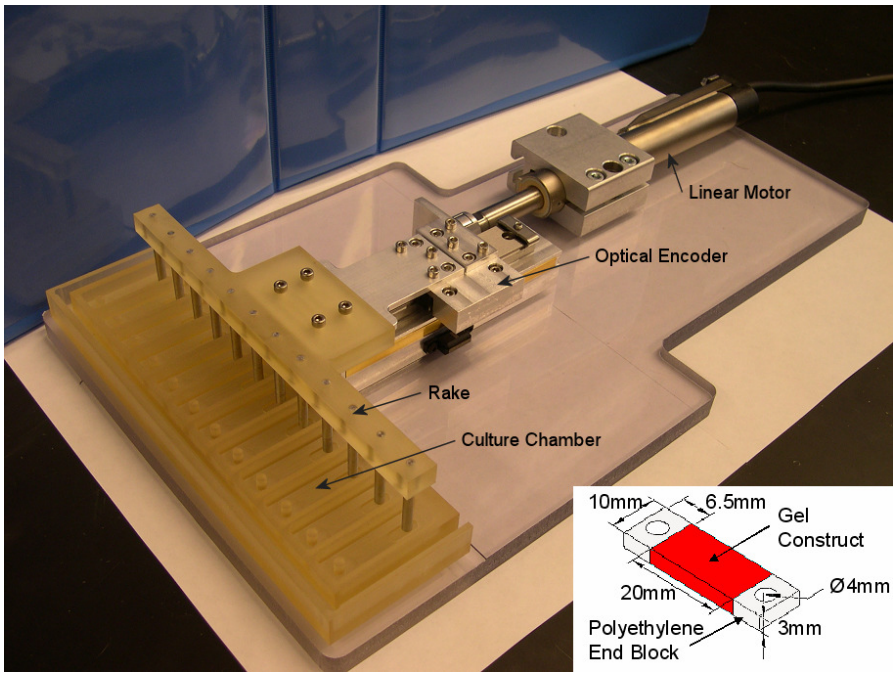

Figure 4.1: Tensile loading system. The tensile loading system consisted of a linear motor that applied cyclic tensile displacements to the fibrin constructs via a linear sliding table and rake attachment. Motion was controlled by a Trio Motion controller and feedback from an optical encoder. The fibrin constructs (inset) were cast between porous polyethylene end blocks for rigid fixation and connection to the rake attachment.

4.3 RESULTS

4.3.1 Unloaded Time Course

At day 2, BMSCs cultured with the chondrogenic supplements TGF-β1 and dexamethasone expressed significantly lower levels of the chondrocytic genes, collagen II, aggrecan, and sox-9, than those cultured in the basal medium (Fig 4.2A-C). By day 7 however, cells in the basal and chondrogenic media expressed similar levels of the chondrocytic genes, and by day 12 the chondrogenic group expressed significantly higher levels. Collagen I expression was not significantly different between media conditions during the unloaded time course (Fig 4.2D).

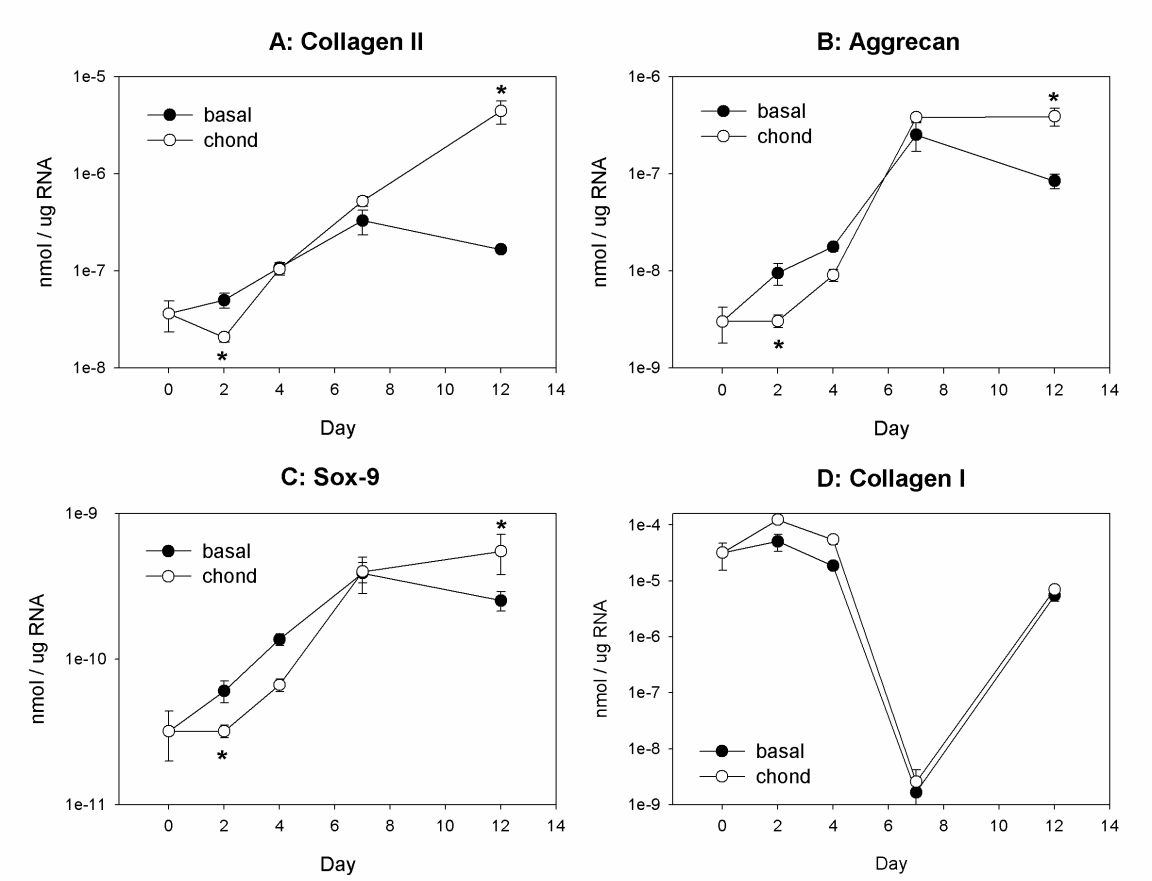

Figure 4.2: Gene expression during unloaded culture. (A) collagen II, (B) aggrecan, (C) sox-9, and (D) collagen I were measured by real-time RT-PCR. Levels of mRNA are expressed on a logarithmic scale as nmol of transcript per μg of total RNA. N=6 / condition, *P<0.05 with basal medium.

Addition of the chondrogenic supplements stimulated sGAG accumulation within the fibrin construct, with significant increases over basal medium at days 7 and 12 (Fig 4.3A). During the 12 day culture period the BMSCs both degraded and contracted the fibrin gel. Constructs in basal medium lost significantly more dry mass than the constructs in chondrogenic medium (Fig 4.3C-D). Similarly, the DNA content in the basal group was significantly lower at day 12 (Fig 4.3B).

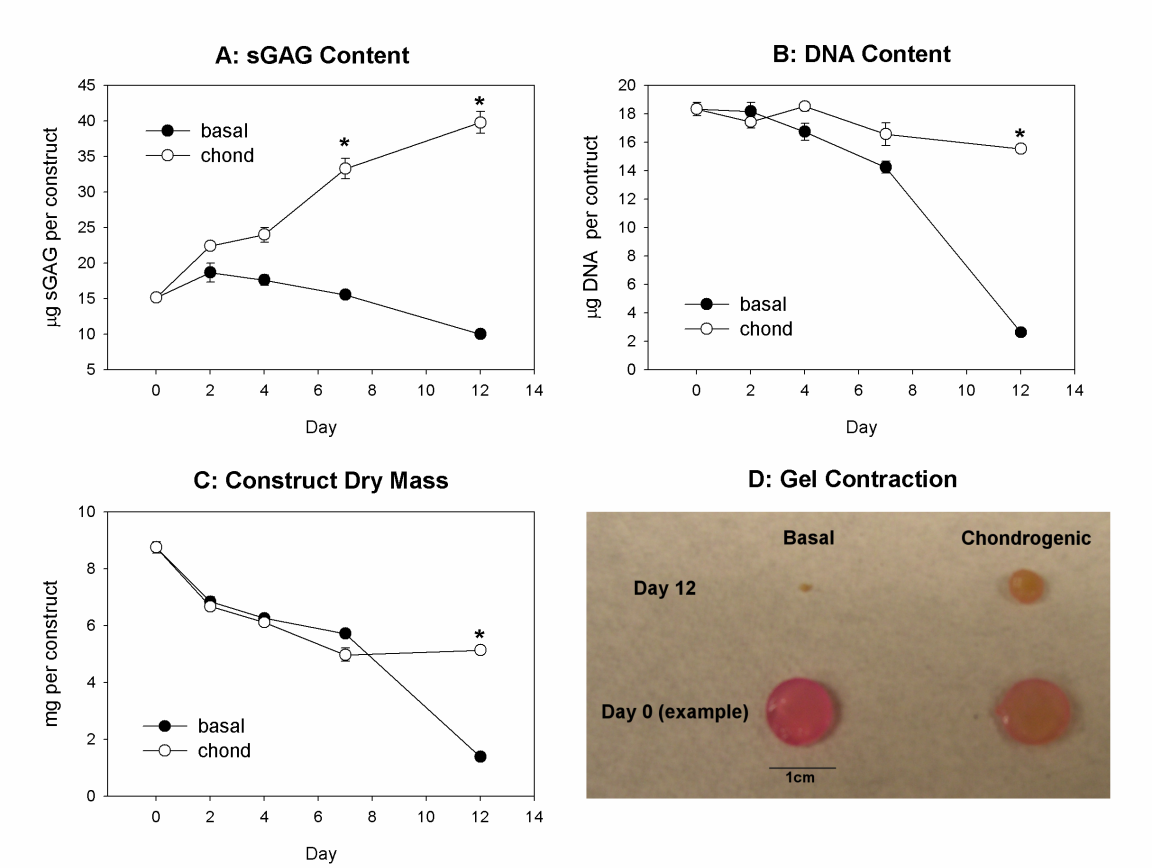

Figure 4.3: Construct matrix composition. (A) sGAG accumulation, (B) DNA content, and (C) construct dry mass were examined over 12 days under free swelling conditions in basal or chondrogenic medium. (D) Representative gels at days 0 and 12. N=6 / condition, *P<0.05 with basal medium.

BMSCs displayed similar morphologies in both basal and chondrogenic media (Fig 4.4A-B). A mix of round cells and spread cells with distinct f-actin stress fibers and cytoskeletal projections could be observed within the constructs. BMSCs within the center of the construct were more rounded (Fig 4.4C), while those on the surfaces had primarily spread morphologies (Fig 4.4D).

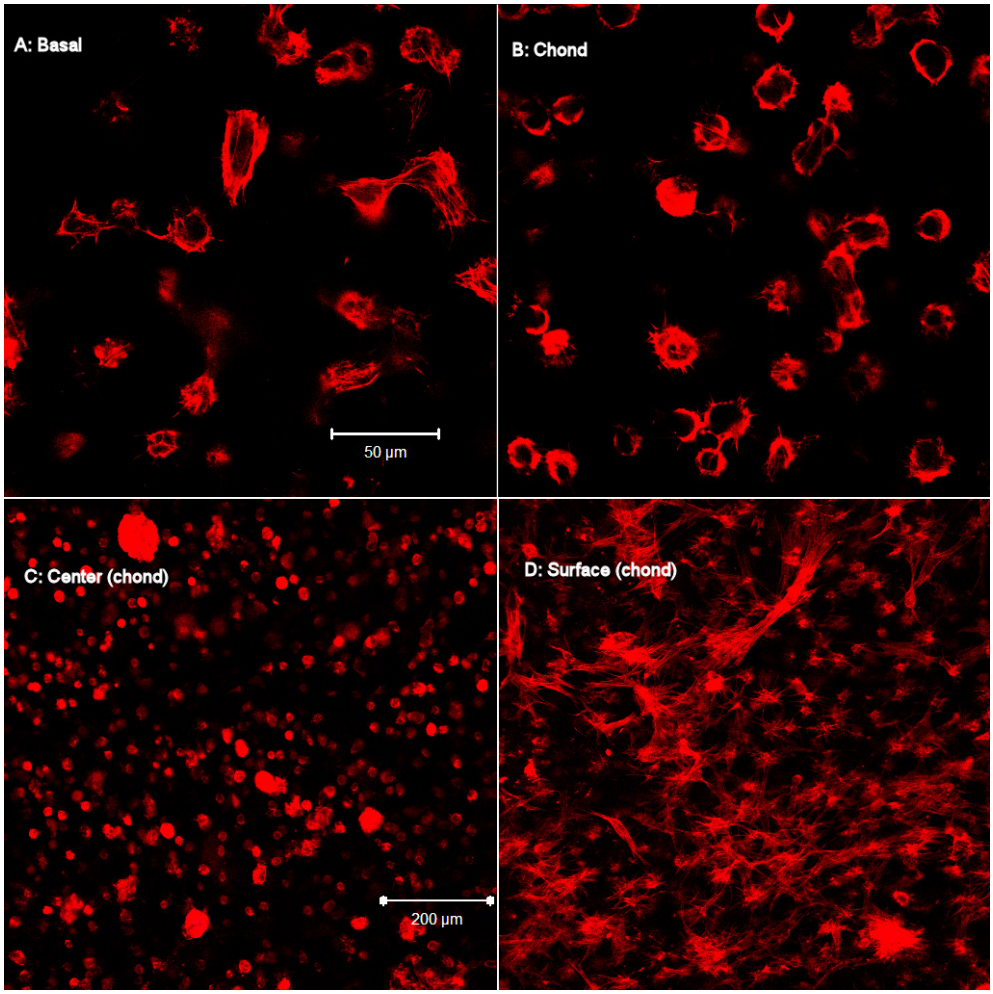

Figure 4.4: BMSC morphology. Cell morphology was examined by staining for the f-actin cytoskeleton and imaging with a confocal microscope at 40X (A-B) and 10X (C-D) magnifications. Representative images from the center of the constructs are shown for cells in (A) basal and (B-C) chondrogenic media, as well as for (D) BMSCs on the surface of the construct.

4.3.2 Loading Duration

After a 4 day pre-culture in either basal or TGF-β1 supplemented medium, fibrin constructs were loaded for 3 or 12 hours. Three hours of cyclic tensile loading of BMSCs in basal medium significantly increased expression of the chondrocytic genes but had no effect on cells in the TGF-β1 medium (Fig 4.5A-C). Interestingly, there was no effect of loading on chondrocytic gene expression when the constructs were loaded

continuously for 12 hours. There was also no significant effect of loading for 3 or 12 hours on collagen I expression (Fig 4.5D). Similar to the unloaded time course, expression of the chondrocytic genes was significantly lower in the TGF-β1 supplemented medium.

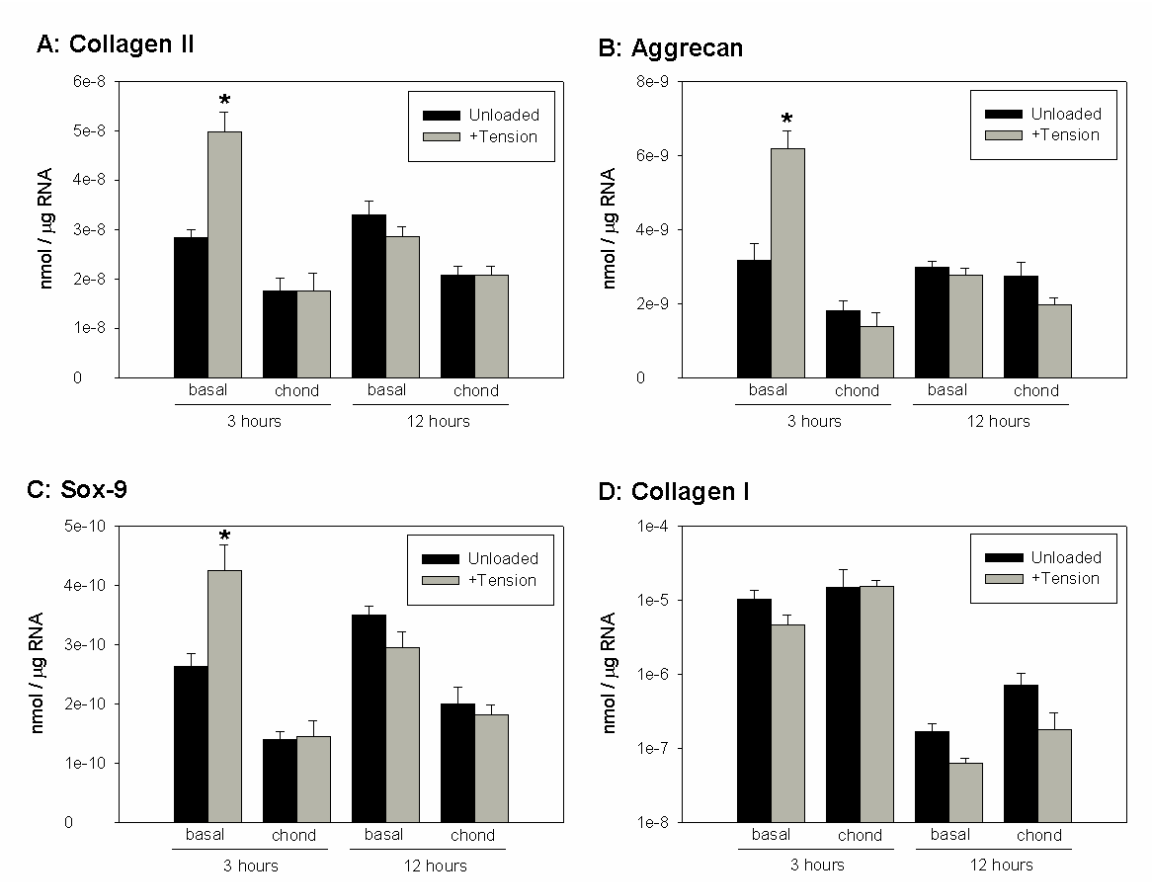

Figure 4.5: Effects of loading duration on mRNA expression. Following a 4 day pre-culture in basal or TGF-β1 medium, the fibrin gels were loaded for 3h or 12h at 1Hz with 10% (peak-peak) displacement. Gene expression was measured for (A) collagen II, (B) aggrecan, (C) sox-9, and (D) collagen I, and mRNA is expressed as nmol per μg of total RNA (logarithmic scale for collagen I only). N=4 / condition, *P<0.05 with unloaded.

4.3.3 Pre-culture Time

Constructs were loaded for 3 hours following 1, 4, or 12 days of pre-culture in basal or chondrogenic media. There were no effects of loading after 1 day of pre-culture

(Fig 4.6). At day 4, cyclic tension significantly increased collagen II expression in the basal medium (Fig 4.6A) and inhibited collagen I expression in the chondrogenic medium (Fig 4.6D). Due to degradation of the fibrin, constructs cultured in basal medium could not be loaded at day 12. For BMSCs in the chondrogenic medium, cyclic tensile loading on day 12 significantly increased collagen I and II expression (Fig 4.6A,D) and had no effect on aggrecan or sox-9 expression (Fig 4.6B,C).

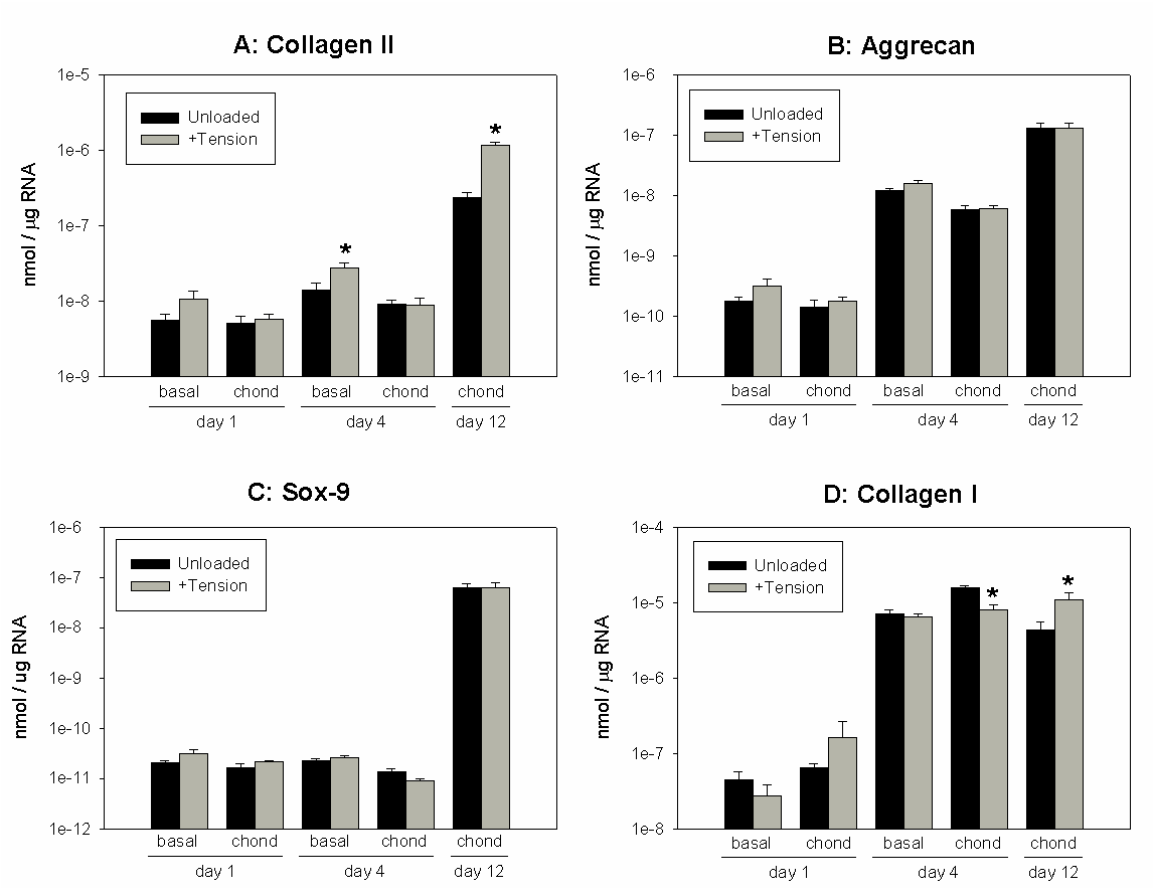

Figure 4.6: Effects of pre-culture on mRNA expression. Following 1, 4, or 12 days of pre-culture in basal or chondrogenic medium, the fibrin gels were loaded for 3h at 1Hz, 10% displacement, and gene expression was measured for (A) collagen II, (B) aggrecan, (C) sox-9, and (D) collagen I. Due to degradation of the fibrin, constructs in the basal medium could not be loaded at day 12. Levels of mRNA are expressed on a logarithmic scale as nmol per µg of total RNA. N=6 / condition, *P<0.05 with unloaded.

The 3 hour loading protocol was extended to 24 hours of intermittent loading to examine the effects of tensile loading on matrix synthesis. For this experiment, 0.1 TIU/ml of aprotinin was used instead of tranexamic acid to prevent fibrinolysis. As a result, there was little degradation of the constructs, and the basal group could be loaded at day 12. In preliminary studies, the addition of 0.1TIU/ml aprotinin did not alter the response of BMSCs to TGF-β1 and dexamethasone (not shown). At day 4, intermittent tensile loading significantly increased protein and PG synthesis for BMSCs in both basal and chondrogenic media (Fig 4.7A-B). At day 12, intermittent loading increased protein synthesis but not PG synthesis. There were no effects of loading on the total sGAG accumulation (Fig 4.7C), but tension did increase the DNA content for constructs in the chondrogenic medium (Fig 4.7D). Intermittent tensile loading did not appear to have an effect on BMSC morphology (not shown); however, variations in cell morphology could be observed throughout the constructs similar to the free-swelling conditions (Fig 4.4)

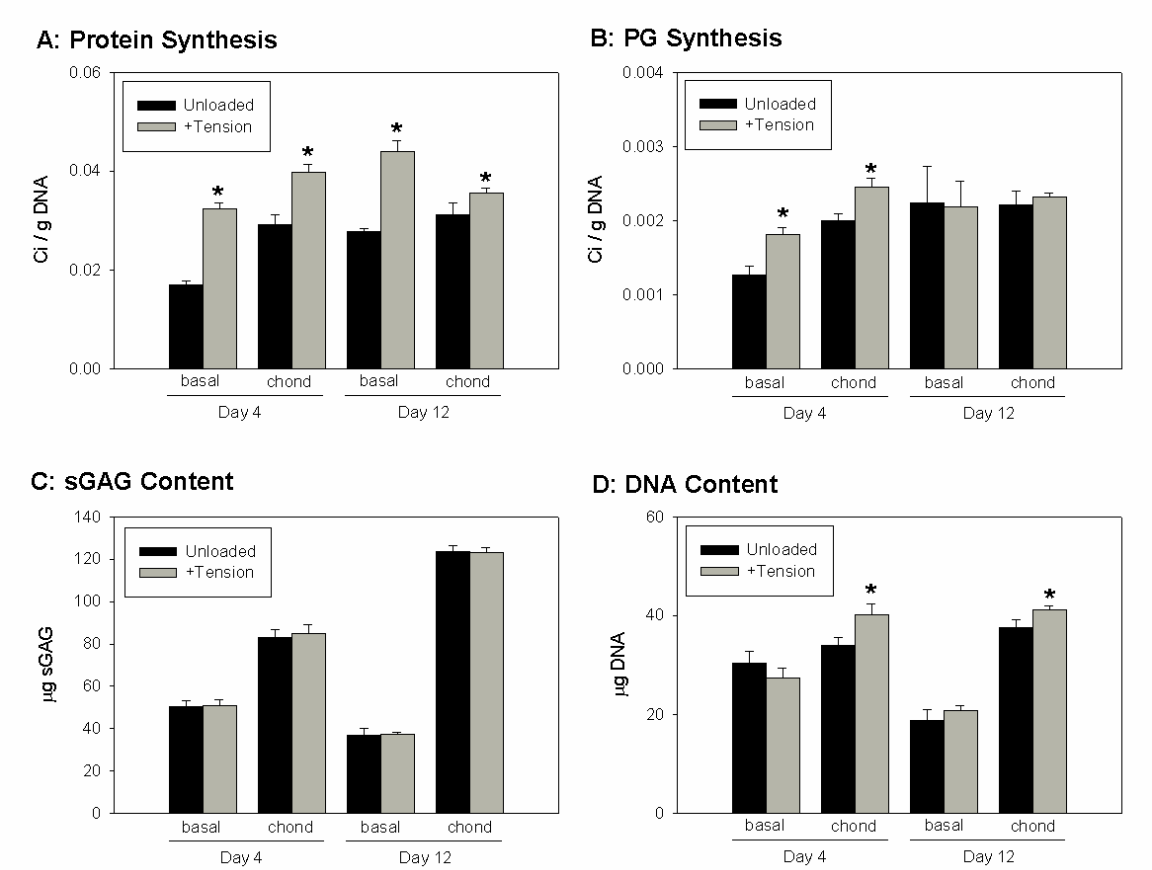

Figure 4.7: Matrix sysnthesis rates during intermittent loading. Constructs were cultured in basal or chondrogenic medium for 4 or 12 days and loaded intermittently (3h on – 3h off) for 24h. (A) Protein and (B) proteoglycan synthesis rates were measured during the 24h loading period by incorporation of 3H-proline and 35S-sulfate, respectively. Aprotinin was used as a fibrinolytic inhibitor in this experiment and prevented gel degradation through day 12. The total (C) sGAG and (D) DNA contents were also measured in the constructs. N=6 / condition, *P<0.05 with unloaded.

4.4 DISCUSSION

The first set of experiments in this study established a model for the chondrogenesis of bovine BMSCs in fibrin gel culture under unloaded conditions. Addition of the chondrogenic supplements, TGF-β1 and dexamethasone, inhibited early chondrocytic gene expression. This unexpected finding may have resulted from

interactions with the fibrin matrix, altering the response to TGF-β1 and dexamethasone[146]. Inhibition of chondrogenesis in fibrin has not been previously reported; however, other studies have only examined time points later than 7 days[141,147]. Despite this early inhibition, BMSCs in both media conditions increased expression of the chondrocytic genes during the first week of culture, suggesting that there was a basal level of chondrogenesis in fibrin. By day 12, BMSCs in the chondrogenic medium had a more intact fibrin matrix, expressed significantly higher levels of the chondrocytic genes, and had accumulated significantly more sGAG, indicating a higher level of differentiation and construct maturation than in the basal medium condition.

After establishing a time course for chondrogenesis in fibrin, the initial response to cyclic tensile loading was examined at day 4, prior to significant changes in gene expression or matrix accumulation. In this experiment, 3 hours of tensile loading specifically stimulated chondrocytic gene expression in the basal medium only, suggesting a possible interaction between TGF-β1 signaling and the mechanosensitivity of BMSCs. Previous studies in our laboratory have shown that dynamic compression of BMSCs in agarose gels increased chondrocytic gene expression and Smad2/3 phosphorylation in the presence of exogenous TGF-β1[96]. The lack of response to tensile loading for BMSCs in TGF-β1 supplemented medium may be a result of the impaired chondrocytic gene expression at this time point or fundamental differences in the response to tension and compression. Future studies directly comparing these different loading modes, as well as the role of TGF-β signaling in the response to cyclic tension, will help to elucidate the mechanisms of mechanotransduction by BMSCs.

Based on the temporal response to cyclic tension observed in the first loading experiment, the effects of short, 3hour loading periods were examined at various stages of differentiation and construct development. Although the effects of loading on collagen II were consistent with the loading duration experiment, increases in aggrecan and sox-9 expression were not significant in this particular experiment. Interestingly, the response to cyclic tension at day 12 was dramatically different than at earlier time points, with large increases in collagen expression and no effect on aggrecan or sox-9 for cells in the chondrogenic medium. The influences of intermittent loading on matrix synthesis rates were consistent with the changes in gene expression. At day 4, loading increased both chondrocytic gene expression and matrix synthesis, while at day 12, loading specifically increased collagen expression and protein synthesis. The distinct responses to cyclic tension at these time points may reflect fundamental differences in the mechanosensitivity of BMSCs at various stages of chondrogenesis. Epigenetic changes in gene regulation that occur during differentiation could potentially influence the sensitivity of the chondrocytic genes to mechanical stimuli. Alternatively, differences in the cells' microenvironments that result from accumulation of a newly synthesized ECM could influence the response to loading. Several studies have shown that adhesion to specific matrix proteins and integrin activation can modulate the effects of mechanical stretch[148,149]. Similarly, accumulation of proteoglycans can affect the availability of growth factors that may be released during deformational loading[150,151].

The specific increases in collagen gene expression and protein synthesis at day 12 provide initial evidence that the combination of chondrogenic medium (TGF-β1 and dexamethasone) with tensile loading may promote fibrochondrocyte-like differentiation.

To our knowledge, this study is the first report on the effects of cyclic tension on the chondrogenesis of bone marrow stromal cells. Previously, stretching of rat limb bud cells on a silicone membrane inhibited expression of collagen II but stimulated fibronectin expression[101], and other loading studies with adult mesenchymal progenitors in 2D[103] and 3D[102] culture have reported stimulation of collagen I gene expression but no effect on collagen II. While the effects of tension on collagen I expression were consistent with our day 12 data, the differences in collagen II expression may be related to the presence of the chondrogenic supplements TGF-β1 and dexamethasone. The potential interaction between growth factors and mechanical stimuli could be a useful strategy for guiding lineage specific differentiation and development of tissue constructs. Furthermore, engineering of tissues such as the meniscus may require graded levels of these stimuli in order to recapitulate the native heterogeneity and unique mechanical function of fibrocartilage.

CHAPTER 5

LONG-TERM TENSILE LOADING REGULATES BMSC DIFFERENTIATION AND CONSTRUCT DEVELOPMENT

5.1 INTRODUCTION

Fibrocartilage tissues, such as the meniscus of the knee, are susceptible to damage from traumatic injuries and have a limited capacity for regeneration. Unrepaired damage to the menisci can often lead to altered joint biomechanics[152] and the onset of osteoarthritis in the underlying articular cartilage[23]. Tissue engineering is a potential strategy for repairing fibrocartilage injuries; however, there are significant challenges for developing tissues with the appropriate composition and structure. Furthermore, the limited availability of autologous fibrochondrocytes presents additional obstacles for obtaining an appropriate cell source. Mesenchymal stem cells may be an alternative cell type for fibrocartilage tissue engineering, but it remains unclear what types or combinations of signals promote fibrochondrocyte-specific differentiation.

In addition to the menisci of the knee, fibrocartilage tissues can be found in the tempromandibular joint disk and at tendon and ligament insertion sites. These tissues are typically characterized by high levels of type I collagen[9], as well as the presence of sulfated proteoglycans[25]. Compared to articular cartilage, fibrocartilage has a higher collagen content (15-25% of wet mass)[9] and lower amounts of the large proteoglycan, aggrecan[2]. Consistent with the tissue composition, fibrochondrocytes express high levels of collagen I and less collagen II and aggrecan than articular chondrocytes[31]. Aside from these patterns of ECM expression, little is known about the fibrochondrocyte phenotype,

thereby creating challenges for evaluating fibrochondrocyte-specific differentiation. Recent studies in our laboratory have provided new insights into the unique responses of fibrochondrocytes to physical and biochemical stimuli[35,36] and identified distinct differences in aggrecan processing between fibrochondrocytes and articular chondrocytes[32]. These findings suggest that high levels of degraded aggrecan may be an additional marker for fibrocartilage tissues and indicator of fibrochondrocyte differentiation.

In vivo, fibrocartilage tissues experience a wide range of compressive, tensile, and shear forces, and the tissue's composition and structure is critical for its diverse mechanical functions. In the meniscus, for example, the osmotic swelling pressure associated with negatively charged proteoglycans allows the tissue to bear compressive forces, while large, circumferential collagen I fibers effectively withstand tensile hoop stresses during joint loading. These structure-function relationships suggest that mechanical forces may be important regulators of fibrocartilage development. In vitro, cyclic tensile loading has been shown to down-regulate proteoglycan synthesis of articular chondrocytes and induce changes in cytoskeletal organization[36]. In addition, cyclic stretching of ligament fibroblasts can stimulate collagen I expression and synthesis. Taken together, these findings provide initial evidence that tensile loading may be a useful strategy for promoting fibrous tissue development. Therefore, we hypothesized that the combination of tension with chondrogenic stimuli, such as TGF-β1 and dexamethsone, may direct fibrochondrocyte-specific differentiation of mesenchymal progenitors.

The studies in the previous chapter indicated that cyclic tensile loading can alter chondrogenic gene expression and matrix synthesis rates of bovine BMSCs. Following induction of chondrogenic gene expression, short periods of tensile loading stimulated collagen I and II expression and protein synthesis rates. The goal of the current study was to extend these loading periods and investigate the effects of long-term cyclic tension on fibrochondrocyte differentiation and the development of a fibrocartilage-like matrix. BMSCs in fibrin gels were allowed to differentiate under chondrogenic conditions for one week prior to loading. The fibrin constructs were then loaded intermittently for 1 or 2 weeks and analyzed for changes in collagen and proteoglycan accumulation. In addition, the patterns of aggrecan processing were compared to native tissues by western blot analysis, and the gene expression levels following loading were measured by real-time PCR. The results of this study demonstrate that the combination of chondrogenic stimuli and tensile forces promotes fibrochondrocyte-like differentiation of BMSCs and has the potential to direct development of a fibrocartilage tissue construct.

5.2 MATERIALS AND METHODS

5.2.1 Materials

Immature bovine hind limbs were from Research 87 (Marlborough, MA). Recombinant human TGF-β1 and basic-fibroblast growth factor (bFGF) were from Peprotech (Rocky Hill, NJ). Bovine fibrinogen, dexamethasone, aprotinin, 1,9 dimethyl methylene blue (DMMB), and Hoechst dye 33258 were from Sigma Aldrich (St. Louis, MO). The ITS+ premix and ProteinaseK were from BD Biosciences (San Jose, CA). Fetal bovine serum was from Hyclone (Logan, UT), and cell culture reagents, including

Dulbecco's Modified Eagles Medium (DMEM), antibiotic/antimycotic, trypsin, non-essential amino acids (NEAA), and phosphate buffered saline (PBS), were from Invitrogen (Carlsbad, CA). 4-12% gradient polyacrylamide gels and prestained standards were also from Invitrogen. The ECF substrate was from GE Healthcare (Piskataway, NJ), and the Protease Inhibitor Cocktail I was from Calbiochem (San Diego, CA).The RNeasy mini kit was from Qiagen (Valencia, CA), and the AMV reverse transcriptase kit was from Promega (Madison, WI). The SybrGreen master mix was from Applied Biosystems (Forest City, CA). The anti-aggrecan G1 and anti-aggrecan G3 antibodies were provided by John Sandy, Ph.D. (Chicago, IL) and the Alexafluor 488 anti-rabbit IgG was from Molecular Probes (Carlsbad, CA).

5.2.2 BMSC Isolation and Expansion

Bone marrow was harvested from the tibiae and femora of an immature calf and physically disrupted by passage through 50ml and 10ml serological pipettes, followed by 16, 18, and 20 gage needles. The marrow was then separated by centrifugation, and the fatty layer was removed. The remaining heterogeneous mixture was rinsed with PBS and pre-plated for 30 minutes to remove the rapidly adherent cells. The remaining cells were then re-plated at approximately 250,000 cells/cm^2 on tissue culture plastic and cultured in low-glucose DMEM with 1% antibiotic/antimycotic, 10% FBS, and 1ng/ml basic-FGF. After 3 days, the non-adherent cells were removed during the first media change. The remaining adherent BMSCs were expanded until nearly confluent, at which time they were trypsinized and replated at 6,000 cells/cm^2. Cells were expanded twice more to near-confluence before seeding in fibrin.

5.2.3 Fibrin gel seeding and culture

BMSCs were seeded into fibrin gels (50mg/ml) at a density of $10x10^6$ cells/ml by combining a fibrinogen/cell suspension in DMEM with bovine thombin (50U/ml final concentration) and casting the gels in rectangular molds between porous polyethylene end-blocks (Chapter 4, Fig. 4.1). Infiltration of the fibrinogen/cell suspension into the polyethylene prior to gelation fixed the gels to the endblocks and provided a rigid support for applying controlled tensile strains to the gels. Fibrin gel constructs were cultured in a chondrogenic medium consisting of high-glucose DMEM with ITS+ premix, NEAA, antibiotic/antimycotic, ascorbate, 0.1TIU/ml aprotinin, 5ng/ml TGF-β1 and 50nM dexamethasone. Media were collected and changed every 2 days.

5.2.4 Cyclic Tensile Loading

The fibrin constructs were cultured under free-swelling conditions for 7 days prior to loading, at which time they were randomly assigned to one of three loading conditions. The free-swelling (FS) constructs were placed in loading chambers and allowed to freely contract and swell over the course of the experiment. Another group was cultured in the loading chambers and held at the day 7 length of 1.4mm (0% displacement). Cyclic tensile strains were intermittently applied to the third group of constructs for up to two weeks using a custom loading system (Chapter 4, Fig 4.1). Sinusoidal displacements of 10% (peak-peak) were applied to the constructs at 1Hz for 1 hour, followed by 3 hours of recovery at 0% displacement, and repeated 6 times daily. Samples were taken after the initial 7 day preculture, and at days 14 and 21, following 7 and 14 days of loading,

respectively. One half of each construct was analyzed for matrix composition by western blot and biochemical analyses, and a slice from the central region was taken for histology. The remaining portions of the constructs were analyzed for gene expression by real time PCR. The length of the constructs under free-swelling conditions was also measured at days 7, 14, and 21.

5.2.5 Western Blot Analysis

Proteoglycans for western blot analysis were extracted from the fibrin gel constructs in 4M guanidine-HCl plus the protease inhibitor cocktail I overnight at 4ºC. Equal portions of the extracts or media samples were pooled (n=6/group) and precipitated in 100% ethanol plus 5mM sodium acetate overnight at -20ºC. The precipitated material was deglycosylated with chondroitinase ABC, keratinase I, and keratinase II for 4 hours at 37ºC in the presence of protease inhibitors. The extract material was then dried and resuspended in a reducing loading buffer. Equal portions of the extract or media samples (approximately 5µg) were separated by electrophoresis on 4-12% tris-glycine gradient gels and transferred to nitrocellulose membranes. The membranes were blocked overnight with 1% non-fat dry milk at 4ºC. The membranes were probed for one hour at room temperature with primary antibodies against the G1 or G3 domains of aggrecan. Secondary detection was performed with an anti-rabbit, alkaline phosphatase antibody. The membranes were developed with a fluorescent ECF substrate and imaged using a Fuji FLA3000 phospho-imager.

5.2.6 Construct Biochemistry

Following extraction, the remaining portion of the constructs were digested with Proteinase K at 60°C. The sGAG contents in the extracts and digests were measured using the DMMB assay[144], and the DNA contents were measured using the Hoechst dye assay[145]. In addition, portions of the extracts and digests were hydrolyzed in 6M HCl at 100ºC and the total collagen contents were measured using the pDAB and chloramines-T assay for hydroxyproline. All biochemical data were reported as the total amount per construct (extract plus digest).

5.2.7 Real Time RT-PCR

RNA was isolated from the fibrin gel constructs using the Tri-spin method[143]. Gels were immediately dissociated in lysis buffer plus 2-mercaptoethanol. RNA was extracted from the fibrin using the Trizol reagent and chloroform and precipitated with 100% isoproponol. The RNA was further purified using the Qiagen RNeasy kit according to the manufacturer's protocol. Total RNA (1µg) was reverse transcribed to cDNA using the AMV reverse transcriptase kit. Gene expression was measured by real-time RT-PCR using the SybrGreen master mix and custom primers for collagen II aggrecan, collagen I, and osteocalcin. The PCR reaction and detection was performed with the ABI Prism 7700 (Applied Biosystems, Forest City, CA).

5.2.8 Immunofluorescence staining and histology

Gel constructs were fixed in 10% neutral buffered formalin for 4h, rinsed in PBS, and dehydrated in 70% ethanol. Samples were subsequently embedded in paraffin and

sectioned at 4μm onto superfrost plus slides. Sections were deparaffinized and rehydrated in water. Sulfated-glycosaminoglycans were stained with Safranin-O. Protein was counter-stained with 0.2% Fast Green and cell nuclei were stained with hematoxylin. Additional sections were stained for collagen with Direct Red. For immunoflurescence staining, sections were de-glycosylated with 0.1U/ml chondroitinase ABC for 1h at room temperature and blocked with 5% BSA for 30min. Sections were then labeled with primary antibodies against aggrecan-G3 (1μg/ml) and a secondary solution with AlexaFluor 488 anti-rabbit IgG (1:100) and Hoechst dye (1:5000). Immunofluorescent slides were preserved with aqueous gel mount and imaged using a Zeiss Axiovert 200 fluorescent microscope.

5.2.9 Data Analysis

All data are presented as the mean ± SEM. Gene expression levels were transformed by a Box-Cox transformation for normality. Data were analyzed by a two factor general linear model with loading conditions and time point as factors. All pairwise comparisons were performed with Tukey's test. Significance was at $P < 0.05$.

5.3 RESULTS

5.3.1 ECM Accumulation and Organization

During the 7 day pre-culture under free-swelling conditions, BMSCs contracted the fibrin matrix by 30% to an average length of 13.87mm (Table 5.1). The 0% displacement group was held at this position for the remaining two weeks, and 1.4mm displacements (10% of day 7 length) were applied to the cyclic tension group. BMSCs in

the free-swelling group continued to contract the gels to 9.68mm and 8.75mm after 14 and 21 days, respectively (Table 5.1). By day 21, this contraction resulted in a 37.5% difference in the construct length for the 0% and +10% groups compared to free-swelling gels.

Table 5.1: Fibrin gel contraction and length differences compared to constrained gels, mean ± SEM, N=6

Day	FS Length (mm)	Contraction (%)	Δ w/ 0% (mm)	Δ w/ 0% (%)	Dynamic Disp (mm)	Dynamic Disp (%)
0	20	0	0	0	0	0
7	13.87±0.35	30.7±1.74	0.13±0.35	0.9±2.52	1.4	10
14	9.68±0.20	51.6±1.00	4.32±0.20	31.6±2.06	1.4	10
21	8.75±0.13	56.3±0.66	5.25±0.13	37.5±1.50	1.4	10

The DNA contents of the fibrin constructs did not significantly vary over the course of the 2 week loading period (Fig 5.1A). The 0% and +10% loading groups released significantly higher amounts of sGAG to the media (Fig 5.1B). After 7 days, cyclic tensile loading significantly increased the total sGAG content within the constructs compared to the FS (12.5% higher) and 0% (10.6%) conditions; however, this effect was lost after 14 days of loading, with no significant differences in sGAG content between any of the loading conditions (Fig 5.1C). Similarly, 7 days of cyclic tensile loading increased the collagen content over FS (33.7%) and 0% (19.0% higher), but not after 14 days of loading. Analysis of the combined sGAG release and day 21 contents indicated that there were no significant differences in the total sGAG produced between any of the groups (not shown).

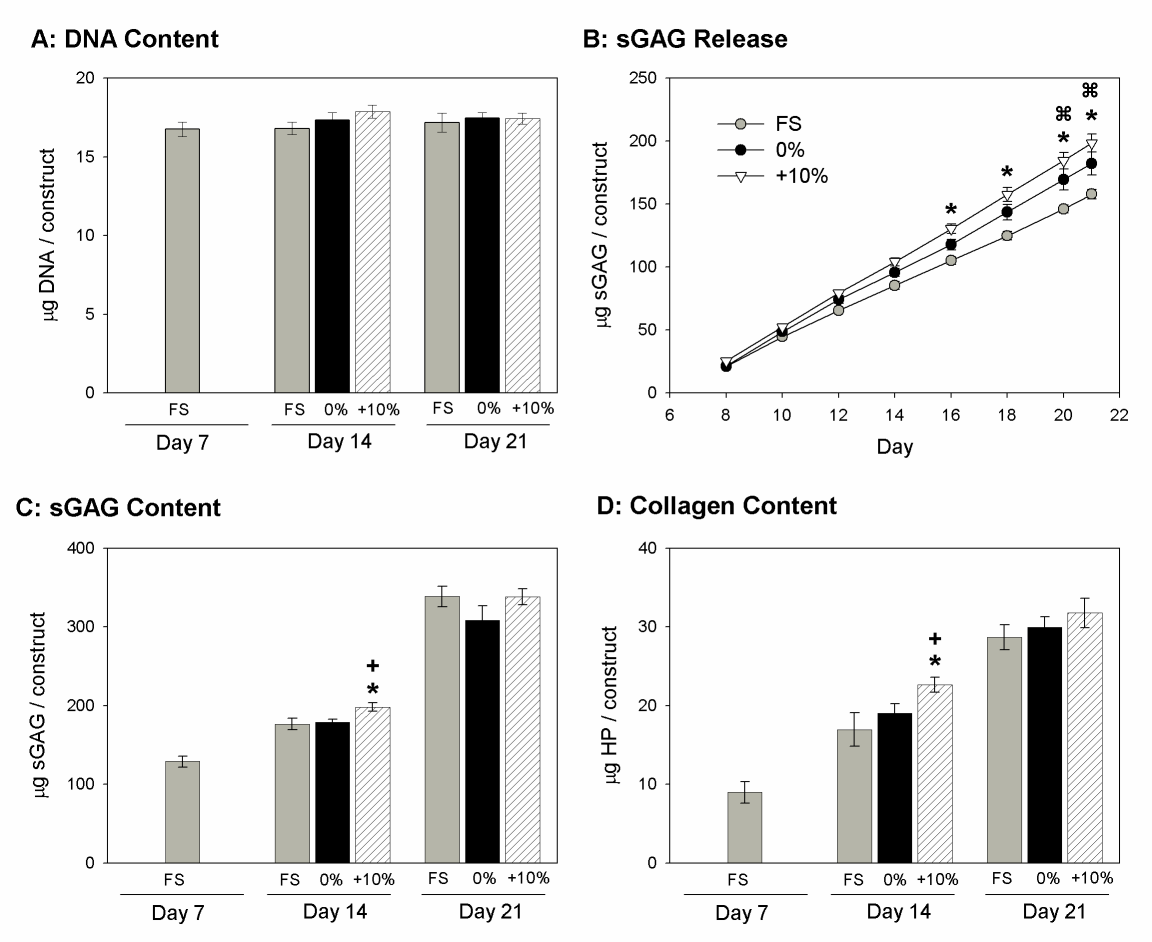

Figure 5.1: Construct biochemistry. Fibrin gel constructs were analyzed for (A) DNA, (C) sGAG, and (D) collagen contents following culture under free swelling conditions (FS), fixed at the day 7 length (0%), or cyclically loaded (+10%). (B) Conditioned media samples were analyzed for sGAG content and reported as the cumulative sGAG released. *P<0.05 for 10% vs, FS, +P<0.05 for 10% vs. 0%, ⌘P<0.05 for 0% vs. FS. N=6/group.

Safranin-O staining of day 21 sections indicated that the sulfated proteoglycans were localized to the pericellular matrix of cells at the periphery of the constructs (Fig 5.2A-C). Intense staining of the fibrin matrix could be seen with the Fast Green counter stain, and higher levels of protein were apparent within the center of the construct. Direct Red staining of day 14 transverse sections revealed distinct collagen fibers in the 0% and +10% constructs, and there appeared to be a preferential alignment with the loading

direction (Fig 5.2D-F). Transverse sections from day 21 constructs were not available for histological examination.

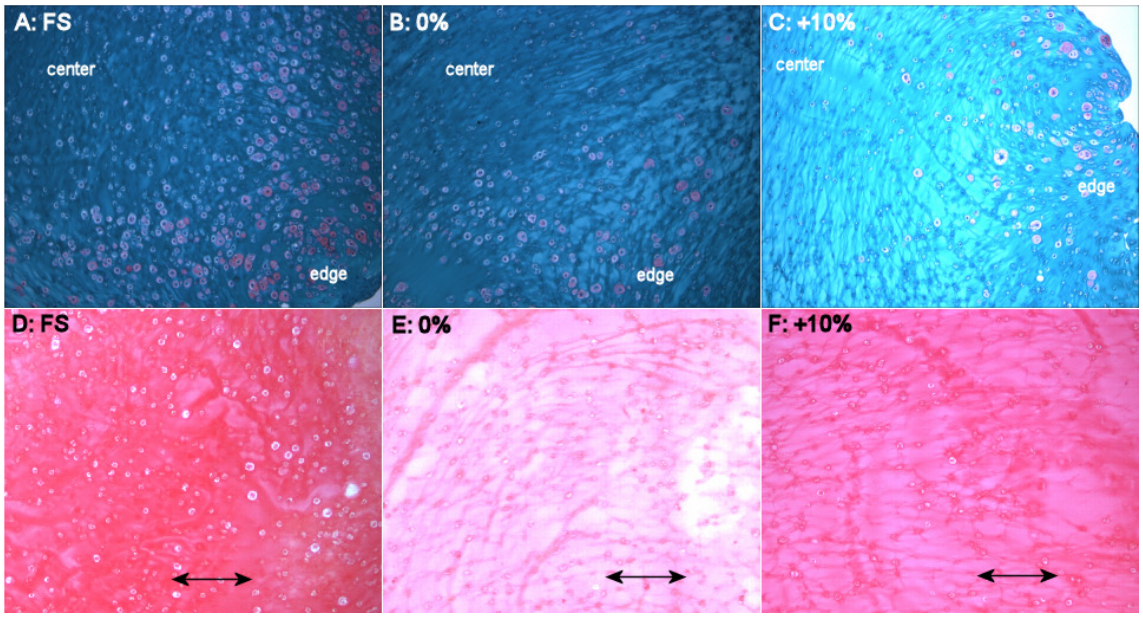

Figure 5.2: ECM organization. Portions of the fibrin gel constructs were formalin fixed, paraffin embedded, and sectioned to 5μm. (A-C) Cross-sections from day 21 constructs were stained for sGAG with Safranin-O and counterstained with Fast Green. (D-F) Transverse sections from day 14 samples were stained for collagen with Direct Red. Arrows indicate the long axis and loading direction of the constructs.

5.3.2 Aggrecan Production and Processing

Western blot analysis of the aggrecan-G1 domain from construct and tissue extracts displayed distinct patterns of aggrecan processing. The presence of full length aggrecan (450kDa) could be observed in both native tissues and the fibrin constructs, and the amount of aggrecan within the constructs appeared to increase with time in culture (Fig 5.3A). The primary form of processed aggrecan within the fibrin constructs was approximately 70kDa, characteristic of aggrecanase (ADAMTS-4/5) mediated cleavage[125], while multiple forms of processed aggrecan could be observed within native tissue. In addition, fibrocartilage (FC) extracts contained higher levels of degraded

aggrecan than articular cartilage (AC). Cyclic tensile loading appeared to increase the abundance of full-length aggrecan in day 21 constructs compared to the fixed 0% displacement, but there were no apparent differences in the abundance of degraded aggrecan between loading conditions.

Two major forms of G3 aggrecan could be observed at 55kDa and 140kDa in the conditioned media samples (Fig 5.3B). The release of these fragments was similar over the course of the experiment under free swelling conditions. However, much higher levels of these cleavage fragments were present in the day 20 media of the 0% and +10% groups. Consistent with these results, less G3 immunofluorescence was seen in sections from the 0% and +10% constructs compared to the free swelling group (Fig 5.3C).

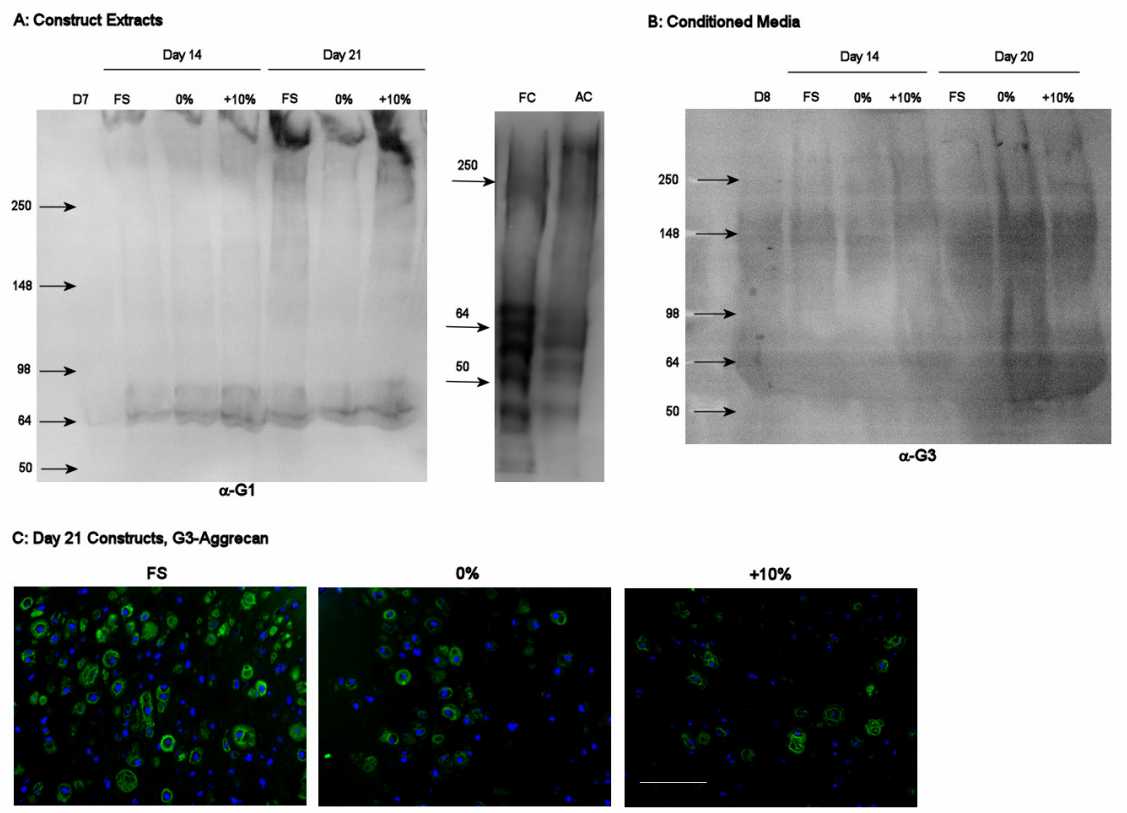

Figure 5.3: Aggrecan production and processing. (A) Extracts from the fibrin constructs and native fibrocartilage (FC) and articular cartilage (AC) were analyzed by western blotting for the aggrecan-G1 domain. (B) Conditioned media samples from days 8, 14, and 20 were analyzed for the aggrecan-G3 domain. (C) Day 21 constructs were examined by immunofluorescence staining for aggrecan-G3 (green) and DNA (blue). Scale bar = 100μm.

5.3.3 BMSC Gene Expression

Collagen II expression increased over the course of the experiment for all loading conditions (Fig 5.4A), and aggrecan expression increased from day 7 to 14 and did not change through day 21 (Fig 5.4B). There were no differences in chondrocytic gene expression between any of the loading conditions at days 14 and 21. Under free swelling conditions collagen I expression decreased from day 7 to 14 and did not change through day 21 (Fig 5.4C). Cyclic tensile loading significantly increased collagen I expression

over the free swell group at days 14 and 21. Osteocalcin expression remained low and near the detection limits of the real time PCR assay throughout the experiment (Fig 5.4D).

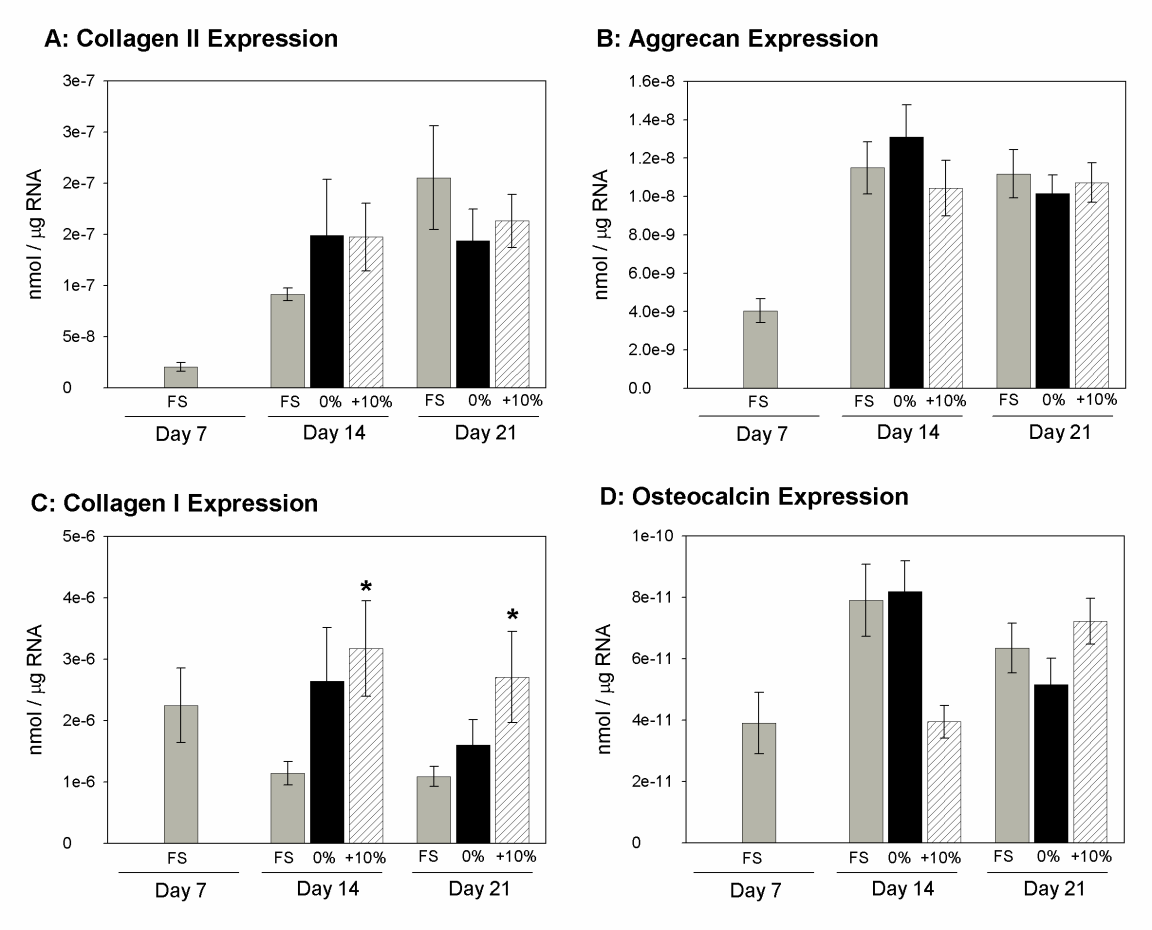

Figure 5.4: BMSC gene expression. The mRNA expression levels of (A) collagen II, (B) aggrecan, (C) collagen I, and (D) osteocalcin were measured by real-time RT-PCR. *P<0.05 for 10% vs. FS, N=6/group.

5.4 DISCUSSION

Successful engineering of fibrocartilage tissues requires the correct accumulation and organization of ECM components in order to achieve a functional tissue replacement. The objective of this study was to investigate the potential for combined tensile loading

and chondrogenic factors to promote fibrochondrocyte differentiation and fibrocartilage development. Consistent with the studies in the previous chapter, culturing BMSCs with TGF-β1 and dexamethasone increased chondrogenic gene expression and matrix synthesis over the course of the experiment, indicating that the cells were differentiating along a chondrogenic lineage. Following a 7 day pre-culture under free swelling conditions, intermittent cyclic tensile loading was applied to the constructs for 1 or 2 additional weeks. To account for BMSC contraction, control constructs were allowed to contract freely or held at the same 0% displacement as the cyclic loading condition. The results of this study indicate that the applied cyclic displacements and static forces generated by cell contraction in constrained constructs elicit distinct responses by BMSCs. While cyclic tension stimulated matrix production during the first week of loading, constraining the constructs increased sGAG release and aggrecan catabolism during the second week. These results provide insights into the potential for these loading modes to differentially regulate BMSC chondrogenesis, as well as their possible application in fibrocartilage engineering.

The tensile forces generated by BMSC contraction in the constrained constructs influenced both matrix organization and proteoglycan processing. As seen with the histological staining for sGAG and collagen, constructs in free-swelling culture had a denser, less organized matrix, while the constrained constructs appeared to have a higher degree of collagen alignment, specifically with the loading direction. The effects of static fixation on matrix organization were similar to other reports with tendon fibroblasts in collagen gels[153], and this strategy has been previously employed for promoting collagen fiber alignment in tissue constructs[153,154]. Based on these findings, static tensile forces

may play an important role in establishing collagen fiber orientation within fibrocartilage tissues like the meniscus or in engineering tissue substitutes with specific ECM orientations.

In addition to influencing matrix organization, constraining the constructs induced catabolic changes in proteoglycan processing. Constructs in the 0% and +10% loading groups released significantly more sGAG to the media compared to the free swelling constructs without changes in the total matrix produced, and western blot analysis of the day 20 media revealed higher apparent levels of the G3-aggrecan fragments in these groups. The lower levels of G3 aggrecan retained in the constrained gels provided further support of these results. The presence of the 140kDa G3 fragment in the media and the 70kDa G1 fragment in the extracts were characteristic of aggrecanase (ADAMTS-4/5) mediated cleavage[135,155], suggesting that aggrecanases are active within this system. Based on these results it appears that static tension upregulates the aggrecanase activity of BMSCs, which is at least partly responsible for the increased sGAG release to the media. Although there were also higher levels of the 55kDa G3 fragment in the media of constrained constructs, this fragment was most likely a product of C-terminal trimming by other proteolytic enzymes and not involved in sGAG release[123]. In addition to stimulating enzymatic cleavage, it is also possible that constraining the constructs inhibited the addition of chondroitin-sulfate chains to the aggrecan core protein as has been previously been reported in cartilage explants exposed to static compression[156].

When compared to the levels of aggrecan degradation observed in the native tissue extracts, the effects of static tension on matrix catabolism suggest that tensile

forces may promote fibrocartilage-like aggrecan processing within a developing tissue. Previous studies in our laboratory have also shown that tensile loading can upregulate the aggrecanase activity of articular chondrocytes after multiple weeks of loading[157]. In addition, distinct patterns of proteoglycan processing have been observed in meniscal[157] and tendon fibrocartilage[158], where higher levels of aggrecan degradation were found in regions experiencing greater tensile forces. Interestingly, static compression has also been reported to inhibit matrix synthesis in the meniscus[35] and increase gene expression of various proteolytic enzymes in intervertebral discs[159], meniscus explants[160], and articular cartilage[161]. Overall, this body of work provides strong evidence that static tensile and compressive forces induce primarily catabolic cellular responses, and this mechanism may be a potential strategy for guiding the formation of tissues with specific patterns of proteoglycan processing.

In contrast to the effects of static tension, cyclic tensile loading had a primarily stimulatory effect on matrix production and collagen I gene expression, consistent with the findings of the previous chapter and in other studies with mesenchymal progenitors[102,162]. Although cyclic tension increased sGAG and collagen accumulation after the first week of loading, these differences were lost after the second week. This response may be due to the high background levels of static tension in the 0% and +10% groups that obscured the stimulatory effects of dynamic loading. Other studies have reported suppressed catabolic responses to interleukin-1 in cyclically stretched chondrocytes and fibrochondrocytes[163], but there was little evidence of this effect in the present study. Alternatively, BMSCs may become less sensitive to mechanical stimuli at later time points due to matrix remodeling or stress shielding; however, the elevated

collagen I mRNA at day 21 suggests that the cells are still responsive to loading. Finally, the strong chondrogenic response to TGF-β1 and dexamethasone may also be the dominating factor regulating matrix synthesis at the later time points. Based on these findings, future studies are likely required to optimize the specific growth conditions and loading parameters for directing construct development during longer culture periods. Similarly, fibrin may not be an ideal material for fibrocartilage development, and the use other scaffolding materials such collagen, alginate, or synthetic polymers may provide for more control over cell adhesion, matrix contraction, and degradation rates.

Overall, the results of this study provide preliminary evidence that combinations of chondrogenic stimuli and tensile forces have the potential to encourage a fibrochondrocyte-like phenotype and development of a fibrocartilage matrix. These conclusions are based on comparisons of the specific changes in matrix production, aggrecan processing, and gene expression observed in this study with the known patterns in native fibrocartilage. As the understanding of fibrocartilage biology improves, so will our ability to evaluate fibrochondrocyte specific differentiation. Nevertheless, the findings in this study provide important insights into the mechanosensitivity of BMSCs to both static and dynamic tensile loading. The distinct responses to these loading modes may represent a potential mechanism for regulating the balance between matrix synthesis and degradation in vivo, and controlling the relative levels of static and dynamic forces in vitro could be an additional means for modulating the composition of engineered tissues.

CHAPTER 6

INHIBITION OF IN VITRO CHONDROGENESIS IN RGD-MODIFIED THREE-DIMENSIONAL ALGINATE GELS

6.1 INTRODUCTION

Mesenchymal progenitor cells are found in numerous tissues throughout the body[65,164,165] and aid in the repair and regeneration of damaged tissues[166]. Bone marrow stromal cells (BMSCs) include mesenchymal progenitors capable of differentiating into various lineages including bone, fat, muscle, and cartilage[66,77,78,115]. BMSCs can easily be cultured and expanded *in vitro*[78,167,168], making them a particularly attractive cell source for tissue engineering applications. Understanding of the specific signals involved in BMSC differentiation is critically important in engineering regenerative therapies that provide the appropriate cues for directing cell fate and tissue development. In addition, these cells provide a useful model system for studying normal regeneration and differentiation of mesenchymal lineages.

Members of the transforming growth factor beta (TGF-β) superfamily, including TGF-β1, TGF-β3, and several bone morphogenetic proteins, have been shown to regulate chondrogenesis during development[80,81] and promote differentiation of BMSCs *in vitro*[82,84,86,87,89]. When cultured in three dimensional environments such as pellet culture or hydrogels, TGF-β1 stimulates chondrogenesis of BMSCs as characterized by increased collagen type-II and proteoglycan synthesis[86,87]. Furthermore, the addition of dexamethasone, a synthetic glucocorticoid, has been shown to enhance TGF-β stimulated

differentiation[78,169]. TGF-β exerts its effects on cell activity by binding to the TGF-β receptor II and recruiting receptor I, which then phosphorylates its targets Smad2 and Smad3[170-172]. Activated Smad2 and Smad3 form a complex with Smad 4 and translocate to the nucleus where they interact with other factors to stimulate transcription of genes such as collagen type II[173,174]. TGF-β1 also functions through Smad-independent pathways, including the mitogen activated kinases ERK1/2, JNK, and p38[175], which have also been shown to play roles in chondrogenesis[175,176]. In addition to promoting chondrogenesis, TGF-β signaling is an important mediator of numerous other processes such as wound healing[177], tumor growth[178,179], and myoblast differentiation[110]. However, the precise mechanisms for regulating these varied responses to TGF-β are not completely understood.

Integrin adhesion to the extracellular matrix (ECM) provides key signals for directing cell function and has been shown to influence the response to TGF-β1. For example, TGF-β1 stimulation of myofibroblast differentiation requires cell adhesion and activation of focal adhesion kinase (FAK)[110]. Furthermore, the magnitude of this response is influenced by the specific type of ECM present, with the greatest stimulation on fibronectin-coated surfaces. Fibronectin and collagen can also differentially mediate the proliferative response to TGF-β1 through interactions between c-Src activation and cyclin expression[180]. In addition to the varied responses on different ECM surfaces, specific integrin receptors have been implicated in regulating the effects of TGF-β1. Dermal fibroblasts from β3 integrin-null mice display accelerated wound healing and enhanced TGF-β signaling[177]. Collectively, these studies demonstrate that integrin adhesion can regulate a wide variety of responses to TGF-β1. Within the context of

chondrogenesis, however, few studies have directly examined the role of cell-matrix interactions. Adhesion to fibronectin has been shown to be necessary for pre-cartilage condensation of chick limb bud cells[111], and the specific isoform of fibronectin present can influence the extent of chondrogenesis[112]. The presence of collagen type II has been shown to enhance TGF-β1 stimulated chondrogenesis of BMSCs[113,169] and chondrocyte matrix synthesis[181]. Although there are some data on the role of cell-matrix interactions in chondrogenesis, it is still relatively unclear how adhesion to specific matrix molecules coordinates with TGF-β and other growth factor signals to regulate the differentiation process.

The arginine-glycine-aspartic acid (RGD) sequence is a common adhesion motif in ECM proteins such as fibronectin, fibrin, and vitronectin[182], and numerous integrin receptors including αvβ3 and α5β1 bind directly to RGD (α5β1 binding requires the synergy site PHSRN in fibronectin)[183,184]. Synthetic, RGD-containing peptides have been incorporated into various biomaterials and tissue engineering scaffolds to promote cell adhesion and improve their biological activity[185]. Although synthetic peptides lack the complete specificity and function of native ECM proteins, they can easily be conjugated to other molecules and allow for greater control over ligand presentation. In addition to promoting cell adhesion, RGD peptides have been shown to influence other processes such as proliferation[186], migration[187], and differentiation[186,188]. For tissue engineering applications, the effects of RGD-modification on cell function may therefore be critical for the ultimate success of the construct.

The purpose of this study was to investigate the influence of integrin adhesion to the RGD motif on the chondrogenesis of BMSCs. Recently, alginate hydrogels modified

with synthetic RGD peptides have been shown to support myoblast differentiation[186] and chondrocyte adhesion[189], and BMSCs seeded in these gels have been employed for repairing bone fractures[190]. In the current study, RGD peptides were conjugated to sodium alginate to examine the response of bovine BMSCs to RGD-engineered three-dimensional (3D) hydrogels in the presence of TGF-β1 and dexamethasone. This system allowed for direct control of the ligand type and density and provided for a thorough investigation into how RGD specific interactions regulate the chondrogenesis of BMSCs.

6.2 MATERIALS AND METHODS

6.2.1 Materials

Low viscosity, high guluronic acid (LVG) sodium alginate was from FMC Biopolymer (Dammen, Norway). The custom peptides GGGGRGESY and GGGGRGDSY, and the soluble peptide GRGDSP were synthesized by Bachem (King of Prussia, PA). 1-ethyl-(diethylaminopropyl) carboiimide (EDC), N-hydroxy-sulfosuccinimide (sulfo-NHS), 2-(N-morpholino)ethanesulfonic acid (MES), dexamethasone, 1,9 dimethyl methylene blue (DMMB), and Hoechst dye 33258 were from Sigma Aldrich (St. Louis, MO). Immature bovine hind limbs were from Research 87 (Marlborough, MA). Recombinant human TGF-β1 and basic-fibroblast growth factor (bFGF) were from Peprotech (Rocky Hill, NJ). ^{35}S-sodium sulfate was from MP Biomedicals (Solon, OH) and the ITS+ premix and ProteinaseK were from BD Biosciences (San Jose, CA). Fetal bovine serum was from Hyclone (Logan, UT), and cell culture reagents, including Dulbecco's Modified Eagles Medium (DMEM), antibiotic/antimycotic, trypsin, non-essential amino acids (NEAA), and phosphate

buffered saline (PBS), were from Invitrogen (Carlsbad, CA). 4-12% gradient polyacrylamide gels were also from Invitrogen, and the micro-BCA protein quantification kit was from Pierce (Rockford, IL). The ECF substrate was from GE Healthcare (Piskataway, NJ), and the Protease Inhibitor Cocktail I was from Calbiochem (San Diego, CA). The RNeasy mini kit was from Qiagen (Valencia, CA), and the AMV reverse transcriptase kit was from Promega (Madison, WI). The SybrGreen master mix was from Applied Biosystems (Forest City, CA).

Blocking antibodies against the β1 (AIIB2) and α5 (BIIG2) subunits were from the University of Iowa Developmental Studies Hybridoma Bank (Iowa City, IA), and the anti-αvβ3 antibody (LM609) was from Chemicon (Temecula, CA). Anti-phospho-Smad2 and anti-Smad2/3 antibodies were from Cell Signaling Technologies (Danvers, MA). The biotinylated anti-rabbit IgG antibody and mouse IgG isotype control were both from Jackson Immunological Research (West Grove, PA), and the alkaline phosphatase-linked anti-biotin antibody was from Sigma Aldrich. Anti-collagen II, anti-fibronectin, FITC streptavidin, and FITC anti-rabbit antibodies were all from Abcam (Cambridge, MA). Alexafluor 594-conjugated phalloidin was from Molecular Probes (Eugene, OR).

6.2.2 RGD Conjugation

The synthetic peptides GGGGRGESY and GGGGRGDSY were conjugated to sodium alginate as previously described[191]. Briefly, EDC and sulfo-NHS were reacted with a 1% alginate solution in MES buffer (0.1M MES, 0.3M NaCl, pH 6.5) for 5 min to form a stable intermediate. The peptides were then added to the solution at 10mg/g alginate and allowed to react overnight at room temperature. The peptide modified

alginate was purified by dialysis (3500 MWCO), lyophilized, and reconstituted at 2%w/v in calcium-free PBS. Alginate solutions for cell culture were sterile filtered through 0.45μm filters. The reaction efficiency and final peptide concentration were estimated by conjugation of a biotinylated derivative of the RGD peptide (GRGDSC-biotin) and dot blotting with fluorescent streptavidin.

6.2.3 BMSC Isolation and Expansion

Bone marrow was harvested from the tibiae and femora of an immature calf and physically disrupted by passage through 50ml and 10ml serological pipettes, followed by 16, 18, and 20 gage needles. The marrow was then separated by centrifugation, and the fatty layer was removed. The remaining heterogeneous mixture was rinsed with PBS and pre-plated for 30 min to remove the rapidly adherent cells. The remaining cells were then re-plated at approximately 250,000 cells/cm^2 on tissue culture plastic and cultured in low-glucose DMEM, 1% antibiotic/antimycotic, 10% FBS, and 1ng/ml basic-FGF. After 3 days, the non-adherent cells were removed during the first media change. The remaining adherent BMSCs were expanded until nearly confluent, at which time they were trypsinized and replated at 6,000 cells/cm^2. Cells were expanded twice more to near-confluence before seeding on or in alginate. Consistent with previous reports[128], BMSCs isolated in this manner were positive for the cell surface markers CD29 and CD44 and negative for CD45 as determined by flow cytometry.

6.2.4 Alginate Gel and Surface Preparation

Alginate surfaces were created in the bottom of non-tissue culture treated 48-well plates. 200µl of 2% alginate was combined with 20µl of 100mM $CaCl_2$ in individual wells and allowed to cross-link for 45 min. The surfaces were then rinsed with PBS and seeded with 50,000 BMSCs per well. For the 3D gel constructs, BMSCs were suspended in sterile 2% alginate at $10x10^6$ cells/ml and cast into 6mmØ x 4.5mm cylindrical molds (~120µl). The gels were cross-linked by diffusing 100mM $CaCl_2$ through a nylon mesh over the top of the molds for 45 min. The alginate gels were removed from the molds, rinsed with PBS, and transferred to culture media.

6.2.5 Experimental Design

To verify that BMSCs specifically adhered to the RGD modified alginate, cells were seeded on surfaces made from unmodified, 1µM RGE, 0.1µM RGD, and 1µM RGD alginate and cultured in serum free medium (DMEM plus 1% ITS+). BMSC morphology was examined by light microscopy at times up to 24 h after seeding. Cell spreading was quantified by counting the number of spread and round cells in 6 randomly selected fields per condition. The influence of ligand density on cell spreading was examined after 24 h on unmodified, 0.1µM RGD, and 1µM RGD surfaces and in the presence of varying concentrations (0, 0.01, 0.1, and 1mM) of a soluble RGD peptide (GRGDSP) in the medium. The specific integrins involved in spreading were identified by seeding BMSCs on unmodified, 0.1µM RGD, and 1µM RGD surfaces and in the presence of 20µg/ml of mouse IgG or blocking antibodies against the $\beta1$, $\alpha5$, or $\alpha v\beta3$ integrins. Cell morphology was again examined 24 h after seeding.

The effects of RGD interactions on chondrogenesis were investigated in 3D alginate gels. BMSCs were seeded into 1μM RGE or 1μM RGD modified alginate gels and cultured up to 7 days in basal medium (DMEM, antibiotic/antimycotic, ITS+, NEAA, ascorbate) or chondrogenic medium (basal medium plus 10ng/ml TGF-β1 and 100nM dexamethasone). Gene expression, sulfated glycosaminoglycan (sGAG) content, and DNA content of the gels were measured at days 4 and 7, and cell morphology and collagen II deposition were examined at day 7. To investigate the effects of RGD density on chondrogenesis, varying ratios of RGE/RGD modified alginate were mixed while maintaining a total bulk peptide density of 1μM. BMSCs were seeded into 3D gels with effective bulk RGD densities of 0, 0.05, 0.1, 0.5, and 1μM and cultured for 7 days in basal or chondrogenic media with or without 0.1mM soluble RGD blocking peptide. The sGAG synthesis rates, total sGAG contents, and DNA contents were examined at the end of the culture period.

Since Smad2/3 activation is one of the primary signaling mechanisms for TGF-β stimulation of chondrogenesis, the effects of the RGD-modified alginate on this pathway were examined as a first step towards understanding the mechanism by which RGD interactions influence differentiation. A time course for initial Smad2 activation in 3D gel culture was first established by measuring the levels of phospho-Smad2 after 0.5, 1, 4, and 24 h in chondrogenic medium. Smad2 phosphorylation was then examined in 1μM RGE and RGD gels at 4 and 24 h after the addition of the chondrogenic medium (initial signaling response) and again at the end of the 7 day culture period. Smad2 activation was quantified as the relative band intensity of phospho-Smad2 to total Smad2.

The integrin blocking antibodies used to inhibit cell spreading were also employed to examine the role of these specific receptors in chondrogenesis. BMSCs were seeded into 1μM RGE and RGD alginate gels and cultured in basal medium plus mouse IgG (isotype control) or chondrogenic medium plus mouse IgG, anti-β1, anti-α5, or anti-αvβ3 antibodies. All antibodies were used at 20μg/ml, and the gels were examined for total sGAG and DNA contents after 6 days in culture. Additionally, the gels cultured in basal and chondrogenic media plus IgG were stained for fibronectin.

6.2.6 Real Time RT-PCR

BMSCs were released from the gels by dissociating the alginate in PBS plus 100mM EDTA and collected by centrifugation at 1500*g* for 5 min. Lysis buffer was added to the cell pellet, and total RNA was isolated using the Qiagen RNeasy kit according to the manufacturer's protocol. Total RNA (1μg) was reverse transcribed to cDNA using the AMV reverse transcriptase kit. Gene expression was measured by real-time RT-PCR using the SybrGreen master mix and custom primers for collagen II (X02420), aggrecan core protein (NM_173906), Sox-9 transcription factor (AF278703), collagen I (AB008683), fibronectin (K00800), osteocalcin (AY17787)[78], and PPAR-γ2 (NM_181024)[78]. The PCR reaction and detection was performed with the ABI Prism 7700 (Applied Biosystems, Forest City, CA).

6.2.7 Matrix Synthesis and DNA Content

During the final 24 h of culture, the radiolabeled precursor ^{35}S-sodium sulfate was included in the culture medium at 5μCi/ml to measure sGAG synthesis. At the end of the culture period, radiolabel incorporation was quenched with 4 sequential 30 min washes in PBS plus 0.8mM sodium sulfate at 4°C. The gels were weighed, lyophilized, reweighed and digested with Proteinase K and 100mM EDTA at 60°C. Radiolabel contents were measured using a liquid scintillation counter. The total sGAG contents were measured using the DMMB assay[144], and the DNA contents were measured using the Hoechst dye assay[145].

6.2.8 Immunofluorescence Staining for ECM Proteins

Portions of the alginate gels were fixed in 10% neutral buffered formalin for 20 min and stored in PBS at 4°C. The gels were blocked with 5% FBS and 1% Triton X100 for 30 min and labeled with either anti-collagen II or anti-fibronectin rabbit antibodies for 90 min at 37°C. The gels were rinsed thoroughly and stained with a solution containing Hoechst dye, Alexa Fluor 594-phalloidin, and a FITC-conjugated anti-rabbit IgG antibody for 90 min at 37°C. The gels were rinsed again and imaged using a laser scanning confocal microscope (LSM 510, Zeiss, Oberkochen, Germany).

6.2.9 Western Blot Analysis

The alginate gels were homogenized in cold lysis buffer containing 1% protease inhibitor cocktail and 2mM sodium orthvanadate and snap-frozen in liquid nitrogen. The samples were later concentrated with a Microcon 30kDa filter, and the total protein was

measured using the micro-BCA assay kit. Equal amounts of total protein (20μg) were loaded in each lane of a 4-12% gradient polyacrylamide gel and separated under reducing conditions. Protein was transferred to a nitrocellulose membrane and blocked overnight in 1% non-fat dry milk at 4°C. Membranes were probed with primary rabbit antibodies against phospho-Smad2 and Smad2/3, followed by a secondary incubation with biotinylated anti-rabbit IgG antibody and a tertiary incubation in alkaline phosphatase-conjugated anti-biotin antibody. Membranes were developed with the ECF substrate and analyzed using a Fuji Image Analyzer (Fuji, Tokyo, Japan). Protein levels were quantified by measuring the intensity of the phospho-Smad2 or total Smad2 bands in each lane and subtracting the background intensity.

6.2.10 Data Analysis

All data are presented as the mean ± SEM. The fractions of spread cells were transformed using an arcsine function, and gene expression levels were transformed by a Box-Cox transformation for normality. Data were analyzed by a two factor general linear model with RGD density/gel type and media conditions as factors. Dunnet's test was used to compare treatments with the blocking antibodies to the isotype control. All other pairwise comparisons were performed with Tukey's test. Significance was at $P < 0.05$.

6.3 RESULTS

6.3.1 BMSCs Adhere and Spread on RGD-Alginate Surfaces via β1 and αvβ3 Integrin Receptors

BMSCs seeded on the surfaces of unmodified or RGE-modified gels remained rounded and aggregated together (Fig 6.1A-B) while cells on RGD-modified alginate surfaces rapidly adhered and spread (Fig 6.1C-D). There was also greater spreading on the 1μM surfaces than on the 0.1μM surfaces. BMSCs reached nearly maximal spreading on RGD surfaces after 8 h, and there was virtually no spreading observed on unmodified alginate or RGE controls through 24 h (Fig 6.1E). Cell spreading was blocked by the soluble RGD peptide (GRGDSP) in the media in a dose dependent manner (Fig 6.1F). On surfaces presenting a low RGD density (0.1μM), 1mM and 0.1mM concentrations of the soluble RGD significantly decreased the percentage of spread cells after 24 h, while on surfaces presenting higher RGD (1μM) only 1mM soluble RGD significantly reduced spreading. Cell spreading was significantly reduced by the β1-specific antibody on the 0.1μM, but not on the 1.0μM surface (Fig 6.1G), and spreading was significantly reduced by the anti-αvβ3 antibody on both densities of RGD (Fig 6.1G). The anti-α5 antibody did not significantly affect cell spreading, as would be expected since α5β1 binding requires the fibronectin synergy site[183,192]. These results demonstrate that BMSCs specifically adhere to the RGD sequence of peptide-modified alginate gels, and adhesion involves both β1 and αvβ3 integrins.

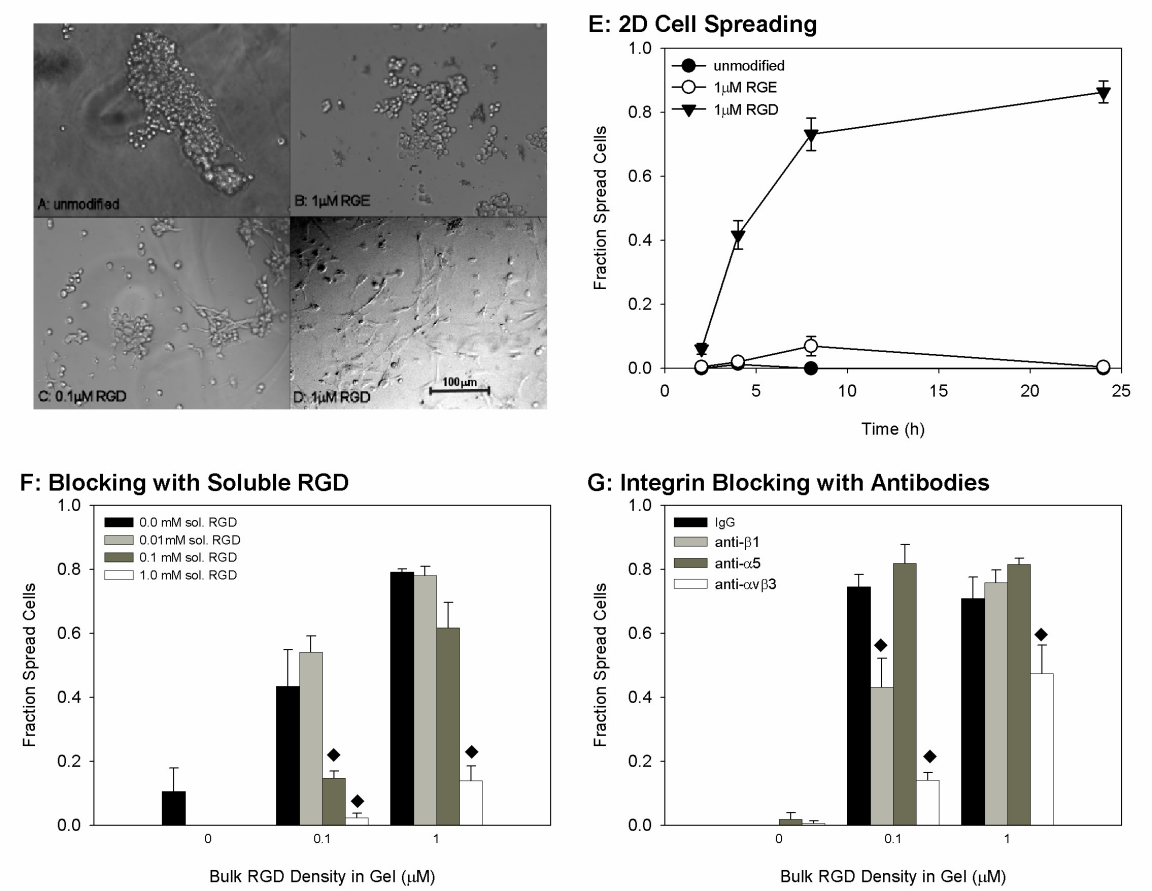

Figure 6.1: 2D cell spreading. BMSC morphology was examined on 2D surfaces of (A) unmodified, (B) RGE-modified, or (C-D) RGD-modified alginate after 8 h in serum-free DMEM. (E) The fraction of spread cells was quantified over a 24 h time course on various alginate surfaces. (F) The effect of ligand density on cell spreading was examined 24 h after seeding on RGD modified surfaces with bulk densities of 0, 0.1, and 1μM and in the presence of varying concentrations of a soluble RGD blocking peptide. (G) The roles of specific integrin receptors in cell spreading were examined after 24 h on various RGD-modified alginate surfaces and in the presence of 20μg/ml of integrin blocking antibodies (mouse IgG, anti-β1, anti-α5, and anti-αvβ3). N = 6 fields/group. ◆ P<0.05 relative to 0.0mM soluble RGD or IgG control.

6.3.2 RGD Interactions Inhibit Chondrogenesis in 3D Gel Culture

After 4 days in culture, there were no significant differences between any groups in mRNA expression levels of the chondrocytic genes collagen type II, aggrecan, and Sox-9 (Fig 6.2A-C). After 7 days in the non-adhesive RGE-modified gels, mRNA

expression of collagen II, aggrecan, and Sox-9 were significantly higher for cells cultured in chondrogenic medium compared to basal medium. However, chondrogenic medium did not significantly stimulate chondrocytic gene expression above basal levels for BMSCs cultured in the RGD-modified alginate gels. TGF-β receptor I expression was significantly higher in chondrogenic medium than in basal medium after both four and seven days, with no significant differences between the RGE and RGD gels (Fig 6.2D). Chondrogenic medium stimulated gene expression of collagen type I and fibronectin in both RGE- and RGD-modified alginate, with slightly lower expression levels in the RGD alginate at day 7 (Fig 6.3A-B). Chondrogenic medium did not stimulate expression of the osteogenic specific gene osteocalcin or the adipogenic specific gene PPAR-γ2 in either gel type (Fig 6.3C-D).

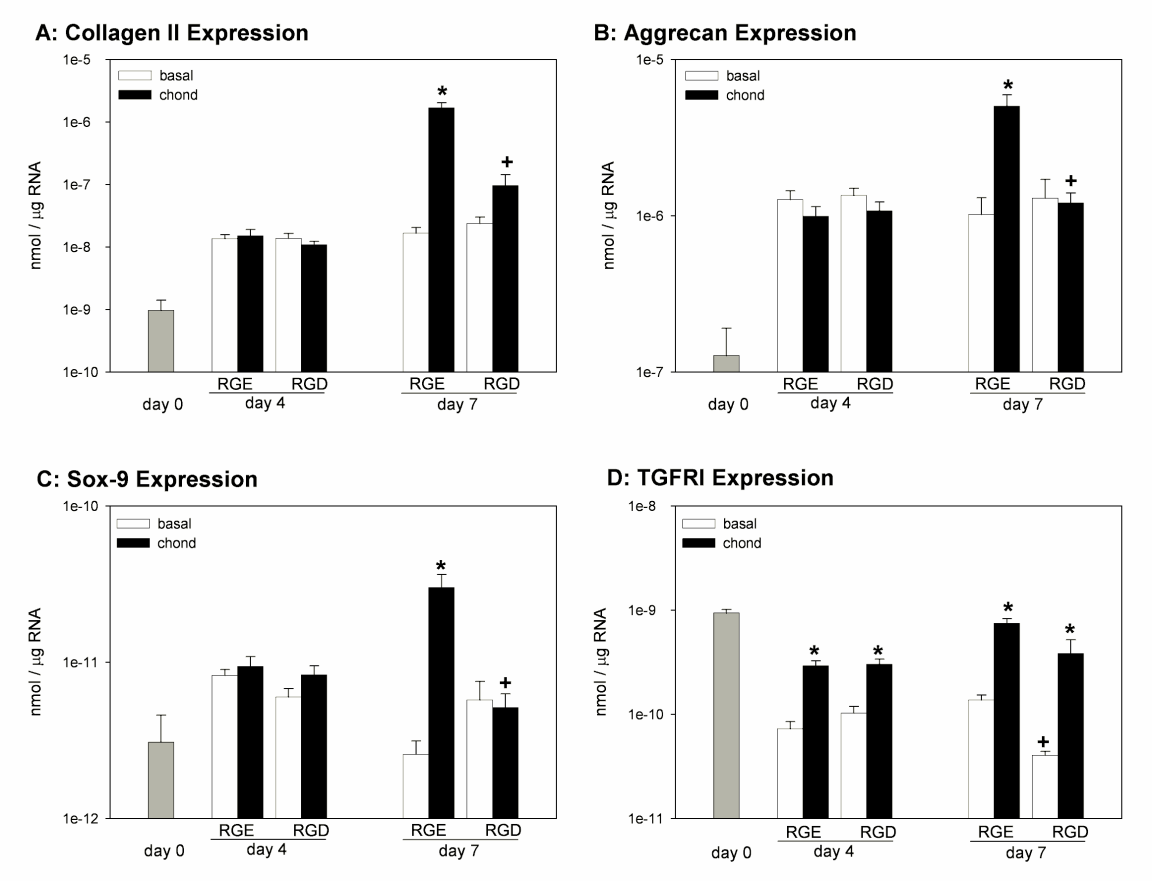

Figure 6.2: Chondrocytic gene expression. BMSCs were cultured in 3D RGE- or RGD-modified gels for up to 7 days in basal or chondrogenic medium. Gene expression was measured by real-time RT-PCR for (A) collagen II, (B) aggrecan, (C) Sox-9 transcription factor, and (D) TGF-β receptor I. Data are presented on logarithmic scales as nmoles of transcript per μg of total RNA. N=6 / group. * P<0.05 relative to basal. + P<0.05 relative to RGE.

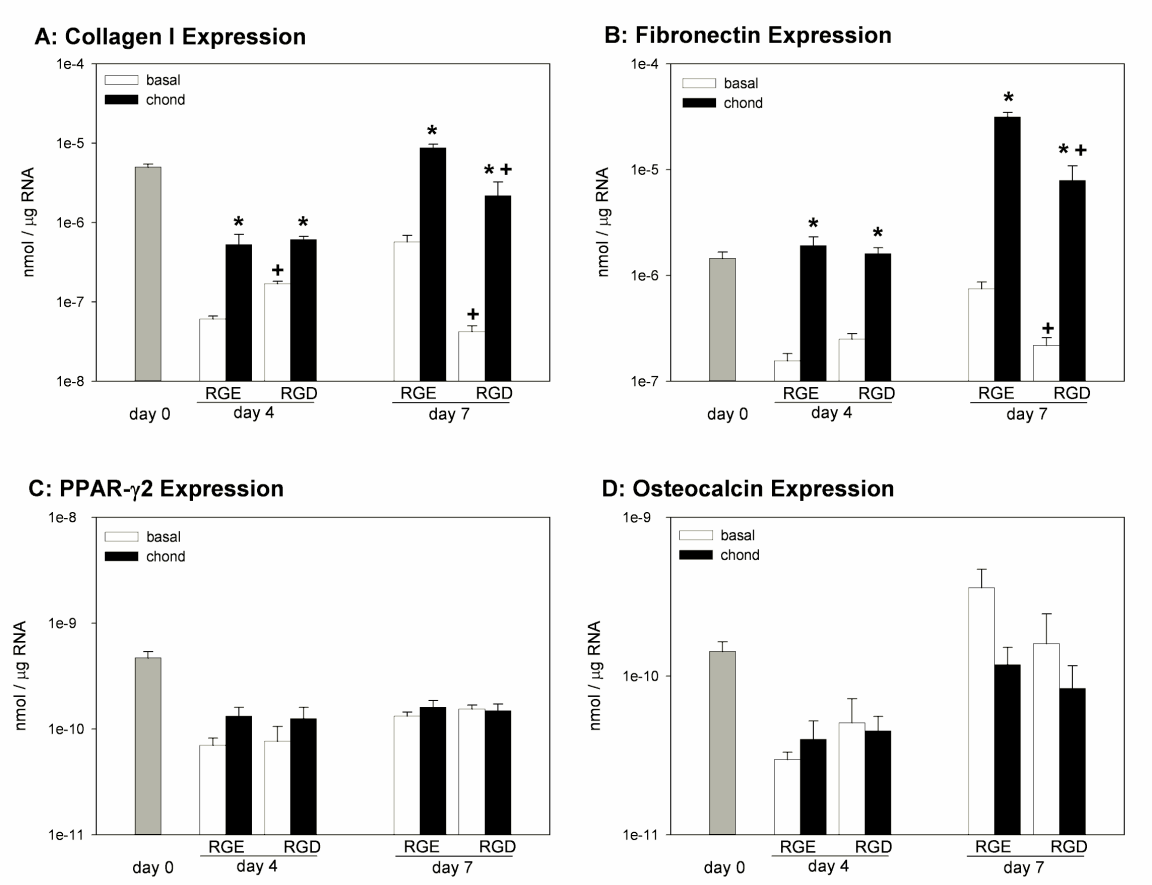

Figure 6.3: Non-specific and alternate lineage gene expression. Gene expression was measured via real-time RT-PCR for (A) collagen I, (B) fibronectin, (C) PPAR-γ2, and (D) osteocalcin. Data are presented on logarithmic scales as nmoles of transcript per μg of total RNA. N=6 / group. * P<0.05 relative to basal. + P<0.05 relative to RGE.

Similar to the effects on gene expression, the chondrogenic medium stimulated cartilaginous matrix synthesis in the RGE-modified gels, but this stimulation was inhibited in the RGD-modified gels. There were no differences in the sGAG contents between media condition or gel type at day 4. However, by day 7 the gels cultured in chondrogenic medium accumulated significantly more sGAG than in basal medium, and stimulation of sGAG production was inhibited in the RGD-modified alginate (Fig 6.4A). Immunofluorescence staining for collagen type II revealed intracellular expression under all conditions, but accumulation of pericellular collagen only in the RGE gels exposed to

chondrogenic medium (Fig 6.5). BMSCs encapsulated in the 3D hydrogels had a primarily rounded morphology (Fig 6.5), which is in stark contrast to the spread morphologies seen on 2D RGD-modified surfaces. Gels cultured in chondrogenic medium had significantly higher DNA contents at day 7 than those in basal medium, suggesting that the supplements TGF-β1 and dexamethasone promoted cell survival and/or proliferation. In addition, the RGD gels in chondrogenic medium had higher DNA contents than the RGE gels at days 4 and 7.

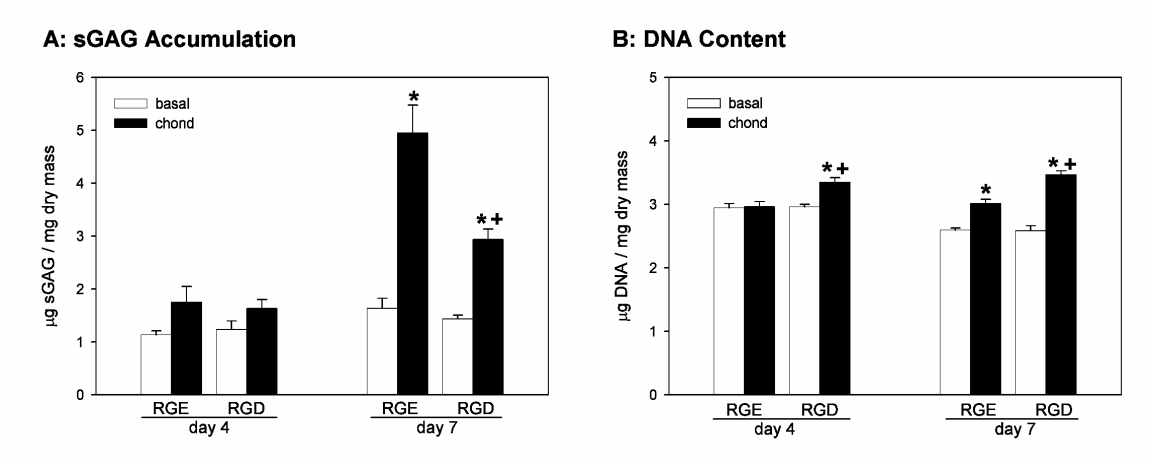

Figure 6.4: sGAG and DNA content. BMSCs were cultured in 3D RGE- or RGD-modified gels for up to 7 days in basal or chondrogenic medium. (A) Total sGAG accumulation and (B) DNA content. N=6 / group. * P<0.05 relative to basal. + P<0.05 relative to RGE.

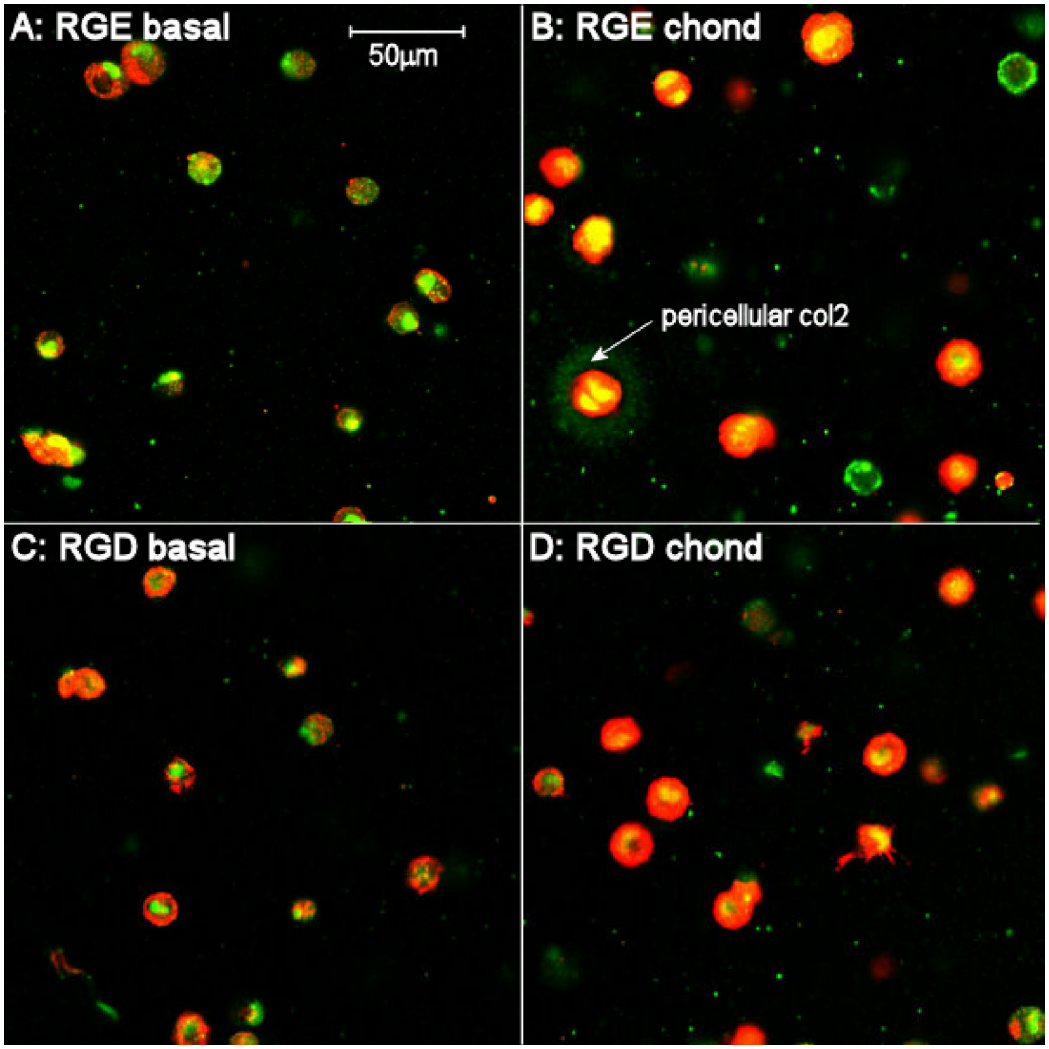

Figure 6.5: 3D morphology and collagen II synthesis. Representative confocal microcope images of (A-B) RGE- and (C-D) RGD-modified gels cultured for 7 days and stained for the F-actin cytoskeleton (red) and collagen II (green).

6.3.3 RGD Density Modulates the Inhibition of Chondrogenesis

To quantify the effects of RGD density on chondrogenic differentiation, BMSCs were seeded into varying ratios of RGE/RGD modified alginate with effective RGD densities ranging from 0-1μM. After 7 days in culture, chondrogenic medium stimulated ^{35}S-sulfate incorporation (indicative of the sGAG synthesis rate) and total sGAG accumulation (Fig 6.6A-B). This response was inhibited in a dose dependent manner by

increasing densities of RGD conjugated to the alginate. The presence of 0.1mM RGD in the media induced partial recovery of sGAG synthesis and accumulation in the gels with the highest RGD densities (0.5 and 1.0μM). In this particular experiment, the chondrogenic medium again increased the DNA content over basal medium, but there were no significant differences among the various RGD densities (Fig 6.6C).

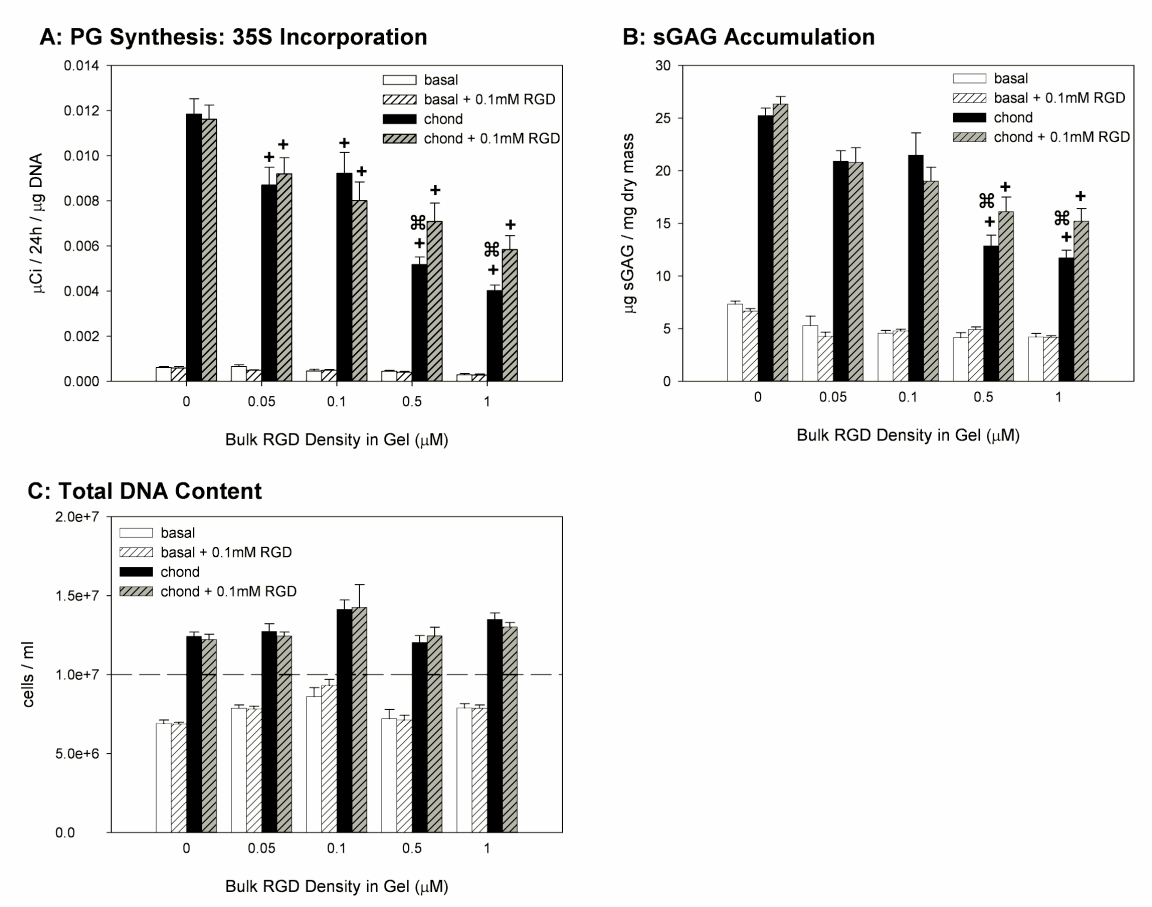

Figure 6.6: RGD density effects on chondrogenesis. The effective bulk RGD density in the gel was varied by mixing different ratios of RGE/RGD modified alginate prior to seeding. The gels were cultured in basal or chondrogenic media with or without 0.1mM soluble RGD blocking peptide. (A) sGAG synthesis rates on the 7th day of culture and (B) total sGAG accumulation and (C) DNA content after 7 days. N=6 / group. + P<0.05 relative to 0μM RGD gels. ⌘ P<0.05 relative to 0.1μM RGD gels.

6.3.4 RGD Interactions Inhibit Chondrogenesis Independently of Smad2 Phosphorylation

The addition of TGF-β1 and dexamethasone stimulated Smad2 phosphorylation over basal medium, with the highest apparent activation at 4 h (Fig 6.7A). At this time point, there were no significant differences in Smad2 phosphorylation between cells in the RGE and RGD gels (Fig 6.7B). Additionally, stimulation of Smad2 phosphorylation was maintained through 24 h and decreased somewhat after 7 days in culture, with no significant differences between RGE-and RGD-modified gels.

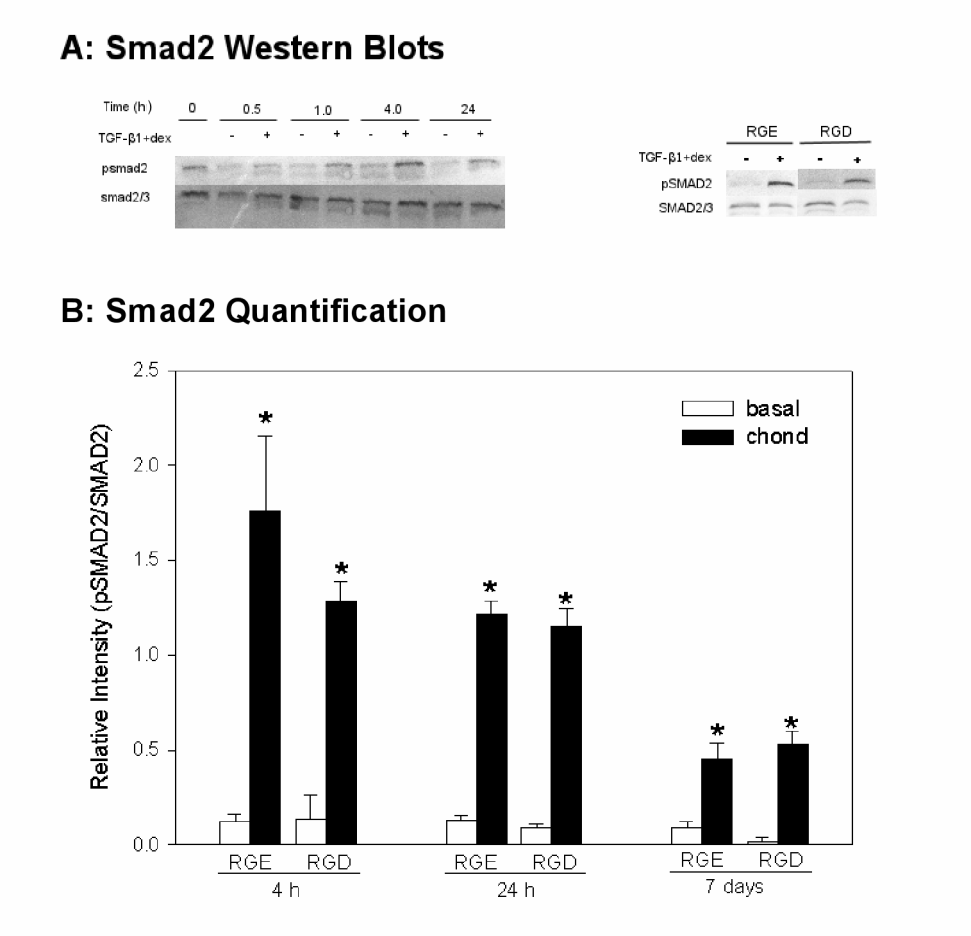

Figure 6.7: Smad2 phosphorylation. The effects of RGD interactions on TGF-β/Smad signaling were examined by western blot analysis of Smad2 phosphorylation. (A) Time course for Smad2 activation in the RGE-modified gels following introduction of the chondrogenic supplements. (B) Initial (4 and 24 h) and final (7 days) levels of Smad2 phosphorylation were quantified by the band intensity of phospho-Smad2 relative to total Smad2. N = 4-5 bands / group. * $P<0.05$ relative to basal.

6.3.5 Integrins α5 and β1 Regulate Chondrogenesis of BMSCs

In the RGE-modified gels, stimulation of sGAG accumulation by chondrogenic medium was significantly inhibited by the anti-α5 antibody but not by the anti-β1 or anti-αvβ3 antibodies. Similar to previous experiments, stimulation of sGAG synthesis by the chondrogenic medium was inhibited in the RGD-modified gels. The addition of the β1

and α5 blocking antibodies further inhibited sGAG accumulation, but the anti-αvβ3 antibody had no effect. Although these results do not identify a specific receptor involved in RGD inhibition of chondrogenesis, they do implicate α5 and potentially β1 as important mediators of chondrogenesis. The integrin specific antibodies did not significantly affect the DNA content after 6 days (Fig 6.8B) or cell viability after 48 h (not shown), suggesting that the effects on sGAG production were not a result of a decrease in the number of viable cells. Since α5β1 primarily binds to fibronectin, expression was examined by immunofluorescence staining (Fig 6.8C). BMSCs synthesized pericellular fibronectin in both basal and chondrogenic media conditions, and consistent with the gene expression (Fig 6.3B), there was more intense staining in the chondrogenic groups. There were no visible differences between RGE and RGD gels.

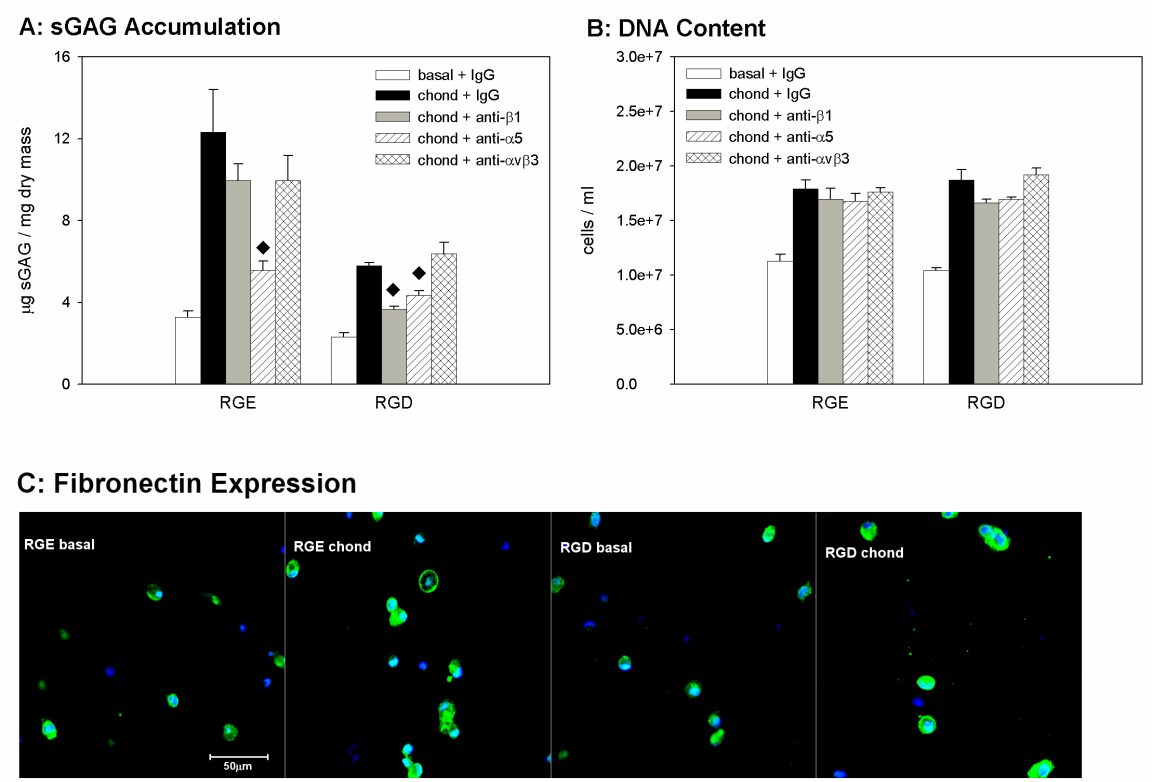

Figure 6.8: Functional blocking of integrin receptors. To investigate the role of specific integrin receptors involved in RGD inhibition of chondrogenesis, BMSC/alginate gels were cultured in basal medium plus 20µg/ml IgG or chondrogenic medium plus 20µg/ml IgG, anti-β1, anti-α5, or anti-αvβ3 antibodies. (A) Total sGAG accumulation and (B) DNA content after 6 days in culture. N = 4. ◆ P<0.05 relative to chond IgG. (C) Confocal microcope images of gels cultured in basal or chondrogenic media with the isotype control and stained for fibronectin (green) and DNA (blue).

6.4 DISCUSSION

The goal of this study was to investigate the effects of RGD interactions on the chondrogenic differentiation of BMSCs in 3D gel culture. Synthetic peptides were conjugated to sodium alginate using a previously established technique, allowing direct control of the ligand type and density presented to the cells. Similar to previous studies, BMSCs adhered and spread on RGD-modified 2D surfaces via integrin receptors[185,189]. The effects of the conjugated RGD peptide on chondrogenesis were then examined in 3D

gel culture. Interactions with RGD significantly inhibited the chondrogenic response to TGF-β1 and dexamethasone in terms of gene expression and matrix synthesis. This inhibition increased with increasing bulk densities of RGD in the gel and was partially rescued by inclusion of an RGD blocking peptide in the media. The mechanism by which RGD inhibits chondrogenesis appears to be independent of Smad2/3 phosphorylation as no differences in Smad2/3 phosphorylation were observed between RGD- and RGE-modified gels.

Interactions with biomaterials play an important role in regulating cell function and matrix accumulation within tissue engineered constructs. For both mature and differentiating cell types, alginate hydrogels have been shown to support the chondrocytic phenotype[56,69,87,89], characterized by round cell morphologies and expression of cartilage matrix molecules. In addition to alginate, other types of scaffolds, such as agarose, poly(glycolic acid), fibrin, and collagen gels have all been used to culture articular chondrocytes[56,99,193] or promote the chondrogenesis of progenitor cells[36,141,194]. However, few studies have directly compared the effects of these materials on chondrocyte and progenitor cell activity. In one report, chondrocytes cultured in agarose accumulated more total proteoglycans and had sulfation patterns more similar to articular cartilage than alginate, collagen, or PGA constructs[56]. In addition, adipose-derived stem cells proliferated more in gelatin matrices than in agarose or alginate, but accumulated similar amounts of sGAG per cell[194]. Although many of these materials support some level of chondrogenesis, development of functional tissue-engineered cartilage may require more rationally designed and optimized biomaterials.

Incorporation of synthetic peptides and adhesive proteins into biomaterials is a potential strategy for regulating cell function. Specifically, the RGD-modified alginate system has been shown to support myoblast differentiation on 2D surfaces[186,191] and osteoblast differentiation in 3D gel culture[195,196]. While some studies have conjugated RGD peptides to materials such as poly(lactic-co-glycolic acid) (PLGA)[197], poly(ethylene glycol) (PEG)[188,195], and alginate[186,188] to promote chondrocyte and progenitor cell adhesion, few have examined the effects on chondrogenesis or the chondrocytic phenotype. In one report, RGD-modified alginate inhibited sGAG synthesis of bovine articular chondrocytes[198]. Similarly, RGD modification of silk protein scaffolds enhanced initial BMSC adhesion and retention, but the RGD peptide had no effect on sGAG accumulation and slightly inhibited collagen II gene expression after four weeks in culture[199]. Together, these results are consistent with our findings that RGD interactions can significantly inhibit BMSC chondrogenesis within the first week of exposure to chondrogenic stimuli.

The inhibitory effect of RGD had the greatest influence on expression of the chondrocytic genes, completely blocking stimulation of collagen II, aggrecan, and Sox-9 by chondrogenic medium. Although interactions with RGD slightly lowered the overall level of collagen I and fibronectin, the chondrogenic medium stimulated a greater fold increase over basal medium in the RGD-modified gels than in the RGE-modified gels. Interestingly, neither the chondrogenic medium nor RGD presentation affected expression of the adipogenic or osteogenic specific markers, suggesting that the BMSCs were specifically differentiating along a chondrogenic pathway and that adhesion to the RGD peptide did not promote differentiation towards one of these alternate lineages. In

this study, the chondrogenic medium significantly increased cell proliferation, and the RGD peptide did not consistently affect this response. However, other studies have reported increased proliferation on RGD-modified surfaces and scaffolds[186]. This discrepancy may be due to differences in the ability of BMSCs to proliferate on 2D surfaces versus within a 3D hydrogel. In addition, the strong stimulatory effect of TGF-β1 may have overwhelmed any effects of the RGD on proliferation. An initial investigation into the mechanism by which RGD interactions inhibit chondrogenesis revealed that there was no effect on Smad2 phosphorylation or gene expression of the TGFβ receptor I. These results suggest that the effects of the RGD are acting downstream of Smad phosphorylation or through Smad independent pathways (e.g. MAP kinases or PKC). Future studies will further examine the role of these pathways, as well as signaling through integrin associated molecules, such as FAK, ILK, and Src.

We propose that integrin binding and signaling are responsible for the inhibitory effects of RGD on chondrogenesis. On 2D surfaces, BMSC spreading could be blocked by a soluble RGD peptide or integrin blocking antibodies in the media, thereby demonstrating that BMSCs directly adhere to the RGD peptide via integrin receptors. In 3D culture, the soluble RGD peptide had no effect on sGAG synthesis in the 0μM RGD gels and partially recovered sGAG synthesis for cells in the gels with the highest RGD densities. Taken together, these results indicate that the signal transduced by RGD binding requires tethering of the ligand to the alginate matrix and that adhesion to RGD appears to have a direct effect on cell activity, as opposed to simply blocking normal cell-matrix interactions. The functional blocking antibodies that inhibited cell spreading in 2D (anti-β1 and anti-αvβ3) did not recover the inhibitory effects of RGD on sGAG

synthesis in 3D. Conversely, the β1 antibody further inhibited sGAG production in the RGD gels, and the αvβ3 had no effect. Since numerous integrin receptors recognize the RGD motif, it is possible that other integrins may be responsible for the inhibitory effect on chondrogenesis. Other studies have also demonstrated that specific receptors, such as αvβ3, can play distinct roles in adhesion and spreading while other integrins, such as α5β1, are more important for differentiation[108,200]. The differential effect of the anti-β1 antibody in the two gel types may have been a result of the antibody blocking multiple β1 dimers in the RGE gels but more specifically targeting the α5β1 receptor in the RGD gels. Interestingly, α5β1 has recently been reported to negatively correlate with re-differentiation of passaged chondrocytes[201], suggesting that the regulation of chondrogenesis by specific receptors may also vary between cell types or stage of differentiation. It is important to note that although the concentration of 20μg/ml of anti-αvβ3 significantly inhibited cell spreading in 2D, this concentration was not saturating and may not have been high enough to out-compete the RGD ligand in 3D.

In addition to the bulk ligand density, the spatial organization of the RGD peptide may play an important role in regulating cell function. Integrin clustering has been reported to be necessary for the formation of focal complexes[202] and recruitment of integrin-associated signaling molecules[107]. On 2D surfaces, patterning of RGD ligands in clusters increased cell motility over more uniform distributions[187], and the formation of RGD islands in 3D alginate gels stimulated osteoblast differentiation to a greater extent than a uniform ligand distribution with the same bulk density[196]. Adhesion to uniformly distributed RGD peptides in the alginate gel may prevent integrin clustering and signaling, and thereby inhibit the response to TGF-β1 and dexamethasone. It is

important to note, however, that based on the molecular weight of LVG alginate and degree of RGD substitution, previous models would estimate the ligand spacing for a 1μM bulk density to be approximately 50-100nm[203], which is similar to previously reported spacings required for cell spreading and focal adhesion formation[202]. Although dramatic cell spreading was observed on 2D surfaces, encapsulation of the BMSCs in the 3D gel resulted in primarily rounded morphologies and potentially altered the presentation of the RGD ligands, either of which may have subsequently influenced differentiation. Future studies should therefore carefully examine the role of ligand organization and integrin clustering in regulating the response to RGD, particularly in a 3D environment.

While RGD adhesion in a 3D alginate gel appears to inhibit chondrogenesis, adhesion to other ligands may be critical for differentiation. We found that the chondrogenic medium stimulated fibronectin gene expression and synthesis. In addition, the anti-α5 antibody significantly inhibited sGAG accumulation in both RGE and RGD gels. Given that the α5β1 integrin receptor specifically binds to fibronectin, these results and others[111,112], provide a strong indication that α5β1 adhesion to fibronectin is important for *in vitro* chondrogenesis of BMSCs. In the context of tissue engineering, it may therefore be possible to enhance chondrogenesis by designing scaffolds that incorporate native fibronectin or mimic its ability to engage α5β1 integrins[200]. Alternatively, the combination of various biomimetic peptides may be a useful strategy for engineering tissues with heterogeneous cell populations or retaining a sub-population of undifferentiated progenitors. Overall, these results demonstrate the strength and specificity with which cell-matrix interactions can regulate chondrogenesis and

emphasize the importance of designing appropriate scaffolds and biomaterials for tissue engineering applications.

CHAPTER 7

INTERACTIONS BETWEEN INTEGRIN LIGAND DENSITY AND CYTOSKELETAL ORGANIZATION REGULATE BMSC CHONDROGENESIS

7.1 INTRODUCTION

Cell shape is closely linked to the phenotype of mature articular chondrocytes, which display primarily rounded morphologies in vivo. During in vitro culture however, chondrocytes will readily adhere and spread on 2D surfaces. These changes in morphology are associated with a gradual loss of collagen type II and proteoglycan synthesis[204]. Disruption of the f-actin cytoskeleton with cytochalasin D is known to inhibit this dedifferentiation process[205], while culturing chondrocytes in 3D hydrogels preserves their rounded morphology and chondrocytic phenotype[22]. Although cell morphology is an important regulator of the mature chondrocyte, the role of cytoskeletal organization in the chondrogenesis of mesenchymal progenitors is less clear. The use of chemical inhibitors to block actin polymerization or actin-myosin contractility have yielded differing responses depending on the cell types and culture conditions examined[206-208], suggesting that cell morphology and cytoskeletal organization play complex and regulated roles in the process of chondrogenesis.

Integrin adhesion to the extracellular matrix provides anchorage for the cell and a direct link between the f-actin cytoskeleton and the surrounding environment. Upon binding with their ligands, integrin receptors can cluster and form focal complexes[104,187],

which directly connect to f-actin filaments through the scaffolding proteins vinculin and talin[106]. In this manner, cell adhesion to the ECM can direct the formation of actin stress fibers and influence the overall organization of the cytoskeleton. In addition, cytoskeletal dynamics are regulated by the family of small GTPases including RhoA, Rac, and cdc42[209]. Rho kinase (ROCK) is one of RhoA's effectors and is responsible for myosin light chain (MLC) phosphorylation and actin-myosin contractility[210,211]. The RhoA/ROCK signaling pathway mediates multiple cellular activities such as migration[212], proliferation[213], and differentiation[214], and can influence the response to growth factors[215] and integrin adhesion[216].

Cell morphology is an important regulator of differentiation for multiple cell types. Recently, the role of cytoskeletal organization in mesenchymal lineage selection was examined using micropatterned surfaces and inhibitors of RhoA/ROCK signaling[214]. In this report, cell adhesion and spreading stimulated osteogenesis through RhoA activation of ROCK, while more rounded cell morphologies enhanced adipocyte differentiation via RhoA inactivation. Although these results indicate that cytoskeletal organization is a key factor in mesenchymal stem cell differentiation, the influence on chondrogenesis remains unclear. Several studies have reported enhanced chondrogenesis in chick limb bud cells by disrupting f-actin polymerization during monolayer culture[206]. However, the application of cytochalasin D or the ROCK inhibitor (Y-27632) to micromass cultures of ATDC or mouse limb bud cells inhibited the expression of collagen II and aggrecan genes[208]. Taken together, these reports suggest that the influence of cytoskeletal organization on chondrogenesis may depend on the degree of cell spreading and involve additional signals from the surrounding microenvironment.

Given the direct connection between integrin receptors and the actin cytoskeleton, adhesion to the ECM could play an important role in modulating the influence of cytoskeletal organization on the differentiation of mesenchymal progenitors. Therefore, the objective of this study was to investigate the effects of interactions between integrin adhesion and cytoskeletal organization on the chondrogenesis of BMSCs. In these experiments RGD peptides were conjugated to agarose hydrogels, and integrin adhesion to the RGD motif promoted BMSC spreading in a density dependent manner. This system allowed for the controlled presentation of specific adhesive ligands and varying degrees of cytoskeletal organization. The influence of these defined cell-matrix interactions on the chondrogenic response of BMSCs to TGF-β1 and dexamethasone was examined over a range of RGD densities and in the presence of the inhibitors cytochalasin D and Y-27632. Furthermore, the specificity of these responses to chondrogenesis was evaluated by investigating osteogenic differentiation within the same modified agarose gels. The results of this study demonstrate that cytoskeletal organization influences the chondrogenesis of BMSCs and depends on the integrin ligand density of the surrounding ECM.

7.2 MATERIALS AND METHODS

7.2.1 Materials

The synthetic peptides GRGESP and GRGDSP were from Bachem (King of Prussia, PA), and the sulfo-SANPAH cross-linker was from Pierce (Rockford, IL).

Seaprep agarose was from Cambrex (Frederick, MD). Dexamethasone, 1,9 dimethyl methylene blue (DMMB), Hoechst dye 33258, and phosphatase substrate 104 were from Sigma Aldrich (St. Louis, MO). Immature bovine hind limbs were from Research 87 (Marlborough, MA). Recombinant human TGF-β1 was from R&D Systems (Minneapolis, MN), and basic-fibroblast growth factor (bFGF) was from Peprotech (Rocky Hill, NJ). The ITS+ premix and ProteinaseK were from BD Biosciences (San Jose, CA). Fetal bovine serum was from Hyclone (Logan, UT), and cell culture reagents, including Dulbecco's Modified Eagles Medium (DMEM), antibiotic/antimycotic, trypsin, non-essential amino acids (NEAA), and phosphate buffered saline (PBS), were from Invitrogen (Carlsbad, CA). The RNeasy mini kit was from Qiagen (Valencia, CA), and the AMV reverse transcriptase kit was from Promega (Madison, WI). The SybrGreen master mix was from Applied Biosystems (Forest City, CA). Cytochalaiasin D and Y-26732 were from Calbiochem (San Diego, CA).

The functional blocking antibody against the β1 integrin (AIIB2) was from the University of Iowa Developmental Studies Hybridoma Bank (Iowa City, IA), and the anti-αvβ3 antibody (LM609) was from Chemicon (Temecula, CA). The mouse IgG isotype control was from Jackson Immunological Research (West Grove, PA). The anti-vinculin antibody was from Sigma Aldrich (St. Louis, MO), and the FITC anti-mouse antibody was from Abcam (Cambridge, MA). The anti-NITEGE antibody was provided by John Sandy Ph.D. (Rush University, Chicago, IL). AF594 phalloidin, AF488 anti-rabbit IgG, and the live/dead staining kit were from Molecular Probes (Eugene, OR).

7.2.2 BMSC isolation

Bone marrow was harvested from the tibiae and femora of an immature calf and physically disrupted by passage through 50ml and 10ml serological pipettes, followed by 16, 18, and 20 gage needles. The marrow was then separated by centrifugation, and the fatty layer was removed. The remaining heterogeneous mixture was rinsed with PBS and pre-plated for 30 min to remove the rapidly adherent cells. The remaining cells were then re-plated at approximately 250,000 cells/cm^2 on tissue culture plastic and cultured in low-glucose DMEM, 1% antibiotic/antimycotic, 10% FBS, and 1ng/ml basic-FGF. After 3 days, the non-adherent cells were removed during the first media change. The remaining adherent BMSCs were expanded until nearly confluent, at which time they were trypsinized and replated at 6,000 cells/cm^2. Cells were expanded twice more to near-confluence before seeding on or in alginate. Consistent with previous reports[128], BMSCs isolated in this manner were positive for the cell surface markers CD29 and CD44 and negative for CD45 as determined by flow cytometry.

7.2.3 Peptide-Agarose conjugation

The synthetic peptides GRGESP and GRGDSP were conjugated to agarose hydrogels with the sulfo-SANPAH cross-linker similar to previous studies[217]. The primary amines on the peptides were reacted with the NHS-ester group of the sulfo-SANPAH at room temperature for 4h in the dark with a 10-fold molar excess of the cross-linker. Seaprep agarose solutions were prepared in Ca^{++}/Mg^{++}-free PBS, autoclaved, and cooled to 37ºC. One part of the peptide/sulfo-SANPAH solution was combined with three parts of 4% Seaprep Agarose and mixed thoroughly. The mixture

was exposed to 365nm UV light for 3min to activate the photoreactive groups of the sulfo-SANPAH and conjugate the peptide to free CH-groups in the agarose. The agarose was allowed to gel at 4ºC for 20min and washed multiple times with PBS to remove the unbound peptide and cross-linker. The conjugation efficiency and resulting peptide density were estimated by immunoblotting for a biotinylated peptide.

7.3.4 Cell seeding and gel culture

Prior to cell seeding, the 3% modified agarose gels were melted at 45ºC and cooled to 37ºC. BMSCs were then seeded into the cyclindrical (4mmØ) gels by resuspending the cells in the melted agarose at a density of 10e6 cells/ml and casting the cell suspension into custom molds. The gels were cooled at 4ºC for 30min and transferred to fresh culture medium. The basal, chemically defined medium consisted of DMEM, ITS+ Premix, NEAA, antibiotic/antimycotic, and ascorbate, and the chondrogenic medium was supplemented with 10ng/ml TGF-β1 and 100nM dexamethasone. For the integrin blocking experiments, BMSCs were incubated with 20μg/ml of anti-αvβ3, anti-β1, or mouse IgG for 20min in DMEM prior to seeding into agarose, and the gels were cultured overnight in chondrogenic medium with 20μg/ml of the same antibodies. In some experiments the chondrogenic medium was further supplemented with 10μM Y-27632, 0.3μM of cytochalasin D, or the carrier (0.01% DMSO). The fetal bovine serum (FBS) supplemented medium consisted of DMEM, 10% FBS, NEAA, antibiotic/antimycotic, and ascorbate. BMSC seeded gels were cultured up to 8 days under the specified conditions and media were collected and changed every 2 days.

7.2.5 Fluorescence imaging and analysis

Agarose gels were fixed with 10% neutral-buffered formalin for 30min at 4ºC and rinsed in PBS. Portions of the fixed gels were blocked with 5% FBS and permeabilized with 1% Triton-X100. Vinculin localization was examined by staining with the anti-vinculin antibody (1:100), and secondary detection was performed with the anti-mouse FITC antibody (1:100). Aggrecanase activity was detected with antiserum against the aggrecan-NITEGE neoepitope (1:100) and the anti-rabbit FITC antibody. The F-actin cytoskeleton was visualized by staining with AF594-phalloidin (1:50), and DNA was labeled with Hoechst dye (1:2000). Cell viability and morphology were also assayed by staining with the calcein AM and ethidium homodimer from the live/dead kit. The agarose gels were imaged with a Zeiss 510 laser scanning confocal microscope (Zeiss, Heidelberg, Germany). Fluorescence images of the f-actin cytoskeleton or calcein AM stain at 10X magnification were analyzed with Scion Image software (Frederick, MD). The area (A) and perimeter (P) for an individual cell were used to calculate the circularity: circularity = $4\pi A/P^2$. Preliminary analyses indicated that the absolute circularity values increased with higher objective power and image resolution, but the relative differences in circularity between treatments did not change. Therefore, the 10X magnification was selected to provide a larger sample size.

7.2.6 Biochemical Assays

The agarose gel constructs were weighed wet, lyophilized, and sequentially digested with ProteinaseK (1mg/80mg tissue) at 60ºC overnight and agarase (4U/construct) at 45ºC for 4h. The sGAG content was measured using the 1,9

dimethylmethylene blue assay[129], and DNA content was measured using the Hoechst dye assay[145]. Media samples were also analyzed for sGAG content using the DMMB assay. To measure alkaline phosphatase activity, gels were rinsed in PBS for 20min, immersed in 1% Triton-X100, and snap frozen to lyse the cells. The agarose gels were homogenized and centrifuged at 1200xg. The lysate was then removed and analyzed for alkaline phosphatase activity by measuring the amount of p-nitrophenyl generated from p-nitrophenyl phosphate.

7.2.7 Real-time RT-PCR

RNA was isolated from the agarose gels using the Tri-spin method[143]. Gels were immediately dissociated in lysis buffer plus 2-mercaptoethanol. RNA was extracted from the gel using the Trizol reagent and chloroform and precipitated with 100% isoproponol. The RNA was further purified using the Qiagen RNeasy kit according to the manufacturer's protocol. Total RNA (1μg) was reverse transcribed to cDNA using the AMV reverse transcriptase kit. Gene expression was measured by real-time RT-PCR using the SybrGreen master mix and custom primers for collagen II, aggrecan, collagen I, and osteocalcin. The PCR reactions and detection were performed with an ABI Prism 7700 (Applied Biosystems, Forest City, CA).

7.2.8 Data Analysis

All data are presented as the mean ± SEM. The fractions of spread cells were transformed using an arcsine function, and gene expression levels were transformed by a Box-Cox transformation for normality. Data were analyzed by a two factor general

linear model with RGD density/gel type and media conditions as factors. Dunnet's test was used to compare treatments with the blocking antibodies to the isotype control. All other pairwise comparisons were performed with Tukey's test. Significance was at $P < 0.05$.

7.3 RESULTS

7.3.1 RGD-modified agarose gels promote quantifiable changes in 3D cell morphology

BMSCs were seeded into 3% agarose gels modified with 0, 200, or 400μM densities of the RGD peptide. After 24h in chondrogenic medium, cell spreading could be observed in the RGD-modified gels by fluorescence staining of the f-actin cytoskeleton and confocal microscopy (Fig. 7.1A). BMSCs displayed distinct cytoskeletal proejections, and there appeared to be more spread cells within the 400μM gels than the 200μM gels. These changes in morphology were quantified by analyzing three 10X images from each density and calculating the circularity of individual cells. The distribution of circularities in the unmodified gels displayed a large peak at 0.9 (Fig. 7.1B), indicative of highly rounded cells (circularity = 1 for a perfect circle). The size of this peak decreased with increasing RGD density, and the circularity distribution shifted towards lower circularities, characteristic of greater cell spreading. The fraction of cells with circularities less than 0.75 (below the major peak in 0μM gels) was calculated for each field, and the presence of the RGD peptide significantly increased the fraction of spread cells in a density dependent manner (Fig 7.1C). Furthermore, the 400μM RGD

density significantly reduced the average circularity of the spread cells compared to the 0 and 200μM densities (Fig 7.1D), indicating that interactions with the peptide also increased the degree of cell spreading. These results demonstrate that RGD-modified agarose gels promote quantifiable and density dependent changes in BMSC morphology.

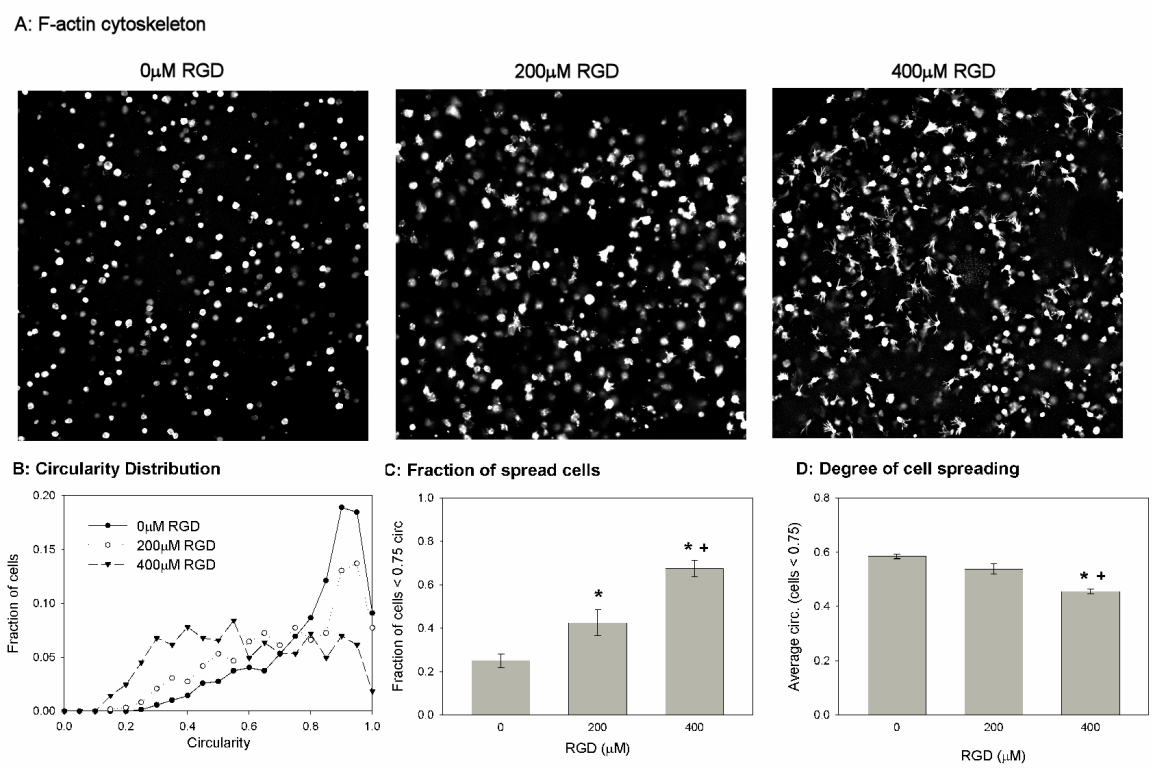

Figure 7.1: Quantification of 3D BMSC morphology. BMSCs were seeded in agarose gels modified with 0, 200, or 400μM RGD. Gels were cultured overnight in chondrogenic medium and stained with AF594-phalloidin. (A) Fluorescence images of the f-actin cytoskeleton were taken with a confocal microscope at 10X magnification. (B) The distribution of cell circularities from 3 random fields was plotted for each RGD density, and (C) the fraction of spread cells was calculated for each field as the fraction with circularities less than 0.75. (D) The degree of spreading was measured by the average circularity of the spread cells (<0.75 circ). N = 3 fields/density, *P<0.05 with 0μM, +P<0.05 with 200μM.

7.3.2 Cell spreading involves αvβ3 integrin adhesion

Integrin mediated spreading in RGD-modified agarose was examined by immunofluorescence detection of vinculin and functional blocking with integrin specific

antibodies. BMSCs in the RGD-modified gels displayed large projections of the f-actin cytoskeleton that co-localized with vinculin, while cells in the RGE-modified gels remained rounded and had lower levels of vinculin (Fig 7.2A). Blocking with the anti-αvβ3 antibody significantly reduced cell spreading, and blocking with the anti-β1 antibody significantly increased spreading (Fig 7.2B). Together, these results indicate that the observed changes in cytoskeletal organization were associated with integrin adhesion and specifically involve the αvβ3 receptor.

Cell spreading could also be inhibited with 10μM Y-27632, which inhibits ROCK activity, or with 0.3μM cytochalasin D, which prevents actin polymerization. These doses were based on a preliminary dose-response experiment and represent the minimum amount required to significantly reduce 3D cell spreading (not shown). Treatment with Y-27632 or cytochalasin D at these levels for 24h did not affect cell viability (Fig 7.2C), and significantly reduced cell spreading in 200μM RGD gels (Fig 7.2D). In addition, BMSCs were able to fully recover their spread morphology 24h after removal of the inhibitors (Fig 7.2D), thereby verifying that there were no cytotoxic or sustained inhibitory effects of these compounds on BMSC activity.

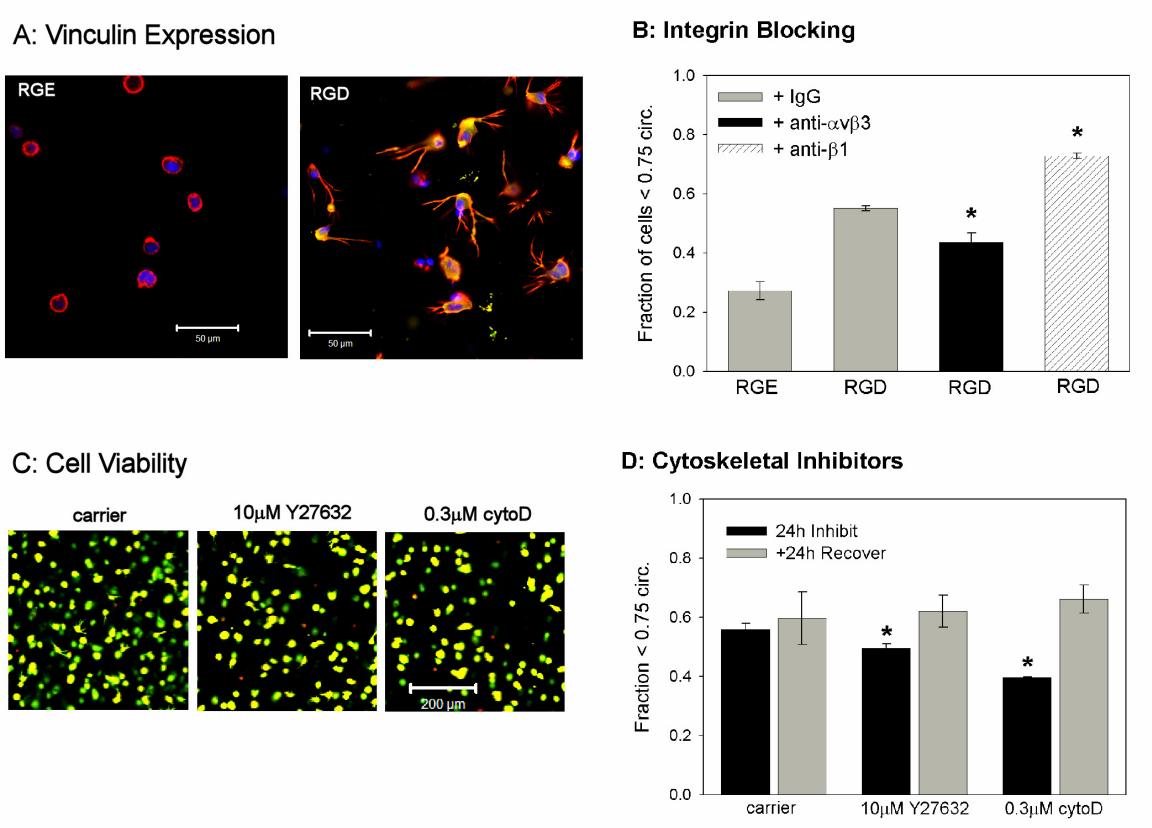

Figure 7.2: Integrin dependent spreading and cytoskeletal organization. (A) Vinculin localization (green) and the f-actin cytoskeleton (red) were examined by confocal microscopy (blue=DNA) 24h after seeding BMSCs in 400μM RGE or RGD modified gels. (B) Specific integrin receptors were blocked with 20μg/ml of anti-β1 or anti-αvβ3 antibodies prior to seeding BMSCs into 200μM RGE/RGD gels. Cell spreading was quantified by analyzing fluorescence images of the f-actin cytoskeleton. (C) BMSC viability was evaluated by live/dead staining following a 24h treatment with 10μM Y-27632, 0.3μM cytochalasin D, or carrier (0.1% DMSO), and (D) the influence of these inhibitors on cell spreading was measured by analyzing images of the calcein AM stain after 24h of inhibitor treatment and again 24h after removing the inhibitors. All experiments were in chondrogenic medium (10ng/ml TGF-β1 and 100nM dexamethasone). N=3 fields/condition, *P<0.05 with IgG or carrier.

7.3.3 Interactions with RGD-modified agarose inhibits BMSC chondrogenesis

To examine the effects of RGD adhesion on chondrogenesis within the agarose gel system, BMSCs were seeded into unmodified, 400μM RGE-, or 400μM RGD-modified gels and cultured for 7 days in basal or chondrogenic (10ng/ml TGF-β1 and

100nM dexamethasone) medium. At day 7 the DNA content was significantly higher in the chondrogenic groups with no differences between between gel types (Fig 7.3A). The chondrogenic medium also significantly stimulated sGAG production over the basal condition (Fig 7.3B). There were no differences in sGAG accumulation between unmodified and RGE gels, but there was significantly less sGAG in the RGD-modified gels (Fig 7.3B). These results demonstrate that interactions with the RGD-modified agarose inhibit the chondrogenic response of BMSCs to TGF-β1 and dexamethasone.

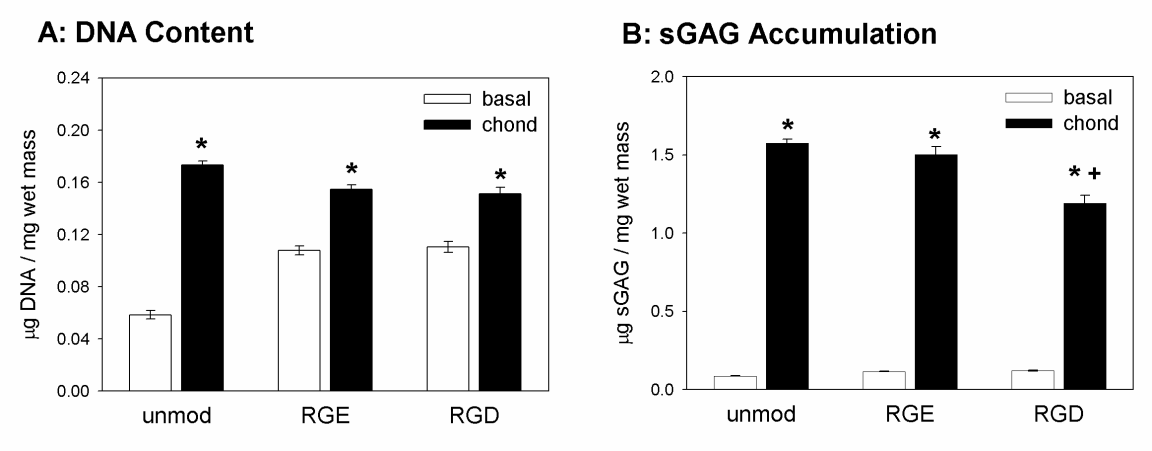

Figure 7.3: Effects of RGD adhesion on chondrogenesis. BMSCs were seeded into unmodified, 400μM RGE, or 400μM RGD gels and cultured for 7 days in basal or chondrogenic medium. (A) The DNA content within the gels was measured using the Hoechst dye assay, and (B) the level of sGAG accumulation was measured with the DMMB assay. N=6 gels/condition, *P<0.05 with basal, +P<0.05 with RGE.

7.3.4 RGD density and cytoskeletal organization modulate sGAG accumulation and release during BMSC chondrogenesis

The influences of RGD density and cytoskeletal organization on BMSC chondrogenesis were investigated by seeding cells into agarose with varying densities of the RGD peptide and culturing the gels in chondrogenic medium supplemented with Y-

27632, cytochalasin D, or carrier (0.01% DMSO). RGD densities ranging from 0 to 400μM were generated by varying the ratio of RGE to RGD while maintaining 400μM of total peptide in all gels. Analysis of the f-actin images at 24h demonstrated that cell spreading increased with increasing RGD densities similar to the previous experiments (Fig 7.4A). Addition of 10μM Y-27632 did not significantly alter cell morphology in this particular experiment, while 0.3μM of cytochalasin D completely blocked cell spreading in the 200μM and 400μM gels. After 6 days in culture, RGD interactions did not significantly affect the DNA content within the gels, but the presence of Y-27632 decreased the DNA content in the 400μM RGD gels only (Fig 7.4B). RGD densities of 40, 200, and 400μM significantly inhibited sGAG accumulation in a dose-dependent manner (Fig 7.4C). The Y-27632 compound decreased sGAG accumulation to similar levels at all RGD densities. Disruption of the f-actin cytoskeleton with cytochalasin D resulted in similar amounts of sGAG accumulation across all RGD densities, effectively lowering the sGAG contents in 0 and 4μM gels and increasing the sGAG content in 400μM gels as compared to the carrier treatment (Fig 7.4C). These findings indicate that the density-dependent effects of RGD adhesion on BMSC chondrogenesis involve changes in the f-actin cytoskeleton.

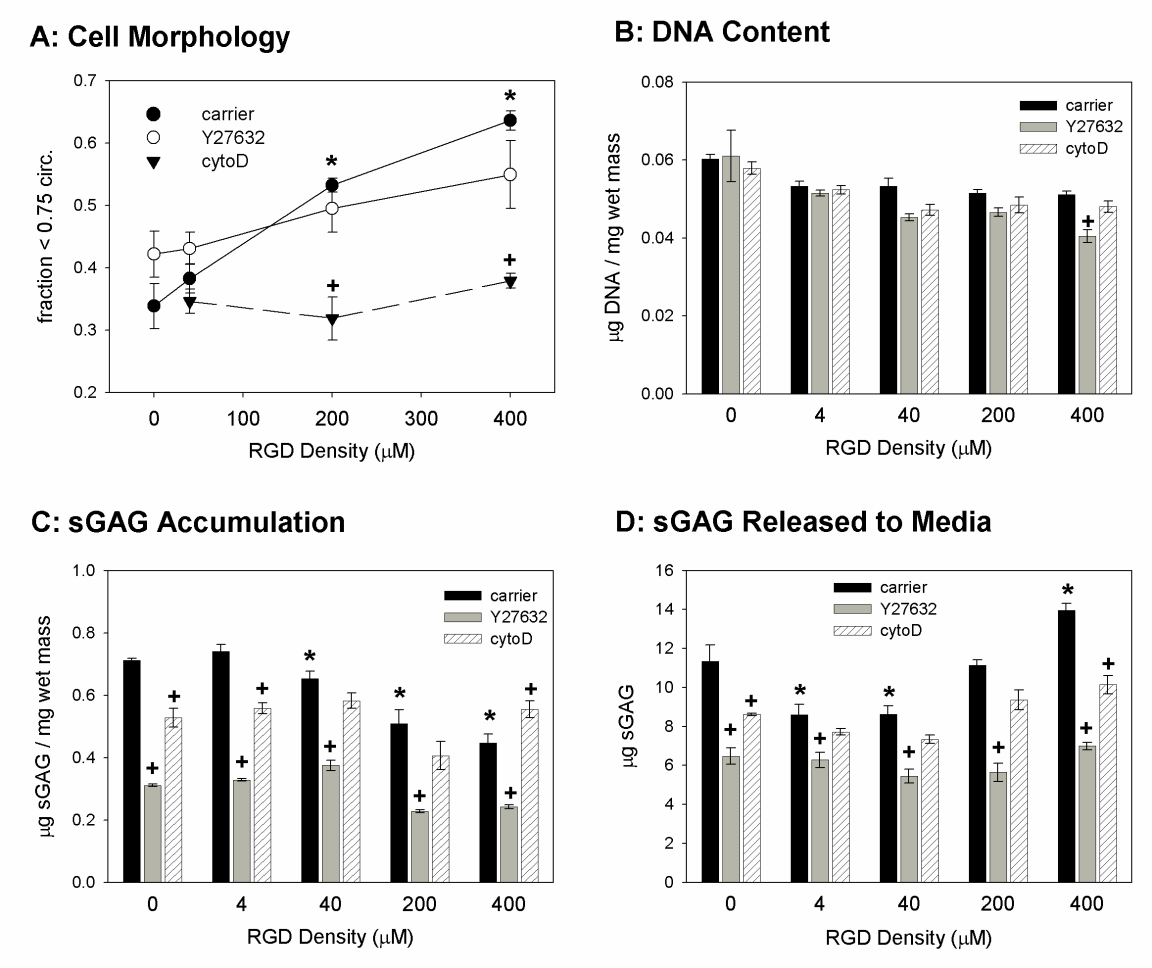

Figure 7.4: Influence of RGD density and cytoskeletal organization on chondrogenesis. BMSCs were seeded into modified agarose gels with 0, 4, 40, 200, and 400μM densities of RGD and cultured up to 6 days in chondrogenic medium supplemented with carrier (0.01% DMSO), 10μM Y-27632, or 0.3μM cytochalasin D. (A) Cell morphology was measured by analyzing fluorescence images of the f-actin cytoskeleton 24h after seeding. N=3 fields/condition (B) The DNA content was measured using the Hoechst dye assay. (C) The sGAG accumulation within the gels and (D) cumulative sGAG released to the media were measured by the DMMB assay. N=4 gels/condition, *P<0.05 with 0μM, +P<0.05 with carrier at same RGD density.

BMSC morphology in the 0, 40, and 400μM RGD gels was also examined after 6 days of culture with Y-27632 and cytochalasin D. Small cytoskeletal projections could be observed in the 0μM gels by day 6 (Fig 7.5A), and BMSCs in the 40μM gels appeared to have larger projections and actin stress fibers (Fig 7.5B). Cells in the 400μM gels

formed multi-cell clusters with clear actin stress fibers (Fig 7.5C). Addition of the ROCK inhibitor did not appear to affect cell morphology at any RGD density, while cells treated with cytochalasin D displayed rounded morphologies at each density and did not aggregate together in the 400μM gels (Fig 7.5A-C). Given the similar levels of DNA across RGD densities, it appears that RGD adhesion promotes cell migration and aggregate formation within the agarose gels, and this process requires organization of the f-actin cytoskeleton.

In contrast to the effects on sGAG accumulation, the cumulative sGAG released to the media was significantly higher for the 400μM gels than for the 0μM gels (Fig 7.4D). Addition of Y-27632 inhibited sGAG release at all RGD densities, and cytochalasin D significantly reduced sGAG release at the 0 and 400μM densities only. The levels of sGAG released to the media were small compared to those retained within the gels, and the total sGAG production (media plus gel, not shown) displayed the same trends as the sGAG accumulation data. Immunofluorescence detection of the NITEGE neoepitope revealed higher levels of aggrecanase mediated aggrecan degradation in the 400μM RGD gels (Fig 7.5D). The NITEGE signal was localized within the multi-cell aggregates and in the extracellular space, and treatment with cytochalasin appeared to block NITEGE generation. Taken together, these results suggest that RGD adhesion and cell spreading promote a catabolic release of sGAG that is in part mediated by aggrecanase specific cleavage of the aggrecan core protein.

A: 0μM RGD

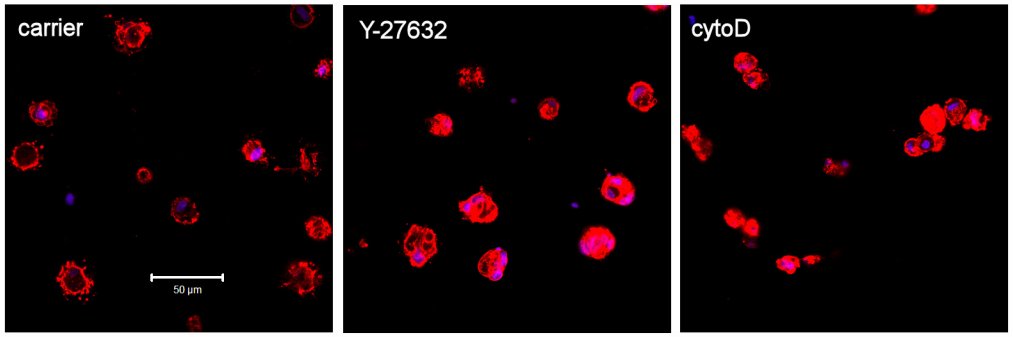

B: 40μM RGD

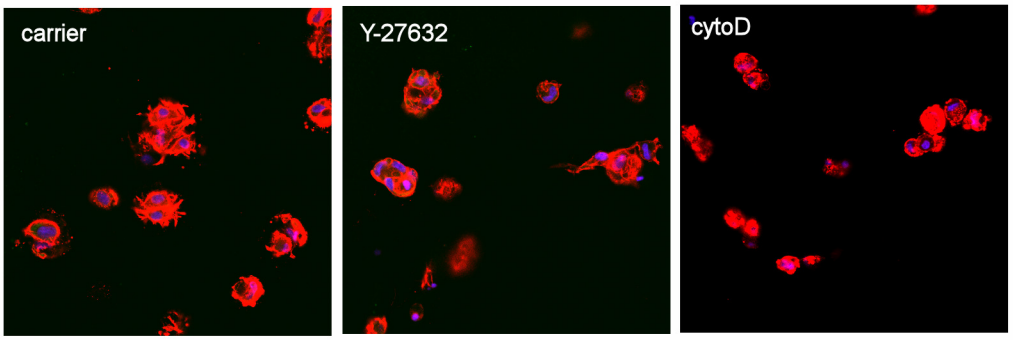

C: 400μM RGD

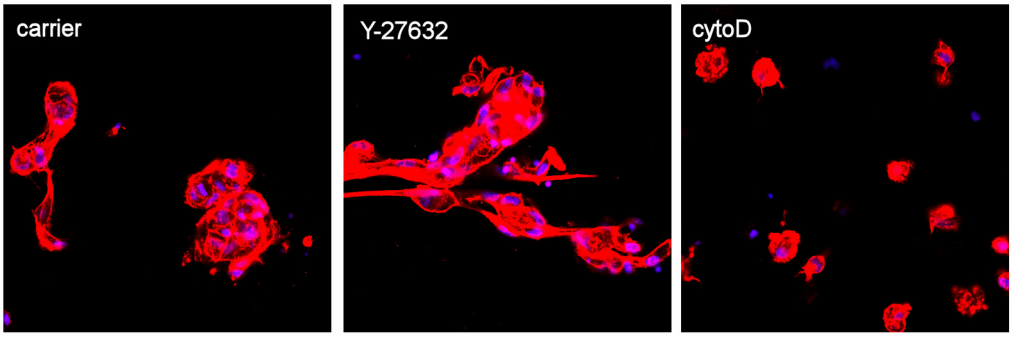

D: NITEGE Localization

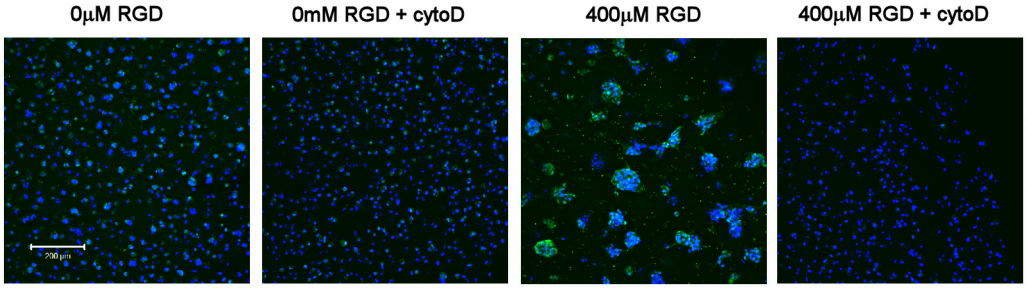

Figure 7.5: Day 6 morphology and NITEGE localization. Cell morphology was examined after 6 days in (A) 0, (B) 40, and (C) 400μM RGD gels cultured with the carrier, Y-27632, or cytochalasin D (red=f-actin, blue=DNA). (D) Aggrecanase activity was detected by immunostaining with antiserum against the aggrecan –NITEGE neoepitope (green=NITEGE, blue=DNA).

7.3.5 RGD adhesion differentially regulates chondrogenic and osteogenic responses of BMSCs.

To investigate the specificity of RGD interactions on chondrogenesis, BMSCs were seeded into 200μM RGE or RGD-modified gels and cultured for 8 days in chondrogenic or 10% FBS supplemented medium. The mRNA levels of chondrogenic and osteogenic genes were measured by real-time RT-PCR. In the RGE gels, BMSCs cultured with the chondrogenic medium expressed significantly higher levels of collagen II and aggrecan than cells in the serum-supplemented medium, but BMSCs in the 10% FBS medium expressed significantly higher amounts of the osteogenic marker, osteocalcin. In the presence of the chondrogenic medium, RGD adhesion significantly inhibited chondrogenic gene expression but had no effect on osteogenic gene expression. Conversely, RGD adhesion had no effect on chondrogenic gene expression in serum-supplemented medium but significantly increased osteocalcin and collagen I expression. These distinct responses to RGD-modified agarose in chondrogenic and 10% FBS media suggest that RGD adhesion differentially regulates BMSC chondrogenesis and osteogenesis depending on the specific biochemical stimuli.

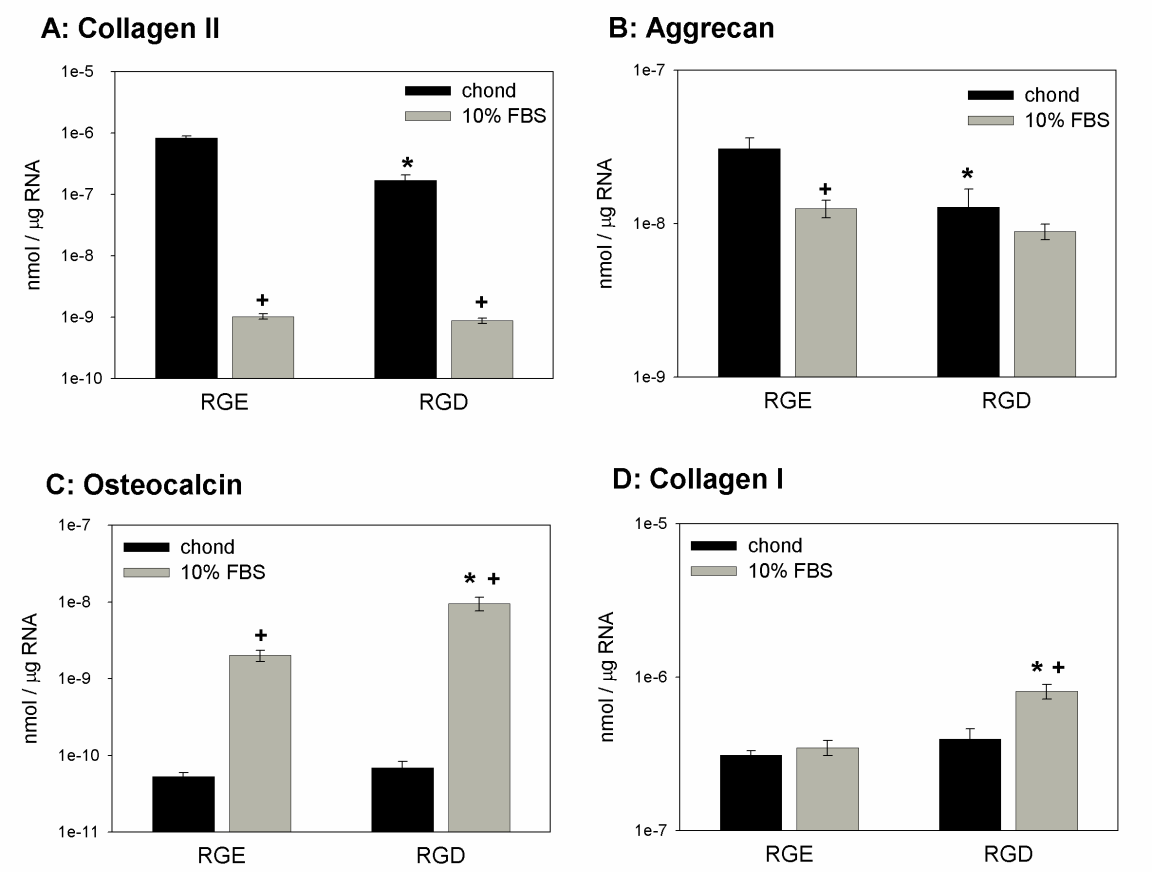

Figure 7.6: Influence of RGD adhesion and culture conditions on mRNA expression. BMSCs in 200µM RGE or RGD gels were cultured for 8 days in chondrogenic (10ng/ml TGF-β1 and 100nM dexamethasone) or 10% serum-supplemented medium. Expression of the chondrogenic genes, (A) collagen type II and (B) aggrecan, and the osteogenic genes, (C) osteocalcin and (D) collagen type I, were measured by real-time RT-PCR. N=4 / condition, *P<0.05 with RGE, +P<0.05 with chond.

The density dependent effects of RGD adhesion on the osteogenic response of BMSCs were examined by seeding cells into 0, 4, and 200µM RGD gels and measuring the alkaline phosphatase activity after 8 days of culture in 10% FBS medium. Similar to the previous experiment, RGD adhesion had no effect on the DNA content within the gels but significantly increased alkaline phosphatase activity in a dose-dependent manner. These results demonstrate that in addition to the effects on gene expression, RGD interactions enhance alkaline phosphatase activity, characteristic of increased osteogenic

differentiation, and BMSCs display opposite density dependent responses to RGD during osteogenic and chondrogenic differentiation.

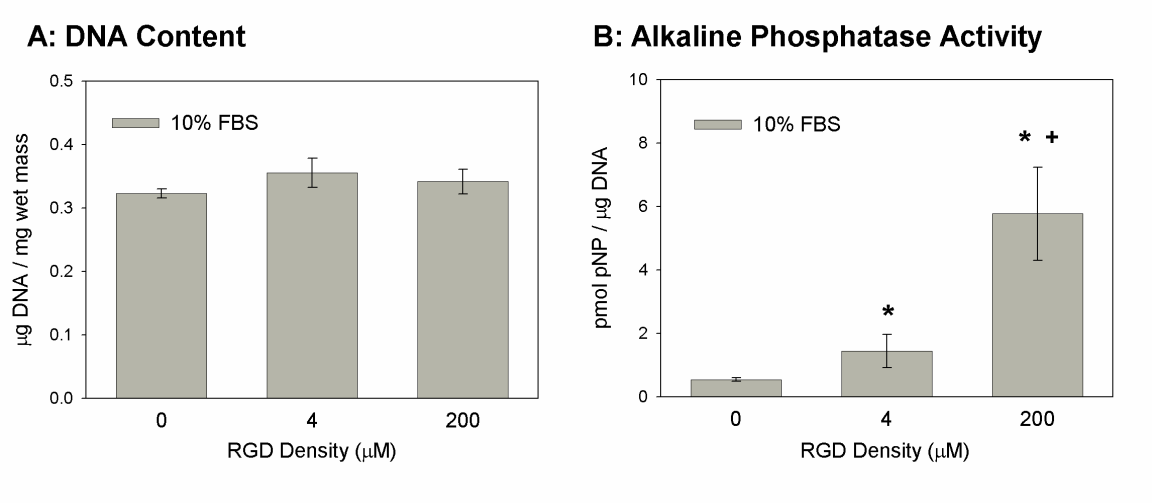

Figure 7.7: RGD density dependent effects on osteogenesis. BMSCs were seeded into 0, 4, and 200μM RGD-modified agarose gels and cultured for 8 days in 10% FBS supplemented medium. (A) The DNA content was measured by the Hoechst dye assay, and (B) the alkaline phosphatase activity was measured by production of p-nitrophenyl (pNP) from the Sigma 104 phosphatase substrate. N=6 / condition, *P<0.05 with 0μM, +P<0.05 with 4μM.

7.4 DISCUSSION

The goal of this study was to examine the interactions between integrin ligand density and cytoskeletal organization in regulating the chondrogenesis of mesenchymal progenitor cells. For this investigation, agarose hydrogels were modified with synthetic RGD peptides to present controlled densities of cell adhesive ligands within a three-dimensional culture environment. In this system, integrin adhesion to the RGD peptide promoted quantifiable and density dependent increases in BMSC spreading, and interactions with the RGD-modified gels inhibited the chondrogenic response to TGF-β1 and dexamethasone concomitant with the changes in cell morphology. Disruption of f-actin polymerization with cytochalasin D blocked BMSC spreading and prevented the

inhibitory effects of RGD adhesion on sGAG production. Interestingly, interactions with the RGD-modified agarose also appeared to facilitate cell migration and aggregation within the gel and promoted the catabolic release of sGAG to the media. The examination of lineage specific markers demonstrated that these responses were specific to chondrogenic differentiation and that RGD adhesion differentially regulated BMSC osteogenesis, depending on the biochemical context. Overall, these findings provide new insights into the role of cell morphology in the regulation of chondrogenesis and demonstrate the ability of coordinated signals from growth factors and the ECM to promote differentiation along specific mesenchymal lineages.

Previous studies have reported varying roles for the f-actin cytoskeleton in the process of chondrogenesis. For example, disruption of actin polymerization with cytochalasin D enhanced the chondrogenesis of chick limb bud cells in monolayer[206], but the addition of Y-27632 and cytochalasin to micromass cultures inhibited chondrocytic gene expression[207]. The results of the current study suggest that the degree of cytoskeletal organization may be an important regulator of differentiation. For the rounded cells in 0μM RGD gels, disruption of the f-actin cytoskeleton inhibited the chondrocytic phenotype, but for cells in 400μM RGD-modified agarose, blocking cell spreading actually increased sGAG production. These findings provide a potential explanation for the different responses observed in monolayer and micromass cultures and indicate that a minimal level of cytoskeletal organization may be required for optimal chondrogenesis and maintainence of the chondrocytic phenotype.

In the present study, the ROCK inhibitor Y-27632 significantly reduced sGAG production to similar levels at all RGD densities. In addition, the influences of Y-27632

on differentiation occurred without significantly altering cell morphology, and the inhibitor appeared to have no effect on BMSC aggregation in the 400μM gels. Although ROCK is known to influence cytoskeletal organization by promoting actin-myosin contractility[210,211], one of its targets, myosin light chain (MLC), can also be phosphorylated by myosin light chain kinase (MLCK)[218]. Therefore, the formation of cytoskeletal projections and cell aggregation observed within the modified agarose gels may involve actin-myosin contractility independent of ROCK activity. Despite having little effect on cell morphology, the significant inhibition of sGAG production suggests that ROCK signaling interacts with other regulatory pathways. This result is consistent with a previous study in which constitutively active ROCK stimulated osteogenesis independently of changes in cell shape[214]. Furthermore, blocking RhoA signaling has been shown to inhibit TGF-β induced Smad2/3 phosphorylation in smooth muscle cells[219]. Together, these reports provide additional evidence that ROCK regulates differentiation downstream of cytoskeletal organization.

In any study, the use of chemical inhibitors is limited by the potential for cytotoxic or non-specific effects on cell activity. The application of 10μM Y-27632 and 0.3μM cytochalasin D did not have noticeable effects on cell viability or the DNA content at low RGD densities. In addition, BMSCs were able to recover their spread morphologies within 24h following inhibitor removal, suggesting that these doses did not have a toxic effect on cell function. It is possible that the inhibitors had non-specific effects on other signaling molecules or kinases that influence chondrogenesis; however, other investigations have reported similar effects on cell activity using both 10μM Y-27632 and dominant negative RhoA[214,219]. Although there are no current indications of

toxicity or non-specific effects on BMSC differentiation, other strategies for perturbing ROCK signaling and cytoskeletal organization would help to strengthen the findings presented in this study.

Interactions between integrin adhesion and cytoskeletal organization are critical for the formation of focal complexes and signal transduction. In this study, functional blocking of αvβ3 integrins inhibited 3D cell spreading, but blocking with the anti-β1 integrin antibody significantly increased cell spreading. These results suggest that both receptors compete for the RGD ligand, but the αvβ3 integrin appears to be specifically involved in cell spreading and cytoskeletal organization, consistent with previous reports[108]. In this manner, αvβ3 integrin adhesion within the modified agarose system may regulate chondrogenesis through changes in cell morphology. Cytoskeletal organization also provides feedback to integrin signaling by stabilizing the formation of focal complexes[107,220] and recruiting signaling molecules such as FAK, ILK, and src. Therefore, disrupting f-actin polymerization or inhibiting contractility may prevent the normal cell-matrix interactions that are important for chondrogenesis[111], as well as the inhibitory effects of RGD adhesion. It is interesting to note that in the previous study (Chapter 6), interactions with RGD-modified alginate inhibited BMSC chondrogenesis without changes in cell morphology, and this response did not involve αvβ3 integrins. Taken together, these studies suggest that αvβ3 integrin adhesion indirectly regulates chondrogenesis through changes in cell morphology, while signaling by other integrin receptors, such as the β1 subunit, may influence differentiation independently of cytoskeletal organization.

In addition to cell spreading, RGD adhesion promoted cell aggregation within the agarose hydrogels and stimulated the catabolic release of sGAG to the media. These responses are consistent with TGF-β1 stimulation of cell migration during processes such as wound healing[177] and tumor cell invasion[179,221]. Cell migration is known to involve the αvβ3 integrin receptor[177,222] and is associated with increased proteolytic activity[223,224]. Similarly, the changes in chondrocyte morphology that occur during chondrocyte dedifferentiation have been implicated in interleukin-1 production and an inflammatory phenotype[225]. The results of the current study support these observations and further demonstrate that integrin adhesion to the ECM can induce aggrecanase-mediated degradation of proteoglycans.

The process of chondrogenesis is tightly regulated by many signals from the surrounding microenvironment. This study clearly showed that the integration of signals from growth factors and the ECM provide a mechanism for directing the lineage-specific differentiation of mesenchymal progenitors. In addition to furthering the current understanding of stem cell differentiation, these findings may have important implications for the use of BMSCs in cell-based therapies or tissue engineering. The development of appropriate biomaterials, as well as the optimization of cell culture conditions, will be essential for controlling cell fate within a tissue engineered construct.

CHAPTER 8

CONCLUSIONS AND RECOMMENDATIONS

8.1 SUMMARY

Cartilage tissue engineering represents an exciting potential strategy for providing permanent and functional regeneration of healthy cartilage tissues, but these treatment options have yet to be successfully implemented in a clinical setting. One of the primary obstacles for cartilage engineering is obtaining a sufficient supply of cells capable of regenerating a functional cartilage matrix. Mesenchymal progenitors can easily be isolated from multiple tissues, can be expanded in vitro, and possess a chondrogenic potential, but it remains unclear what types or combinations of signals are required for lineage-specific differentiation and tissue maturation. The overall goal of this dissertation was to investigate how the coordination of biochemical stimuli with cues from mechanical forces and the extracellular matrix regulate the chondrogenesis of bone marrow stromal cells (BMSCs). Specifically, these studies explored the potential for cyclic tensile loading and chondrogenic factors, TGF-β1 and dexamethsone, to promote fibrochondrocyte-specific differentiation of BMSCs. In addition, the roles of integrin adhesion and cytoskeletal organization in BMSC differentiation were examined within engineered hydrogels presenting controlled densities of integrin adhesive ligands. Together, these studies provided fundamental insights into the regulatory mechanisms involved in the chondrogenesis of mesenchymal progenitor cells.

The studies presented in Chapter 3 characterized the production, organization, and processing of various proteoglycans and proteins by BMSCs within a tissue engineered construct and cultured with exogenous TGF-β1. Although BMSCs produced an ECM containing collagen type II and aggrecan, the total amount of matrix was significantly

lower than that produced by articular chondrocytes (ACs) under the same conditions. Furthermore, there were distinct differences in the composition of the pericellular matrix, indicating that the BMSCs were not fully differentiated chondrocytes. Interestingly, the aggrecan produced by these cells was primarily full-length, and there appeared to be little proteolytic degradation of the ECM within this system. The results of these experiments clearly indicated that the addition of TGF-β1 alone was insufficient to promote chondrocyte maturation and development of a functional tissue construct. Additionally, the differences in the pericellular matrix produced by BMSCs and ACs provided initial indications that specific cell-matrix interactions may regulate the chondrocytic phenotype and differentiation of progenitors.

Chapters 4 and 5 investigated the ability of cyclic tensile loading to guide fibrochondrocyte differentiation and fibrocartilage development during in vitro chondrogenesis of BMSCs. In these studies, the introduction of short periods of cyclic tension at different stages of chondrogenesis differentially altered BMSC gene expression and matrix synthesis rates. At early time points, tensile loading up-regulated chondrocytic gene expression, proteoglycan synthesis, and protein synthesis, but at later time points, tension specifically increased collagen I and II expression and protein synthesis only. These results suggest that the mechanosensitivity of BMSCs changes during chondrogenic differentiation and construct development. In addition to the early effects on gene expression and matrix synthesis rates, longer periods of intermittent tension influenced matrix accumulation and processing within the tissue constructs. In these experiments, one week of cyclic tensile loading significantly increased collagen (33.7%) and sGAG accumulation (12.5%); however, after two weeks of loading, these effects were lost. Furthermore, constraining the constructs in the 0% and +10% loading conditions enhanced the catabolic release of sGAG to the media, most likely through increased aggrecanase activity. Long-term, cyclic tensile loading also altered the patterns of BMSC gene expression, with increases in collagen I expression after one and two

weeks of loading, but no changes in collagen II, aggrecan, or osteocalcin gene expression. Taken together, the greater relative stimulation of collagen I gene expression and total collagen production with cyclic tension suggests that this form of physiologically relevant loading promotes a fibrochondrocyte-like phenotype for BMSCs during in vitro chondrogenesis. In addition, tensile forces generated by BMSC contraction increased aggrecan degradation, characteristic of a more fibrocartilage-like tissue.

The objective of Chapters 6 and 7 was to examine the roles of cell-matrix interactions in modulating BMSC chondrogenesis. In these studies, peptides containing the RGD motif were conjugated to alginate and agarose hydrogels and allowed for the controlled presentation of integrin adhesive ligands within a 3D, non-adhesive culture environment. BMSC interactions with the RGD-modified alginate specifically inhibited chondrocytic gene expression and matrix synthesis in a density dependent manner. These effects occurred without changes in 3D cell morphology and did not involve the $\alpha v\beta 3$ integrin receptor. In contrast, RGD-modified agarose gels promoted quantifiable and density-dependent changes in BMSC morphology, which involved $\alpha v\beta 3$ integrin adhesion. In this system, interactions with the RGD peptide also inhibited chondrogenesis and could be blocked by disrupting cytoskeletal organization. The results of these studies suggest that integrin specific adhesion to the ECM can regulate chondrogenesis directly and through interactions with the f-actin cytoskeleton. In addition, the studies in Chapter 7 demonstrated that RGD adhesion differentially regulates chondrogenic and osteogenic responses depending on the biochemical environment. Overall, these findings provided key insights into the mechanisms by which cell-matrix interactions regulate BMSC differentiation.

8.2 CONCLUSIONS

The research presented in this dissertation advances the current understanding of chondrogenic differentiation and examines several regulatory mechanisms that have important implications for the development of cartilage tissue engineering strategies. The tensile loading studies demonstrated the potential for physiologically relevant forces to guide fibrochondrocyte-like differentiation of mesenchymal progenitors, and the influences of integrin adhesion and cytoskeletal organization on BMSC chondrogenesis indicate that interactions with the ECM can play a significant role in regulating differentiation. Throughout these studies, one of the most fundamental concepts to emerge was the ability for multiple signals from the biochemical environment, mechanical stimuli, and the ECM to interact and direct lineage-specific differentiation.

Compressive loading is a well known regulator of the articular chondrocyte phenotype[64,93,95], and more recently, dynamic compression has been shown to promote the chondrogenesis of progenitor cells[85,96,97]. Although this form of physiologic loading plays an important role in articular cartilage development, the influences of tension on fibrochondrocyte differentiation have received relatively little attention. Previous work in our laboratory has shown that short periods of cyclic tensile loading of articular chondrocytes promoted cell spreading and differentially regulated proteoglycan synthesis depending on the loading duration and subpopulation of articular chondrocytes examined[36,157]. While generally consistent with a more fibrochondrocyte-like phenotype, these responses were different from those observed in the present studies, where cyclic tension stimulated collagen I and II expression and protein synthesis and had little effect on proteoglycan synthesis at later time points. In addition, cyclic tensile loading did not

appear to alter the already spread and contractile phenotypes of BMSCs. These distinct responses may reflect key cell type differences between chondrocytes and BMSCs. Articular chondrocytes produce significantly higher levels of proteoglycans, and BMSCs have greater collagen I mRNA expression, suggesting that high levels of gene expression or synthesis for a specific matrix molecule may be more sensitive to loading. Alternatively, the presence of TGF-β1 and dexamethasone in the BMSC cultures could have influenced the response to loading by enabling the responsiveness of collagen genes or protecting proteoglycan synthesis.

Despite differences in the immediate responses to short-term tension, the effects of longer loading periods on matrix production and turnover were strikingly similar between chondrocytes[157] and BMSCs. In each of these studies, one week of intermittent tensile loading slightly increased sGAG accumulation, but two weeks of loading had no effect on sGAG accumulation and appeared to promote aggrecan catabolism. In the BMSC studies, similar effects were also found for total collagen accumulation. These findings may reflect an adaptive response to loading either through matrix remodeling or changes in the mechanosensitivity of the cells. The deposition of a stiff pericellular matrix could provide stress shielding from mechanical stimuli during intermediate stages of construct development[226]. Similarly, detachment of the cells from the fibrin matrix and adhesion to a newly synthesized ECM may have altered the response to loading[148]. Several studies have implicated specific cell-matrix interactions and integrin adhesion as important mediators of mechanotransduction[101,148,227]. It is also possible that over multiple weeks of loading, the chondrocytes and BMSCs became desensitized to cyclic tension through cytoskeletal reorganization or changes in ion channel activity[228]. Even

during the short-term loading experiments, BMSCs were responsive to 3 hours but not 12 hours of cyclic tension. For longer studies, a more thorough understanding of these mechanotransduction and adaptive mechanisms will likely aid in optimizing loading protocols for providing sustained stimulation of fibrocartilage development.

The influences of cyclic tensile loading on BMSC chondrogenesis were distinctly different from the previously reported effects of dynamic compression. Compressive loading of bovine BMSCs in agarose gels had little effect at early stages of differentiation (day 8), similar to tensile loading, but at later time points (day 16), compression significantly up-regulated collagen I, collagen II, and aggrecan mRNA expression, as well as protein and proteoglycan synthesis[96]. The stimulation of aggrecan expression and proteoglycan synthesis at day 16 in these studies suggests that dynamic compression promotes phenotypic changes more characteristic of articular chondrocytes and may reflect fundamental differences in the cellular responses to tension and compression. Similarly, longer compressive loading experiments reported elevated aggrecan expression[85] and sGAG production, even after multiple weeks of loading[97]. Although the responses to tension and compression may have resulted from cellular sensing of the distinct loading modes, these effects could also reflect differences in mechanotransduction between the fibrin and agarose systems. Direct adhesion and spreading in the fibrin matrix may have elicited a more fibroblastic response, while the rounded morphologies in the agarose gels may have supported chondrocytic changes in gene expression and matrix synthesis.

One of the more interesting responses in the tensile loading studies was the increased sGAG release and aggrecan processing induced by constraining the fibrin

constructs. These increases in proteoglycan catabolism were most likely due to elevated aggrecanase (ADAMTS-4/5) activity[135]. The studies in Chapter 7 also demonstrated that integrin adhesion to the ECM promoted sGAG release and generation of the NITEGE neoepitope through changes in cytoskeletal organization. Therefore, the catabolic responses in the constrained constructs may have been a direct result of increased resistance to matrix contraction and greater cytoskeletal tension. This mechanism is further supported by the observations of low proteolytic activity in the long-term agarose cultures and the presence of a 70kDa aggrecan fragment in the fibrin constructs, characteristic of aggrecanase cleavage[135], even after 7 days of free-swelling culture. Interestingly, western blot analysis of the aggrecan cleavage fragments did not reveal detectable levels of the MMP-generated fragments, suggesting that there is little MMP-mediated degradation in this system. Although cytoskeletal contractility has been implicated in stimulating the proteolytic activity of other enzyme systems[229-231], these are the first reports for direct activation of aggrecanases in response to cell spreading and cytoskeletal tension.

In the tensile loading studies, the combination of multiple signals from growth factors, cyclic tensile deformations, and cytoskeletal tension promoted the differentiation and development of a fibrocartilage-like matrix. Similar to this in vitro system, the coordination of various signals from the surrounding environment may also guide fibrocartilage formation in vivo. In limb development, the menisci arise from cellular aggregates during joint formation[232]. Experiments inhibiting muscle contraction and joint loading within the embryo have revealed that mechanical stimuli are not required for early meniscus formation, but play an essential role in the tissue's maturation[233]. For

example, the tissue only acquires higher collagen II mRNA expression within the inner region at later stages of development[24,234]. At the same time, circumferentially oriented collagen I fibers develop within the tensile regions[23,27], suggesting that both compressive and tensile forces regulate fibrocartilage development. Recent reports have also observed higher aggrecanse activity within the outer region of the menisci[32], which may reflect the substantial levels of tension and cell spreading in this zone[27]. In other tissues, such as tendon and ligament, proteoglycan deposition in the fibrocartilage regions is associated with increased compressive loading and TGF-β1 expression[235,236]. Overall, these studies suggest that the precise combinations of multiple types of mechanical stimuli and growth factor signals also regulate fibrocartilage tissue formation in vivo.

In Chapter 6, RGD-modified alginate gels inhibited the chondrogenic response to TGF-β1 and dexamethasone. These inhibitory effects influenced mRNA expression, as well as matrix synthesis. Furthermore, RGD adhesion inhibited chondrogensis in a density dependent manner, and sGAG synthesis could be partially rescued by blocking with a soluble RGD peptide in the media. These results suggest that the influence of RGD interactions on BMSC differentiation required tethering of the ligand to the ECM, and may have involved interactions with the f-actin cytoskeleton. Encapsulation within the alginate hydrogels, however, did not allow for BMSC spreading or detectable changes in cytoskeletal organization. These observations could reflect the independent roles of cell shape and integrin signaling in regulating differentiation, or a minimal level of cytoskeletal organization may be required to support integrin clustering and RGD signal transduction, but not significantly alter cell shape. In these studies, blocking the αvβ3 integrin receptor reduced cell spreading on 2D surfaces, but blocking had no effect on the

response of BMSCs to RGD-alginate in 3D. This finding further supports the idea that specific integrins are responsible for inhibiting chondrogenesis independently of changes in cell morphology.

Although αvβ3 integrin adhesion did not directly influence BMSC chondrogenesis, the functional blocking of α5 subunits significantly inhibited sGAG accumulation in both RGE- and RGD-modified gels. In addition, chondrogenic medium up-regulated fibronectin expression, and pericellular fibronectin could be detected in the alginate gels. These results indicate that α5β1 adhesion to fibronectin may be important during the initial stages of BMSC chondrogenesis and are consistent with expression patterns in the pre-cartilage condensations of developing limbs[111]. It is interesting to note that in Chapter 3 higher levels of fibronectin were found in the BMSC constructs than the AC constructs, and the spatial distribution of fibronectin appeared to negatively correlate with sGAG. Moreover, fibronectin expression is only transiently up-regulated during mesenchymal condensation and gets down-regulated at later stages of cartilage development[112]. Therefore, BMSC adhesion to fibronectin may be essential for the early stages of chondrogenesis but actually inhibit the maturation of BMSCs during longer-term culture. Recent studies have even isolated a resident population of progenitors from articular cartilage based on the ability to rapidly adhere to fibronectin-coated surfaces[237]. These findings underscore the potential for specific cell-matrix interactions to not only promote differentiation, but also maintain resident populations of progenitor cells within the tissue.

The final set of studies in Chapter 7 examined the interactions between integrin adhesion and cytoskeletal organization in the regulation of BMSC chondrogenesis. In

agarose gels, integrin adhesion to the RGD peptide promoted quantifiable changes in 3D cell morphology. Although the RGD density in the agarose was 10 to 100-fold higher than the alginate, the differences in cell spreading in these two systems was most likely due to the structure of the scaffold rather than differences in ligand density. In preliminary studies, BMSCs were able to spread on 2D agarose surfaces with RGD densities that also promoted cell spreading in 3D (40-400μM), while agarose surfaces with the same molar densities as the RGD-modified alginate (1μM) did not support cell spreading. These results indicate that the presentation of the RGD ligand was different within these two systems, and many of the peptides in the agarose were inaccessible to the cells. Therefore, it is difficult to directly compare the absolute ligand densities between gel types or to draw conclusions about integrin spacing and signal transduction. Recent advances in FRET (fluorescence resonance energy transfer) -based probes have allowed for the direct measurement of integrin binding and may be a useful tool for addressing these issues in future studies[238,239].

Similar to the RGD-alginate gels, interactions with RGD-modified agarose specifically inhibited BMSC chondrogenesis in a density dependent manner. The disruption of the f-actin cytoskeleton with cytochalasin D blocked these density dependent effects, indicating that the cytoskeleton plays an important role in mediating the effects of RGD adhesion. However, it remains unclear whether cytoskeletal organization enables RGD signal transduction through integrin receptors or whether cell shape influences other functions downstream of integrin signaling. The inhibitory effects of cytochalasin D treatment on cells in the 0μM RGD gels demonstrates that a minimum level of cytoskeletal organization is required for chondrogenesis and that disrupting f-

actin polymerization may block the effects of both normal cell-matrix interactions and RGD adhesion. In contrast, culturing articular chondrocytes on monolayers of various ECM proteins, including collagen I, collagen II, and fibronectin, does not alter their rapid dedifferentiation, suggesting that cell shape may be the primary determinant of the chondrocytic phenotype[20]. Clearly, the cooperation between integrin adhesion and cytoskeletal organization plays an important role in regulating chondrogenesis, but future investigations will likely be required to fully elucidate the mechanisms of these interactions.

The RhoA/ROCK pathway may be a point of convergence for the influences of cell shape on mesenchymal cell differentiation. In these studies, inhibiting ROCK activity with Y-27632 significantly reduced sGAG production to similar levels across all RGD densities, but had little effect on cell morphology. Although the possibility exists for non-specific effects of the inhibitor, these findings and others[214] suggest that ROCK regulates differentiation downstream of cytoskeletal organization. Previous studies have shown that constitutively active ROCK stimulated osteogenesis independently of changes in cell shape[214]. In the RGD-modified agarose gels, Y-27632 did not affect cell migration or aggregate formation indicating that BMSCs retained actin-myosin contractility. In addition to myosin light chain, ROCK also phosphorylates LIM-kinase1[240] and 2[241], which are responsible for inhibiting actin depolymerization and enhancing the transcriptional activity for serum response factor (SRF) elements[242,243]. Therefore, ROCK activity may regulate differentiation through changes in SRF transcription without altering the gross cytoskeletal morphology. In future work, the use of constitutively

active or dominant negative ROCK constructs may help to further understand the details of this pathway and its potential influences on chondrogenesis.

The experiments in Chapter 7 revealed that RGD adhesion differentially regulates chondrogenic and osteogenic gene expression depending on the specific culture conditions. These findings most clearly demonstrate the ability for interactions between multiple signals to direct lineage specific differentiation. The distinct responses to RGD adhesion may be regulated at the level of osteogenic and chondrogenic transcription factors. Sox-9 is the master transcription factor for chondrogenesis and becomes activated in response to TGF-β1 stimulation[244], and Runx2 is a primary transcription factor for osteogenic differentiation[245,246]. Recent reports have indicated that Sox-9 inactivates Runx2, thereby simultaneously promoting chondrogenesis and repressing osteogenic responses[247]. This regulatory switch potentially explains how RGD adhesion does not stimulate osteogenic gene expression in the presence of chondrogenic medium. Conversely, the inhibitory effects of RGD adhesion on chondrogenesis could act by blocking Sox-9 expression. In addition to TGF-β signaling, β-catenin accumulation through the canonical Wnt pathway has also been shown to stimulate osteogenesis while inhibiting chondrogenesis[248-250] and may be an additional mechanism for determining lineage specificity.

In addition to mechanical forces and integrin adhesion, other factors may play important roles in regulating BMSC chondrogenesis. In Chapter 3, higher levels of sGAG accumulation could be observed in the center of BMSC constructs suggesting that low oxygen tension, similar to the in vivo environment, may encourage chondrocytic matrix production[130]. Cell-cell interactions are also known to be necessary for

chondrogenesis in development[251] and in adult stem cells[175]. In future studies, it will be interesting to examine how cell aggregation in the RGD-modified agarose influences chondrogenesis at time points beyond the first week. Finally, other types of cell-matrix interactions, such CD44 adhesion to hyaluronan, can affect chondrocyte activity[252] and may also play a role in chondrogenic differentiation. Although these factors were not directly examined in this set of studies, they may be important considerations for future investigations.

Chondrogenic differentiation is clearly a complex, dynamic, and highly regulated process. The studies presented in this dissertation demonstrate that the interactions between growth factors, mechanical stimuli, and the ECM provide robust signals for regulating lineage-specific differentiation. Moreover, the limited chondrogenesis of BMSCs with TGF-β1 alone suggests that additional stimuli are not only important, but are required for chondrocyte maturation and the development of a functional tissue. The findings of this research provide significant insights into the mechanisms of progenitor cell differentiation and will help to guide future endeavors in the field of cartilage tissue engineering and regeneration.

8.3 FUTURE DIRECTIONS

While the loading studies presented here demonstrate the potential for tensile forces to direct fibrochondrocyte differentiation, much work will required to optimize the specific loading and culture conditions that promote the development of a functional fibrocartilage tissue. Dynamic loading parameters, including amplitude, frequency, and duration of cyclic tension, as well as static forces, could contribute to the

mechanosensitivity of BMSCs, and a careful examination of these contributions may help identify loading conditions that stimulate elevated matrix production over multiple weeks. Alternatively, longer pre-culture periods may be necessary to overcome the possible stress shielding effects. Ultimately, successful fibrocartilage replacements will require appropriate mechanical properties to function in vivo, and investigations into the influences of tensile loading on construct mechanics will be essential in future studies.

The complex functions of fibrocartilage tissues in tension and compression create significant challenges for tissue engineering. Furthermore, the spatial variations in matrix composition and organization seen in structures such as the meniscus may present additional obstacles for designing heterogeneous and anisotropic tissues. The combination of multiple types of mechanical stimuli could provide a means for guiding the correct composition and organization of ECM in tissue constructs. In the long-term loading studies, constraining the fibrin constructs encouraged matrix alignment and catabolism, while dynamic loading stimulated matrix synthesis. Therefore, tuning the relative levels of static and dynamic tension to elicit distinct cellular responses may allow for the development of tissues with specific compositions and functions. In addition, combining tensile and compressive forces could also be a useful strategy for regulating the relative amounts of proteoglycan and collagen production. Finally, graded levels of these different stimuli may provide control over the heterogeneity and spatial variations of fibrocartilage constructs. Beyond fibrocartilage, combinations of mechanical stimuli have potential applications in engineering other heterogeneous tissues, such as heart valves, blood vessels, or skin, and the fundamental insights into the role of tensile forces in tissue formation gained by this research will greatly aide in these efforts.

Although RGD adhesion clearly inhibits BMSC chondrogenesis, other cell matrix interactions may be important for in vitro chondrogenesis, and the incorporation of specific biomimetic ligands or growth factors into biomaterials and tissue engineering scaffolds may enhance chondrogenic differentiation. Specifically, the studies in Chapter 6 suggest that $\alpha5\beta1$ integrin adhesion to fibronectin is required during the early stages of BMSC chondrogenesis. In addition, other studies have shown that the presence of collagen type II in alginate hydrogels enhances BMSC chondrogenesis[113]. Therefore, preliminary studies were conducted to examine the effects of integrin specific adhesion to fibronectin and collagen mimetic ligands on mesenchymal progenitor cells (Appendix B). In these studies, recombinant fibronectin fragments ($FnIII^{7-10}$), containing the RGD and PHSRN synergy sites required for $\alpha5\beta1$ binding[192], were conjugated to agarose hydrogels using the sulfo-SANPAH cross-linker (Chapter 7). Similarly, synthetic, triple helical peptides with the GFOGER motif were also conjugated to agarose hydrogels. The GFOGER consensus sequence is found in fibrillar collagens, including types I and II, and has been shown to specifically engage $\alpha2\beta1$ receptors[109]. Agarose hydrogels modified with the $FnIII^{7-10}$ and GFOGER peptides promoted density-dependent, 3D cell spreading, but compared to the RGD-modified agarose, BMSCs required significantly lower molar densities of these ligands for equivalent levels of spreading (Fig B.2). These findings demonstrated that $FnIII^{7-10}$ proteins and GFOGER peptides could be conjugated to agarose hydrogels and retain their adhesive function within a 3D environment.

To investigate the effects on chondrogenesis, BMSCs were seeded into agarose gels modified with RGD, $FnIII^{7-10}$, or GFOGER at densities that promoted approximately 50-70% cell spreading, and the gels were cultured up to one week in basal or

chondrogenic medium. In these experiments, interactions with each of the adhesive ligands significantly inhibited chondrogenic stimulation of sGAG and collagen accumulation (Fig B.3) but had no effect on the total DNA contents. These results are consistent with the effects of different ECM monolayers on chondrocyte dedifferentiation[20] and suggest that cell adhesion and spreading inhibit the chondrocytic phenotype, regardless of the specific integrins or matrix proteins involved. In light of these preliminary studies, perhaps the specific cell-matrix interactions that are important for chondrogenesis also require the correct presentation of ECM proteins in order to maintain round cell morphologies. Alternatively, the roles of fibronectin and collagen may not involve integrin signaling, but rather serve to promote matrix assembly or localize growth factors through other functional domains, such as the heparin and collagen binding sites on fibronectin. Therefore, future investigations should more closely examine the spatial orientation of these ligands, as well as the additional functions of fibronectin and collagen.

A more complete understanding of the regulatory mechanisms of the ECM in BMSC chondrogenesis may eventually lead to rationally designed materials for cartilage tissue engineering. One interesting observation from the studies in Chapter 3 was the lack of collagen VI in the BMSC pericellular matrix. Collagen VI is also found pericellularly in articular cartilage and associates with the small PGs decorin and biglycan[131]. This complex has been hypothesized to help initiate cartilage matrix assembly[133] and bind growth factors such as TGF-β1[132]. In addition to being a potential marker for differentiated chondrocytes, it is possible that collagen VI plays an important role in regulating chondrogenesis and tissue formation. Engineering scaffolds that

incorporate or mimic the effects of collagen VI may be a potential strategy for enhancing BMSC maturation into chondrocytes and improving the development of articular cartilage constructs.

The ultimate success of engineered cartilage and fibrocartilage replacements will depend on the tissues' abilities to perform their basic mechanical and biological functions in vivo. Therefore, the development of animal models and in vivo testing protocols should be an important consideration for future work. Initially, subcutaneous implantation models may be useful for determining the fates of cells within the construct. It will be essential to understand the phenotypic stability of differentiated BMSCs within the vivo environment, particularly following in vitro loading protocols that encourage fibrochondrocyte differentiation. In addition, differences in the biochemical stimuli that are present in vitro and in vivo may also influence the specific responses of mesenchymal progenitors to peptide-modified gels. Beyond these initial studies, more rigorous animal models of cartilage defects will be required for evaluating the constructs' mechanical functions. Key considerations for these types of studies will include the new tissue's mechanical integrity as well as the ability to integrate with the host cartilage. Although RGD adhesion clearly inhibits the early chondrogenesis of BMSCs in vitro, the ability of cells to migrate through RGD-modified constructs may be advantageous for improving tissue integration. Finally, changes in the mechanical environment of BMSCs once implanted in a cartilage or fibrocartilage defect may also influence their differentiation state and tissue development. In vivo work may be years away, but it is important to keep many of these considerations in mind during the initial stages of in vitro studies.

While biomimetic and engineered hydrogels are attractive for tissue engineering applications, they may also provide useful tools for studying fundamental biological processes. These systems allow for the controlled presentation of specific adhesive ligands and quantitative analysis of cell-matrix interactions. Moreover, 3D matrices may more accurately reflect the vivo environment in terms of diffusion rates, matrix stiffness, and cell morphology. The ability to tune these types of parameters would likely be advantageous for studying basic cell functions such as proliferation, migration, and survival. Similar to the studies in this dissertation, the use of engineered cellular microenvironments could provide significant insights into the complex interactions between biochemical and physical stimuli that regulate cell behavior in various tissues and disease states.

APPENDIX A

THE INFLUENCE OF CYCLIC TENSION AMPLITUDE ON CHONDROCYTE MATRIX SYNTHESIS: EXPERIMENTAL AND FINITE ELEMENT ANALYSES

A.1 INTRODUCTION

During normal physiologic loading, cartilaginous tissues primarily bear compressive forces. Based on this function, it has been hypothesized that compressive loading is a key stimulus for chondrocytes, and numerous studies have investigated how both dynamic and static compression influence matrix synthesis[64,95,253-256]. In general, dynamic compression in explant and 3D culture increases chondrocyte synthesis of the major extracellular molecules, type II collagen and aggregating proteoglycans. Furthermore, loading parameters such as magnitude and frequency influence the extent of matrix synthesis[93,95,253].

Although much work has been done with compression, the effects of tensile loading on chondrocyte biosynthesis have received little attention. While it is not generally considered a major component of normal physiologic loading, significant tensile strains can develop near cracks or tears in the tissue as a result of injury or arthritic degradation. Unlike articular cartilage, fibrocartilage tissues normally experience substantial levels of tensile loading. For example, the loading conditions and geometry of the meniscus produce tensile hoop stresses in the structure's circumferentially oriented collagen fibers[23]. Studying the role of tensile loading on

chondrocyte and fibrochondrocyte matrix synthesis is therefore important for understanding both articular cartilage injury and normal fibrocartilage function. In addition to investigating the fundamental cellular responses, oscillatory tension may also be useful for developing tissue engineered constructs by providing a means to control matrix synthesis and organization.

A loading system was previously developed for applying cyclic tension to cells within a three-dimensional fibrin construct[257]. With this system, it was shown that cyclic loading at 10% overall displacement and 1.0 Hz inhibited both chondrocyte and fibrochondrocyte synthesis of protein and proteoglycan as measured by ^{3}H-proline and ^{35}S-sulfate incorporation, respectively. Although these results indicated an inhibition of matrix synthesis due to cyclic tension, only one set of loading parameters has been investigated. As seen in compressive loading, the cellular response may depend on the strain magnitude and loading frequency. The decreases in matrix synthesis previously observed at 10% tensile displacement may reflect an adaptive response to non-physiologic loading conditions. Alternatively, it could represent an injury response to excessive tensile strains. Examining the response to various amplitudes of cyclic tension would further our fundamental understanding of how tensile loading affects matrix synthesis and possibly lead to the development of an optimal loading regime for tissue engineered cartilages.

One complicating factor in studying different amplitudes of tension with the current system is determining the mechanical environment of the cells during dynamic loading. While different amplitudes of tension can be applied to the fibrin constructs, the precise stress and strain distributions have not been determined, making it difficult to

correlate cellular responses with specific mechanical stimuli. In addition, the fibrin construct is a hydrated gel that allows culture media to flow through its porous structure during loading. As a result, different tension protocols may alter the hydrostatic pressures, fluid velocities, and convective transport throughout the construct.

The goal of this study was to investigate the influence of oscillatory tension amplitude on chondrocyte matrix synthesis. Experimental studies examined the biosynthetic response to a range of tension amplitudes at a fixed oscillatory frequency. A finite element model of the fibrin construct was also created to determine how the different amplitudes of overall displacement affect the mechanical environment of cells within the construct.

A.2 MATERIALS AND METHODS

A.2.1 Materials

Bovine stifle joints were from Research 87 (Marlborough, MA). Dimethyl sulfoxide (DMSO), calcium chloride, and Triton X-100 were from Fisher Scientific (Pittsburgh, PA). Fetal bovine serum (FBS) was from Mediatech (Herndon, VA) and fibrinogen and thrombin were from ICN (Costa Mesa, CA). Ascorbate, ε-aminocaproic acid, ammonium acetate, and Hoechst 33258 dye were from Sigma (St. Louis, MO). Proteinase-K and formaldehyde were from EM Science (Gibbstown, NJ) and ^{3}H-proline and ^{35}S-sodium sulfate were from American Radiolabeled Chemicals (St. Louis, MO). Alexa Fluor® 546 conjugated phalloidin (A-22283) was from Molecular Probes (Eugene, OR). Collagen type II antibody (ab300) was from Abcam (Cambridgeshire, UK),

aggrecan antibody was donated by Dr. John Sandy (Shriner's Hospital, Tampa, FL), and the FITC conjugated rabbit IgG antibody was from Sigma (St. Louis, MO). All other cell isolation and culture media reagents were from Invitrogen (Carlsbad, CA).

A.2.2 Cell Isolation and Construct Seeding

Articular cartilage was aseptically harvested from the femoropatellar grooves of a matched pair of immature bovine stifle joints, avoiding the deep vascularized and calcified cartilage layers. Tissue was then minced, and articular chondrocytes were isolated enzymatically using 0.2% collagenase in antibiotic/antimycotic supplemented Dulbecco's Modified Eagle's Medium (DMEM plus 50 μg/mL gentamycin sulfate, 100 μg/mL kanamycin sulfate, 100 U/mL penicillin, 100 μg/mL streptomycin, and 0.25 μg/mL Fungizone) for approximately 40 hours at 37 °C with gentle agitation. Cell solutions were filtered through a 74 μm mesh, centrifuged and washed multiple times, counted using a Coulter Multisizer II, frozen at 1°C per minute in DMEM with 20% FBS and 10% DMSO, and finally stored in liquid nitrogen.

Chondrocytes were later thawed, re-counted, and seeded into 1 mL oval shaped fibrin constructs at a density of $5x10^6$ cells/mL using custom polycarbonate molds. In addition to the cells, the fibrinogen solution was comprised of 50 mg/mL bovine fibrinogen, 2 mg/mL ε-aminocaproic acid, and 10% FBS (final concentrations), with 50 U/ml of the enzyme thrombin added to catalyze the gelation of the fibrinogen/cell mixture. The constructs were incubated for approximately 90 minutes and transferred from the custom molds to 8-well tissue culture plates with supplemented media (DMEM, 10% FBS, 2 mg/mL ε-aminocaproic acid, 10 mM non-essential amino acids, 10 mM

HEPES buffer, 50 mg/mL ascorbate, 0.4 mM L-proline, 50 μg/mL gentamycin, and 0.25 μg/mL Fungizone). Culture media were changed every two to three days throughout the duration of the study.

A.2.3 Cyclic Tensile Loading

After four days of unloaded culture, the final construct geometry was created by punching two 6 mm diameter holes in the constructs using a dermal biopsy punch and a custom template (Fig A.1A). All constructs were cultured for an additional 3 days before being transferred to either the unloaded chambers or tensile loading chambers. Cyclic tension was applied to the fibrin gels using a custom loading device, which consisted of both stationary and moveable pegs inserted into the holes of the constructs. The moveable pegs connected to a DC motor via a linear sliding mechanism, and the magnitude and frequency of tension was controlled by the position of the slide and input voltage, respectively (Fig A.1C).

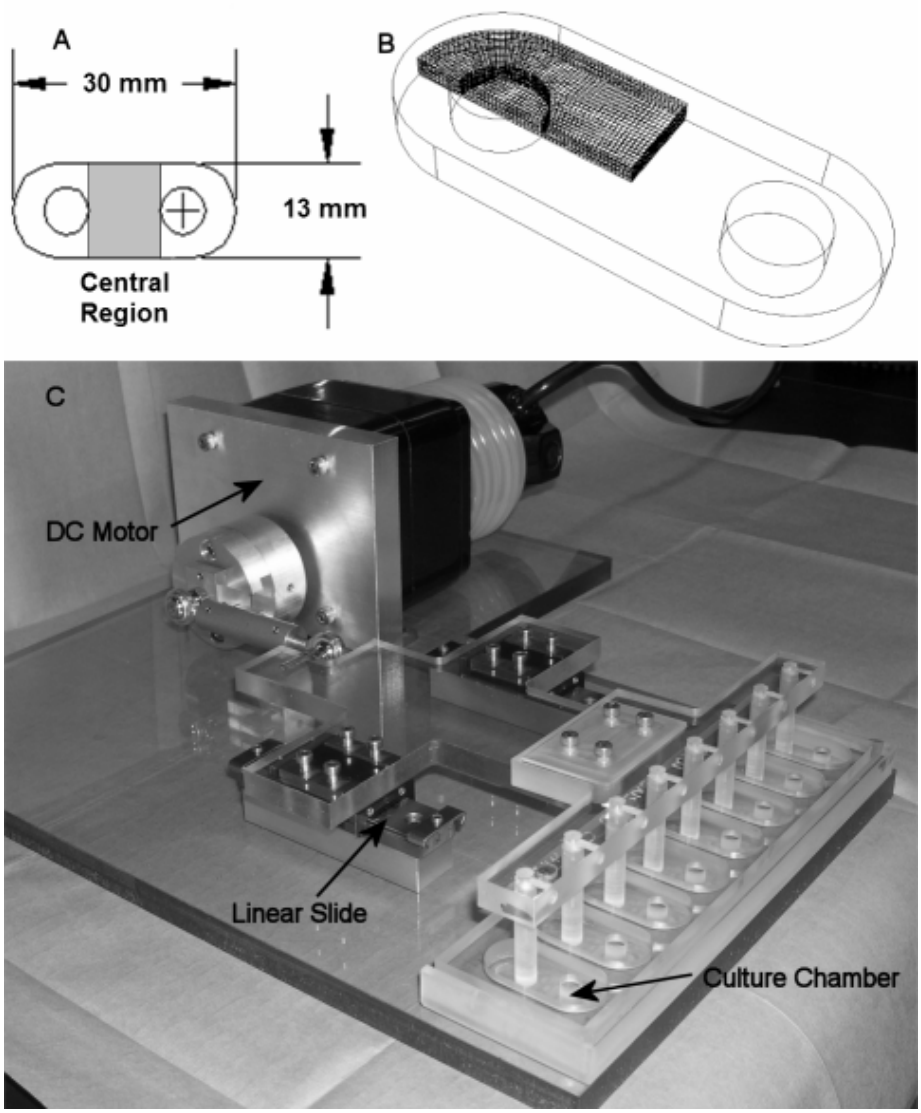

Figure A.1: Tensile loading system. (A) Geometry of the oval fibrin constructs indicating the central region used for biochemical and morphological analysis. (B) The finite element mesh of the gel and peg modeled one-eighth of the construct based on the three symmetry planes. (C) The custom tensile loading system dynamically loaded the constructs within the culture chambers via moveable pegs attached to a linear sliding mechanism and driven by a DC motor.

Two experiments were conducted to examine the effects of various amplitudes of cyclic tension on matrix synthesis. For the first experiment, constructs were subjected to 48 hours of continuous tensile loading at a frequency of 1.0 Hz and displacement amplitudes of 5% or 10% (peak-to-peak). In the second experiment, constructs were

again loaded continuously for 48 hours at 1.0 Hz but with displacement amplitudes of 10% or 20%. For both experiments, unloaded controls were cultured in chambers with fixed pegs to impose diffusive limitations similar to those seen by the loaded groups. During the final 20 hours of culture, the medium for six constructs in each group was further supplemented with 7.4 μCi/mL ^{3}H-proline and 5 μCi/mL ^{35}S-sodium sulfate. Two additional samples from each loading group were later used for confocal imaging.

A.2.4 Biochemical and Morphological Analyses

Constructs for biochemical analysis were washed 4 times for 30 minutes in phosphate buffered saline (PBS) supplemented with 0.8 mM sulfate and 1.0 mM L-proline to remove unincorporated radiolabeled precursors. Constructs were then sliced such that only the central region was used in the analyses, avoiding the areas outside the pegs (Fig A.1A). These pieces were weighed, frozen, lyophilized, weighed again, and solubilized using proteinase-K (80 mg per 1 mg tissue) in 100 mM ammonium acetate for approximately 24 hours at 60 °C. Digest solutions were analyzed for ^{3}H and ^{35}S incorporation as indicators of protein and proteoglycan synthesis, respectively, using a liquid scintillation counter. DNA and total sGAG content were also measured using the Hoechst 33258[145] and 1,9-DMMB[129] dye assays, respectively. All data were normalized to the wet mass of the section analyzed.

Two constructs from each group were analyzed for cell morphology and extracellular matrix deposition using confocal microscopy. Constructs were fixed in 10% neutral buffered formalin for 20 minutes at 4°C, washed twice for 5 minutes in PBS, permeabilized for 20 minutes using 1% Triton X-100, and again washed twice for 5

minutes in PBS. Blocking buffer (5% FBS in PBS) was added to the constructs for at least 10 minutes to minimize nonspecific antibody binding and reduce background staining. A primary solution containing either a 1:100 dilution of rabbit IgG anti-collagen type II or 1:50 dilution of rabbit IgG anti-aggrecan core protein antibodies was added to the constructs and incubated for 60 to 90 minutes with gentle agitation. Constructs were again washed with blocking buffer for at least 10 minutes and then a secondary solution containing 0.1 μg/mL Hoechst 33258 dye, a 1:50 dilution Alexa Fluor® 546 conjugated phalloidin, and a 1:150 dilution of FITC conjugated goat anti-rabbit IgG was added. Constructs were then incubated for 60 to 90 minutes with gentle agitation before finally being washed twice for 5 minutes in PBS. All images were obtained using laser scanning confocal microscopy and oil emersion objectives at a magnification of either 40X or 63X (Zeiss LSM 510).

Biochemical data were analyzed using ANOVA with significance at $p<0.05$ and Tukey's test for post-hoc analyses. All data are presented as mean ± standard error of the means (SEM).

A.2.5 Finite Element Model

A poroelastic finite element (FE) model of the fibrin construct was developed with Abaqus 6.3-3 (HKS, Pawtucket, RI) to analyze the strain distributions during tensile loading (Fig A.1B). The fibrin gel and infiltrating medium were modeled using 6972 linear brick elements coupled with pore pressure (C3D8P), and the peg was modeled using 1536 linear elastic elements (C3D8) were used for the peg. Contact surfaces with the small sliding formulation modeled the interaction between the two objects. The gel

was assigned an isotropic modulus of 22 kPa [258], Poisson's ratio of 0.3, and permeability of $5x10^{-10}$ $m^4/N\text{-}s$ [259], and the peg was assigned a modulus substantially higher than that of the gel (220 MPa). Based on the symmetry, only one-eighth of the construct was required for the FE model, and displacements were constrained across the planes of symmetry. Zero pore pressure was fixed at the construct's free surfaces and there was no fluid flow between the contact surfaces of the gel and the peg. The initial pore pressure throughout the gel was also assumed to be zero. The loading experiments were simulated by sinusoidally displacing the peg 0.5mm, 1mm, or 2mm, corresponding to the 5%, 10%, and 20% loading experiments, respectively. The displacements were applied at a frequency of 1.0Hz for five cycles using 100 uniform time steps and the non-linear geometry option for large deformations. Within the region of interest, principal strains, pore pressures, and fluid velocities at the maximum displacement were calculated for post-processing analysis.

A.3 RESULTS

A.3.1 Radiolabel and Biochemical Analyses

Protein synthesis in cyclically stretched gels was not significantly different than that of the unloaded controls for any amplitude of tension (Fig A.2A). In the first experiment, however, 10% displacement significantly decreased proteoglycan (PG) synthesis ($p<0.05$), while 5% displacement had no effect on PG synthesis (Fig A.2B). In the second loading experiment, both 10% and 20% displacements inhibited PG synthesis compared to the controls ($p<0.05$), but there were no differences between the two loaded groups (Fig A.2B). There were no significant differences between any of the loading

groups in the DNA or total sGAG contents accumulated during the entire nine day culture (data not shown).

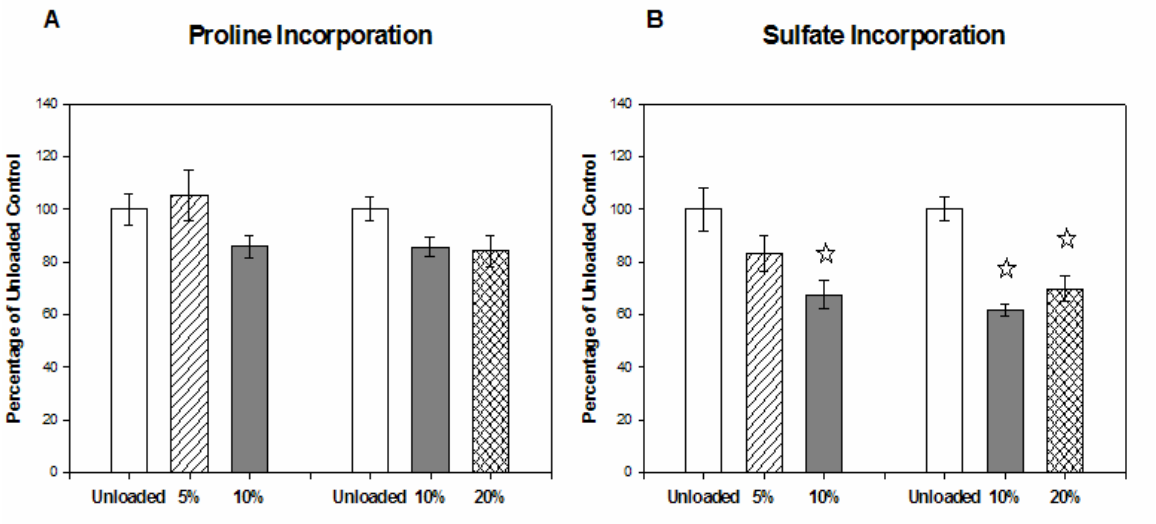

Figure A.2: Matrix synthesis rates. (A) Protein synthesis measured by ^{3}H-proline incorporation was not affected by any amplitude of dynamic tension. (B) Proteoglycan synthesis measured by ^{35}S-sulfate incorporation was inhibited by 10% and 20% tension, but not by 5% tension. N=6 per loading group. ★ $p<0.05$.

A.3.2 Confocal Imaging

Immuno-histochemical staining revealed that the chondrocytes synthesized and assembled extracellular type II collagen (Fig A.3A) and aggrecan core protein (Fig A.3B). Most of the cells also maintained a rounded morphology as indicated by the F-actin cytoskeletal staining. Some of the cells at the surface of the gel had a more spread, fibroblastic morphology. In addition, these cells did not stain positively for extracellular Type II collagen or aggrecan. There were no observable differences in morphology between any of the loading groups.

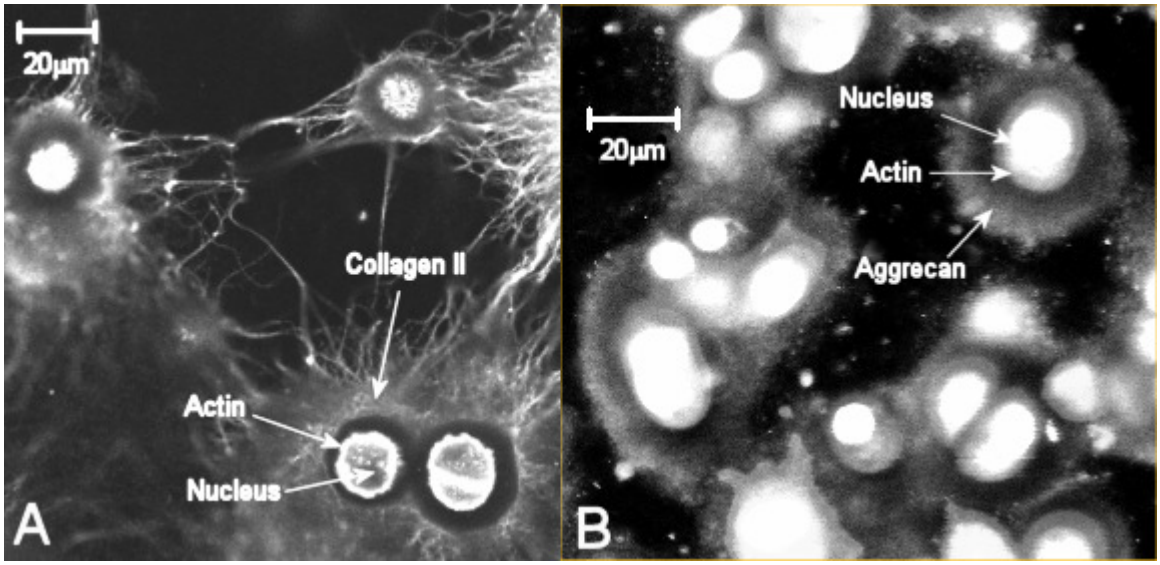

Figure A.3: Cell morphology and matrix organization. For all loading groups, chondrocytes in the construct interiors stained positively for extra-cellular (A) type II collagen and (B) aggrecan core protein and maintained a rounded morphology as seen by F-actin staining with phalloidin.

A.3.3 Finite Element Analysis

Contour plots of the maximum and minimum principal strains show the relative distribution of strains through the middle cross-section of the gel (Fig A.4). At the maximum displacement during cyclic loading, the peak strains are located around the holes in the construct where the peg makes contact. Within the central region (isolated for biochemical analyses), the maximum principal strains were greatest along the outer edge of the construct and varied across the section (XY plane). However, there was little variation in strains through the thickness of the construct (along the Z-direction).

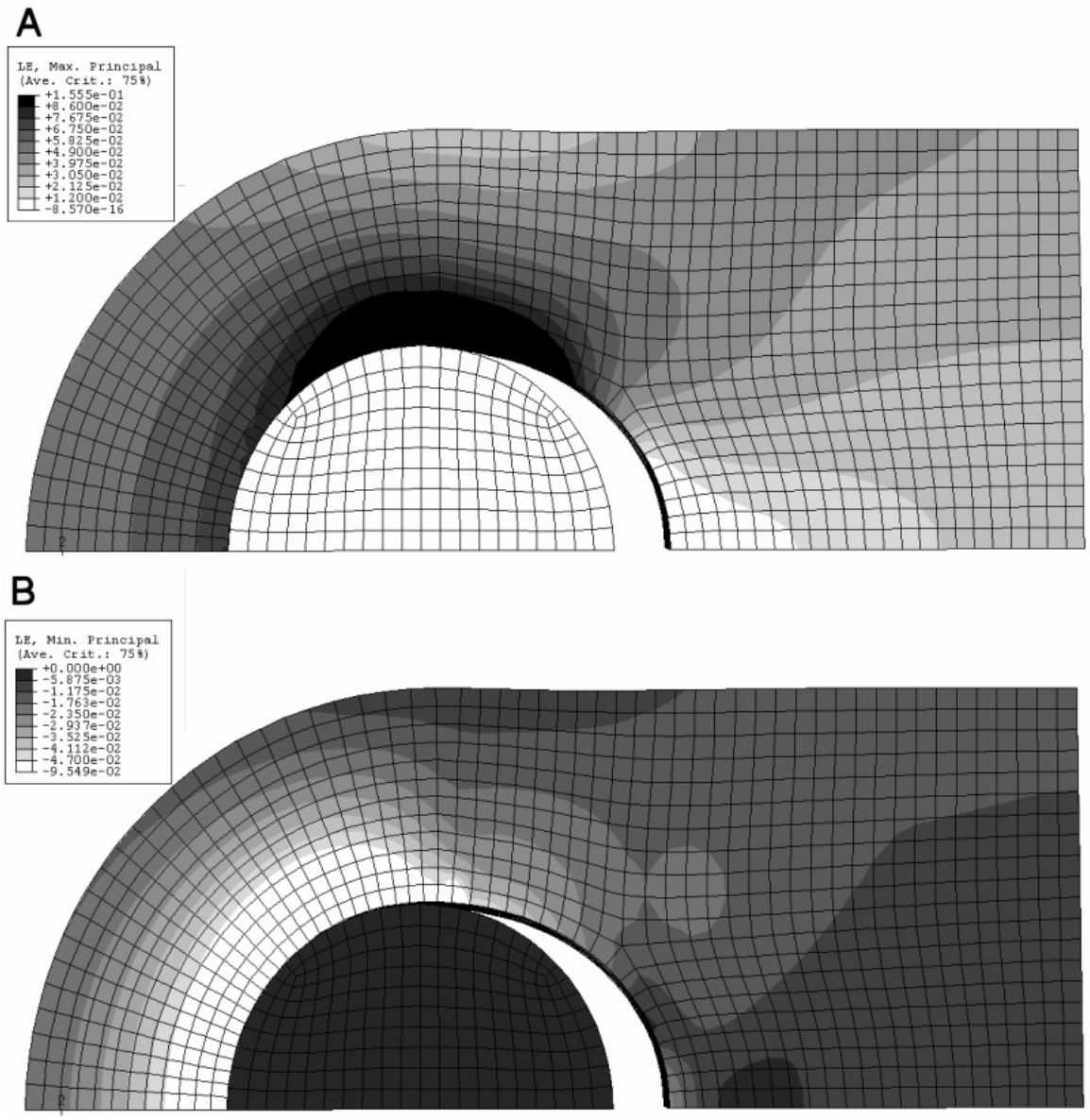

Figure A.4: Principle strains. (A) Maximum principal strains predicted by the finite element model varied across the central region of the construct and were greatest around the hole. (B) Minimum principal strains also varied across the central region and were greatest on the outer edge of the hole.

For 10% total displacement, the maximum principal strains in the region of interest ranged from 0.93–5.2% (Fig A.5). The magnitude of strains was approximately proportional to the overall level of displacement such that the range of maximum principal strains was 0.51 –2.6% for 5% total displacement and 1.8–10% for 20% total

displacement. These results indicate that the principal strains varied greatly within the central region of the construct and there was a large degree of overlap in strains among the different levels of displacement.

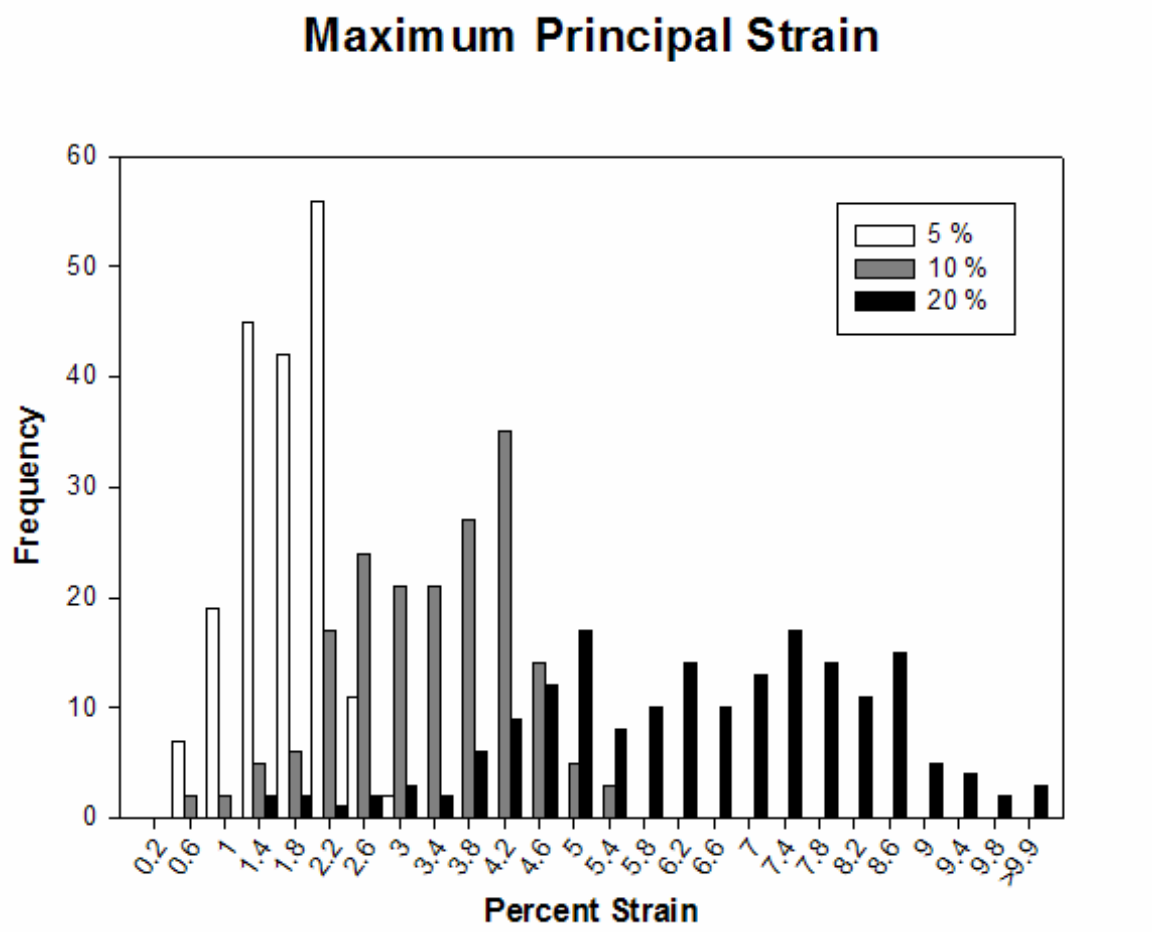

Figure A.5: Strain distributions. The histogram of predicted maximum principal strains for elements within the central region of the construct indicates both a large variation in strain magnitude at each displacement amplitude and large overlaps in strains between the different displacement amplitudes. The strains were approximately proportional to the level of displacement.

The poroelastic behavior of the fibrin gel was examined under tensile loading. A contour plot of the interstitial fluid pressure at the maximum displacement demonstrates how the three-dimensional gradients developed throughout the construct. At this point in the cycle, the pressures were negative (≈-40 Pa) with respect to the surrounding fluid (Fig

A.6A). The negative pressure gradients resulted in fluid flow into the construct in all directions (Fig A.6B,C,D) and velocity magnitudes ranged from 0 to 20μm/s at 10% total displacement. Within the central region of interest, velocities were greatest at the free surfaces, zero at the center of the construct, and varied non-linearly along each axis. In addition, fluid flow was greatest along the Z-axis due to the steep pressure gradient through the thickness of the gel. Similar trends in fluid pressure and velocity were seen for all displacement amplitudes, with magnitudes roughly proportional to the overall displacement.

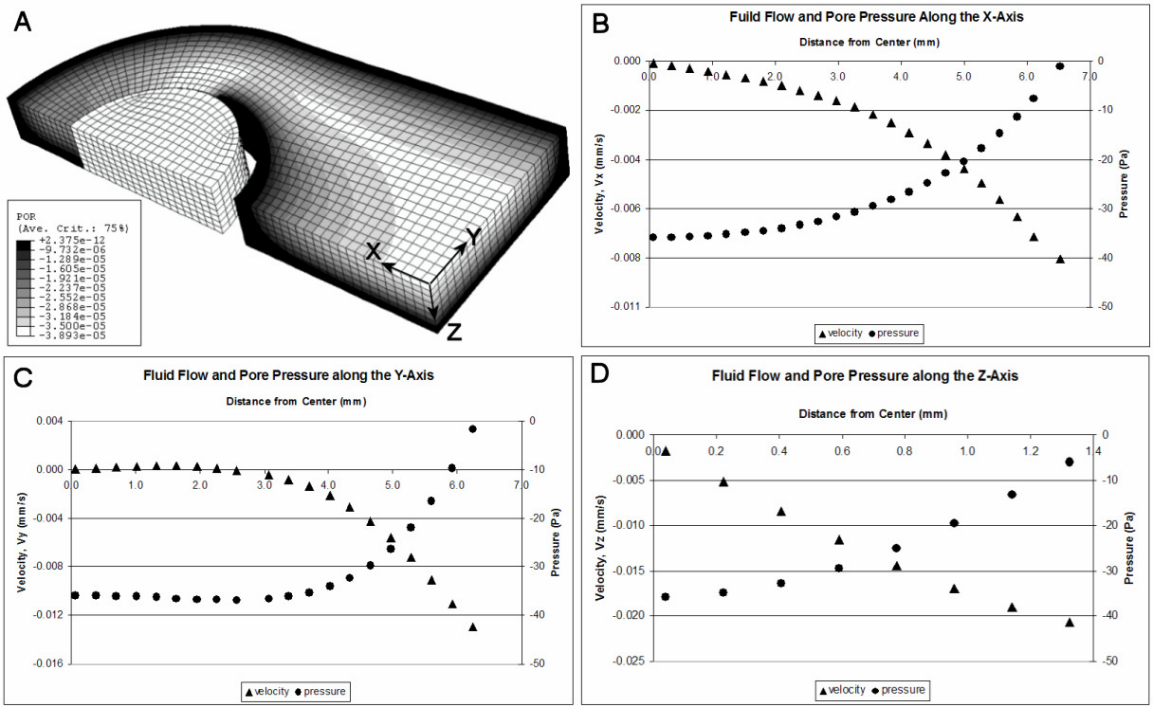

Figure A.6: Poroelastic properties. (A) The predicted hydrostatic pressure (MPa) within the gel was greatest at the center and zero at the outer surface. (B,C,D) The predicted fluid flow varied non-linearly along each of the central axes of the gel and was greatest in the Z-direction due to the high pressure gradients across the thickness. All results correspond to the point of maximal peg displacement.

A.4 DISCUSSION

The goal of this study was to examine how various amplitudes of dynamic tension influence chondrocyte matrix synthesis. In both loading experiments, displacement amplitudes of 10% consistently inhibited proteoglycan (PG) synthesis but not protein synthesis relative to the unloaded controls. The 20% displacement loading also inhibited PG synthesis to the same extent as 10% and did not affect protein synthesis, while the 5% displacement did not decrease PG or protein synthesis. These results suggest that there may be a threshold amplitude of cyclic tension that inhibits chondrocyte production of proteoglycans. This response is also consistent with previous experiments where 10% displacement at 1.0 Hz decreased PG synthesis in chondrocytes and fibrochondrocytes[257]. However, the significant decreases in protein synthesis seen in the previous study were not seen here. This inconsistency may be due to variability in cellular activity between animals or to a relatively small inhibition of protein synthesis, making any effect difficult to consistently detect at statistically significant levels.

A small number of previous studies have investigated the effects of cyclic tension on chondrocyte matrix synthesis in monolayer culture. In general, higher magnitudes of tensile strain (~17%) inhibited PG synthesis while smaller strains (~5%) increased synthesis[260-262]. Although, the local environment and cellular deformations in 3D and monolayer culture are significantly different, these results are fairly consistent with the magnitude dependent inhibition of PG synthesis seen in the current study.

The immunostaining and confocal microscopy images demonstrated that chondrocytes within the fibrin gels maintained their phenotype in all loading groups. These cells stained positively for extracellular type II collagen and aggrecan core protein

indicating synthesis of the major articular cartilage matrix components. In addition, cells within the construct maintained rounded chondrocyte morphologies. Based on the spread morphology and lack of matrix staining, cells at the surface of the construct appeared to dedifferentiate similar to chondrocytes in monolayer culture[204]. In previous studies, cyclic tension induced a significant number of chondrocytes within the gel to take on a three-dimensional stellate morphology[263]. However this phenomenon was not observed in the current study and was most likely due to inter-animal variability

The results of the finite element analyses revealed important insights into the mechanical environment of the fibrin construct during cyclic tensile loading. Within the central region (analyzed for matrix synthesis), there was a fairly wide range of strains. For example, the maximum principal strains at 10% displacement were approximately 1-5%. As a result, the chondrocytes within the central region most likely experienced a wide range of cellular deformations, which could have produced a variety of biosynthetic responses. Previous poroelastic simulations of the micro-environment in articular cartilage predicted large variability in the local cellular strains even for uniform macroscopic strains due to mismatches in the cell-matrix mechanical properties and complexity of the extracellular matrix[264]. Such a non-uniform strain field therefore makes it difficult to isolate how specific amplitudes of dynamic tension affect matrix synthesis.

This issue is further complicated by an overlap in the range of principal strains at different displacement magnitudes. As seen in Figure A.5, the maximum principal strains for the 10% and 20% loading groups overlapped between 1.4% and 5.4% strains, and the 5% and 10% loading groups overlapped between 0.6% and 3.0%. With a large

number of elements in each group experiencing similar deformations, it is not surprising that no significant differences in matrix synthesis were detected between any of the loaded groups. Therefore, it is possible that cyclic tension inhibits PG synthesis in a dose dependent manner rather than as a threshold response, but an experimental system with a more uniform strain field is necessary to distinguish the two hypotheses.

The porolastic model of the fibrin gel also provided interesting information about the hydrostatic pressure and fluid flow distributions, which have been theorized as stimuli of chondrocyte matrix synthesis[94,265-268]. Due to the high permeability of the fibrin gel, the media easily flowed through the construct, and only minimal hydrostatic pressures developed (≈40Pa). As a result, the total stress within the gel was primarily carried by the solid component, unlike articular cartilage tissue where the low permeability causes the total stress to include larger hydrostatic pressures[269]. *In vivo* fluid velocities in articular cartilage have also been estimated within the same order of magnitude as those calculated in this study[266,270], suggesting that cyclic tension inhibits proteoglycan synthesis via deformational loading rather than through changes in convective nutrient transport. As seen with the calculated strain distributions, identifying the extent to which pressure, fluid flow or other aspects of the local environment regulate matrix synthesis is difficult due to the variability throughout the construct.

The combination of loading experiments and finite element analysis allowed for detailed examination of how the amplitude of cyclic tension influences chondrocyte matrix synthesis, and several conclusions can be drawn from this study. (1) Dynamic tension consistently inhibits proteoglycan production. (2) This response depends on the magnitude of tension in either a threshold or dose dependent manner. (3) Mechanical

parameters vary greatly within the central region of the fibrin construct, possibly inducing a variety of cellular responses. Clearly, future studies using an experimental system with a more uniform mechanical environment are necessary to isolate the effects of various amplitudes. In addition, other loading parameters such as strain rate and duration of loading should be investigated to fully characterize the effects of oscillatory tension on chondrocyte matrix synthesis.

APPENDIX B

PRELIMINARY DATA: INFLUENCES OF FNIII7-10 AND GFOGER ON BMSC MORPHOLOGY AND CHONDROGENESIS

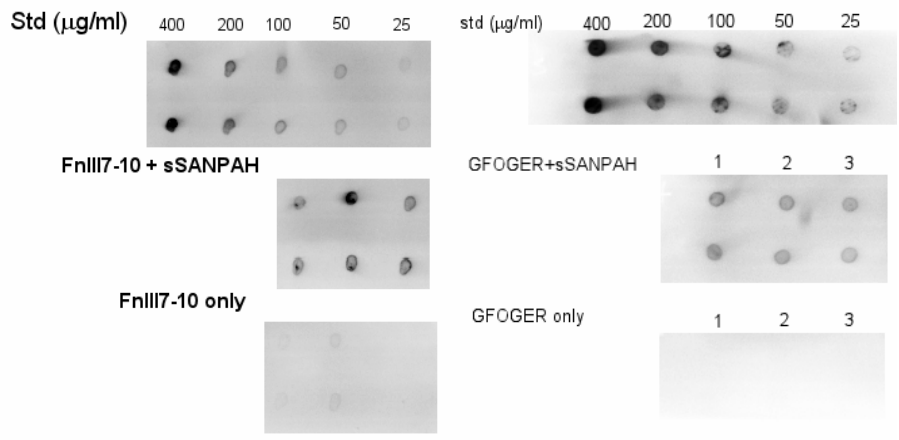

Figure B.1: Immunoblot detection of FnIII7-10 and GFOGER. Biotinylated FnIII7-10 and GFOGER peptides were conjugated to 3% Seaprep agarose as previously described (Chapter 7) with initial densities of 400μg/ml and 200μg/ml, respectively. Agarose gels were washed extensively and digested with agarase. Immunoblot detection with the anti-biotin antibody demonstrated that the ligands were conjugated to the agarose with approximately 25% efficiency, and the unbound ligand was removed by washing.

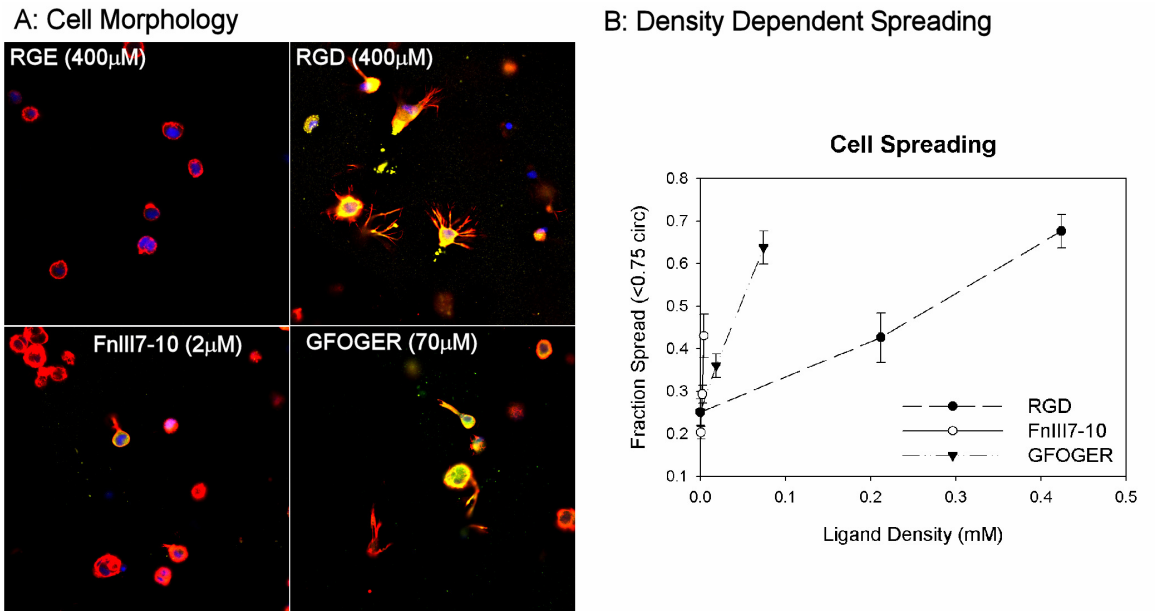

Figure B.2: BMSC morphology in modified agarose gels. BMSCs were seeded into modified agarose gels with varying densities of RGE, RGD, FnIII7-10, and GFOGER. (A) Cell morphology was examined by immunofluorescence staining of the f-actin cytoskeleton (red) and vinculin expression (green) and imaged with a confocal microscope. (DNA = blue). (B) Density-dependent changes in morphology were quantified by calculating the fraction of spread cells (circularity < 0.75) over a range of RGD, FnIII7-10, and GFOGER ligand densities. N=3 fields/condition.

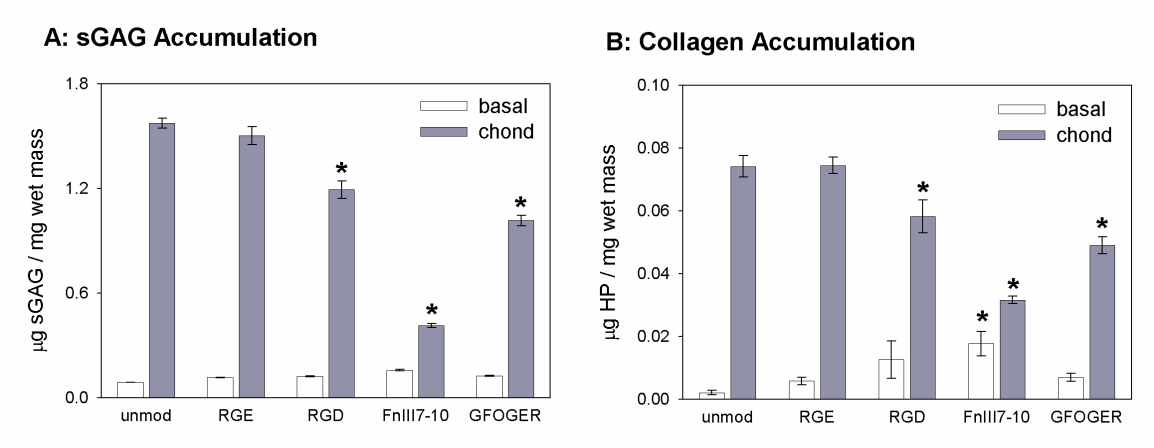

Figure B.3: Influences of FnIII7-10 and GFOGER interactions on BMSC chondrogenesis. BMSCs were seeded into 3% agarose gels that were undmodified or modified with RGE (400μM), RGD (400μM), FnIII7-10 (5μM), or GFOGER (70μM). These ligand densities promoted similar levels of cell spreading (50-70%). BMSCs were cultured up to 7 days in basal or chondrogenic (10ng/ml TGF-b1 and 100nM dexamethasone) medium and analyzed for (A) sGAG and (B) total collagen accumulation. N=6/condition, *P<0.05 with unmod in same medium.

APPENDIX C

LABORATORY PROTOCOLS

C.1 Bone Marrow Harvest and Stromal Cell Isolation

1. Clean away all the tissue around the mid diaphysus of the tibia or femur, then take it into the culture hood. Rinse the bone with ethanol and cut it in half with a hack saw and autoclaved blade.

2. Scoop out the marrow with forceps and a small spatula trying not to scrape the bone too much. Place the marrow in a concial with PBS, about 10-20ml/half bone.

3. Break up the marrow by pipetting up and down until it flows somewhat smoothly (50ml pipet, then 10ml). Pass the marrow through 16, 18, and 20 gage needles. Replace the needle if it clogs, and do not press the syringe too hard or it will kill the cells.

4. Spin down the cells at 1200xG for 20 minutes. Sometimes the cells will spin down easily, sometimes not at all. Diluting in PBS (40ml/conical) or spinning longer can help. Aspirate off the fatty layer and excess blood and resuspend in PBS.

5. To count the cells, take 100µl of the cell suspension plus 100µl of 4% acetic acid (lyses blood cells) and count this sample. The viability may be low and there will be a lot of debris in the sample, but you just need a rough estimate of cells.

6. Pre-plate 20e6 cells in 5ml DMEM for 30min on a TC Petri dish, then transfer to a T-150 and add 25 ml expansion media (low-glucose DMEM, 10% FBS, 1% antibiotic/antimycotic, and 1ng/ml basic-FGF. After 2 days remove the media and rinse vigorously. Add 25ml fresh expansion media and continue culturing until nearly confluent.

7. This is often a good point to freeze the cells (20%FBS and 10%DMSO).

C.2 Peptide Conjugation to Alginate

1. Prepare reaction buffer: 0.1M MES, 0.3M NaCl, pH 6.5

2. Dissolve 1% Pronova LVG in MES buffer (requires warming to 45C and stirring for several hours).

3. Prepare 100X solutions of EDC (82mg/ml) and sulfo-NHS (46.5mg/ml) in the MES buffer immediately before the reaction.

4. Add the EDC and sulfo-NHS to the 1% alginate solution for a final concentration of 0.82mg/ml EDC and 0.465mg/ml sulfo-NHS, vortex and react for 5min at room temperature.

5. Add the RGE/D peptide to the alginate for a final concentration of 0.1mg/ml. Mix thoroughly and allow the solution to react at room temperature overnight.

6. Dialyze against water (20ml alginate in 2L water) to remove the unbound peptide and excess reactants. Change the water after 2h, 24h, and 48h.

7. Lyophilize the purified alginate, reconstitute in ion-free PBS at 2%, and sterile filter with 0.8μm filter.

C.3 Peptide Conjugation to Agarose

*In the dark and sterile

1. Weigh out and dissolve the sulfo-SANPAH (Pierce, MW = 492) in sterile water. Use at least 10X molar excess of the sSANPAH compared to the protein to be conjugated.

2. Give the solution a quick spin and take the supernatant to avoid the undissolved SANPAH. Combine 1 volume of the sSANPAH with one volume of the protein/peptide solution (in PBS) and allow it to react for 4 hours at room temp.

3. Melt the 4% SeaPrep agarose in a 45C water bath or in the autoclave to sterilize, and cool the agarose to 37C.

4. Turn on the UV lamp (365nm wavelength) and allow it to warm up for at least 10min.

5. Add 1 volume of the peptide-sSANPAH mixture to 3 volumes of the agarose and vortex thoroughly.

6. Transfer the mixture to a 12-well-plate. Place the well in the center of the UV light a few inches away from the UV bulb for 3 min. Placing a piece of white paper under the plate will allow the most intense areas of UV to be easily located.

7. Allow the agarose to gel at 4C for 30 minutes.

8. Wash the gel with PBS 5X: 2h and 4 x 24h

Notes:

The volumes and concentrations of the peptide solution and agarose will depend on the experiment.

Avoid placing more than 1ml of the agarose/peptide mixture in each 12-well plate, as this will reduce the washing volume and may not result in even conjugation through the depth of the gel upon exposure to UV light.

The conjugation and washing can be kept sterile by working inside the hood. Alternatively, the agarose can be sterile filtered while it's liquid, but this is really difficult.

C.4 RNA Isolation from Fibrin, Agarose, and Alginate Gels

Fibrin/Agarose:

1. Dissociate the gels in a small volume of RLT Buffer plus BME (~200µl) at 65°C.
2. Add 1ml of Trizol reagent and incubate at room temperature for 15 minutes.
3. Centrifuge at 12000XG for 10 minutes.
4. Transfer the supernatant to a new tube and discard the pellet.
5. Add 200µl of chloroform and vortex.
6. Incubate for 2-3 minutes at room temperature.
7. Centrifuge at 12000XG for 15 minutes. The mixture will separate into a red organic phase, a white interphase, and clear aqueous phase, containing the nucleic acids.
8. Pipette the aqueous phase to a new tube being careful not to mix the phases.
9. Precipitate the RNA with 500µl of isopropyl alcohol.
10. Incubate at room temp for 10 minutes.
11. Centrifuge at 12000XG for 10 minutes.
12. Discard the supernatant and resuspend in 350µl of RLT.

13. Continue with the RNeasy isolation protocol for animal tissues, including homogenization with the Qiashredder.

Alginate:

1. Rinse the gels with ion free PBS.
2. Dissociate the alginate with 100mM EDTA in ion free PBS.
3. Spin at 1200XG for 8 minutes.
4. Remove the supernatant and resuspend in 350µl RLT Buffer plus BME.
5. Continue with the RNeasy isolation protocol for animal tissues, including homogenization with the Qiashredder.

Measuring RNA Quantity:

1. After eluting the RNA from the RNeasy columns, take 5µl and dilute 1:20 into 100µl of nuclease free water in a fresh tube.
2. Store the remaining RNA at -80C.
3. Read the absorbance of each sample at 260 and 280nm with the UV spectrophotometer.
4. Total RNA = OD_{260} * 43µg/ml/OD * 20 * 0.055ml.
5. The ideal 260/280 ratio is 1.8-2.0 and lower ratios indicate protein contamination.

C.5 Reverse transcription for real-time PCR

1. Take a volume from each sample equal to 1µg of total RNA and transfer to a new tube.
2. If the volume is less than 9.75µl, bring the volume up to 9.75µl. If the volume is greater than 9.75µl, speedvac the sample until all the volume has been evaporated and resuspend in 9.75µl of water.
3. Incubate at 70C for 10 minutes to remove secondary structures.
4. While the samples are incubating, prepare the RT-master mix in a new tube. Volumes per reaction:
   $MgCl_2$ 4µl

RT 10X Buffer	2µl
DNTPs	2µl
Oligo dT primers	1µl
RNasin	0.5µl

*Make enough for each sample plus 2 extra and keep everything on ice.

5. Transfer the samples to room temperature for 2 minutes.

6. While the vials are cooling add enough AMV reverse transcriptase to the master mix for 0.75µl per reaction plus 2 extra. *Keep the reverse transcriptase on ice and return to the -20C freezer immediately after use.

7. Add 10.25µl to each sample and centrifuge briefly to collect the reaction mix.

8. Incubate the samples at 42C for 60 minutes.

9. Incubate the samples at 90C for 5 minutes.

10. Transfer to ice for 5 minutes.

11. Add 30µl to each sample to bring the total volume to 50µl.

REFERENCES

1. Ahmed AM, Burke DL. In-vitro measurement of static pressure distribution in synovial joints--Part I: Tibial surface of the knee. J Biomech Eng 1983;105(3):216-25.

2. Mow VC, Ratcliffe A. Structure and function of articular cartilage and meniscus. In: Mow VC, Hayes WC, editors. Basic Orthopaedic Biomechanics; 1997. p 113-177.

3. Maroudas AI. Balance between swelling pressure and collagen tension in normal and degenerate cartilage. Nature 1976;260(5554):808-9.

4. Lai WM, Hou JS, Mow VC. A triphasic theory for the swelling and deformation behaviors of articular cartilage. J Biomech Eng 1991;113(3):245-58.

5. Muir H, Bullough P, Maroudas A. The distribution of collagen in human articular cartilage with some of its physiological implications. J Bone Joint Surg Br 1970;52(3):554-63.

6. Wilson W, Huyghe JM, van Donkelaar CC. Depth-dependent compressive equilibrium properties of articular cartilage explained by its composition. Biomech Model Mechanobiol 2007;6(1-2):43-53.

7. Aspden RM, Hukins DW. Collagen organization in articular cartilage, determined by X-ray diffraction, and its relationship to tissue function. Proc R Soc Lond B Biol Sci 1981;212(1188):299-304.

8. Yarker YE, Aspden RM, Hukins DW. Birefringence of articular cartilage and the distribution on collagen fibril orientations. Connect Tissue Res 1983;11(2-3):207-13.

9. Eyre DR, Muir H. The distribution of different molecular species of collagen in fibrous, elastic and hyaline cartilages of the pig. Biochem J 1975;151(3):595-602.

10. Minns RJ, Steven FS. The collagen fibril organization in human articular cartilage. J Anat 1977;123(Pt 2):437-57.

11. Haynesworth SE, Carrino DA, Caplan AI. Characterization of the core protein of the large chondroitin sulfate proteoglycan synthesized by chondrocytes in chick limb bud cell cultures. J Biol Chem 1987;262(22):10574-81.

12. Maroudas A, Muir H, Wingham J. The correlation of fixed negative charge with glycosaminoglycan content of human articular cartilage. Biochim Biophys Acta 1969;177(3):492-500.

13. Gu WY, Lai WM, Mow VC. Transport of fluid and ions through a porous-permeable charged-hydrated tissue, and streaming potential data on normal bovine articular cartilage. J Biomech 1993;26(6):709-23.

14. Buschmann MD, Grodzinsky AJ. A molecular model of proteoglycan-associated electrostatic forces in cartilage mechanics. J Biomech Eng 1995;117(2):179-92.

15. Bayliss MT, Venn M, Maroudas A, Ali SY. Structure of proteoglycans from different layers of human articular cartilage. Biochem J 1983;209(2):387-400.

16. Hardingham TE, Fosang AJ. The structure of aggrecan and its turnover in cartilage. J Rheumatol Suppl 1995;43:86-90.

17. Murphy G, Hembry RM, Hughes CE, Fosang AJ, Hardingham TE. Role and regulation of metalloproteinases in connective tissue turnover. Biochem Soc Trans 1990;18(5):812-5.

18. Siczkowski M, Watt FM. Subpopulations of chondrocytes from different zones of pig articular cartilage. Isolation, growth and proteoglycan synthesis in culture. J Cell Sci 1990;97 (Pt 2):349-60.

19. Aydelotte MB, Greenhill RR, Kuettner KE. Differences between sub-populations of cultured bovine articular chondrocytes. II. Proteoglycan metabolism. Connect Tissue Res 1988;18(3):223-34.

20. Brodkin KR, Garcia AJ, Levenston ME. Chondrocyte phenotypes on different extracellular matrix monolayers. Biomaterials 2004;25(28):5929-38.

21. Stokes DG, Liu G, Coimbra IB, Piera-Velazquez S, Crowl RM, Jimenez SA. Assessment of the gene expression profile of differentiated and dedifferentiated human fetal chondrocytes by microarray analysis. Arthritis Rheum 2002;46(2):404-19.

22. Kolettas E, Buluwela L, Bayliss MT, Muir HI. Expression of cartilage-specific molecules is retained on long-term culture of human articular chondrocytes. J Cell Sci 1995;108 (Pt 5):1991-9.

23. Messner K, Gao J. The menisci of the knee joint. Anatomical and functional characteristics, and a rationale for clinical treatment. J Anat 1998;193 (Pt 2):161-78.

24. Bland YS, Ashhurst DE. Changes in the content of the fibrillar collagens and the expression of their mRNAs in the menisci of the rabbit knee joint during development and ageing. Histochem J 1996;28(4):265-74.

25. Roughley PJ, McNicol D, Santer V, Buckwalter J. The presence of a cartilage-like proteoglycan in the adult human meniscus. Biochem J 1981;197(1):77-83.

26. Roughley PJ, White RJ. The dermatan sulfate proteoglycans of the adult human meniscus. J Orthop Res 1992;10(5):631-7.

27. Fithian DC, Kelly MA, Mow VC. Material properties and structure-function relationships in the menisci. Clin Orthop Relat Res 1990(252):19-31.

28. Gao J, Messner K. Quantitative comparison of soft tissue-bone interface at chondral ligament insertions in the rabbit knee joint. J Anat 1996;188 (Pt 2):367-73.

29. Skaggs DL, Weidenbaum M, Iatridis JC, Ratcliffe A, Mow VC. Regional variation in tensile properties and biochemical composition of the human lumbar anulus fibrosus. Spine 1994;19(12):1310-9.

30. Ochi K, Daigo Y, Katagiri T, Saito-Hisaminato A, Tsunoda T, Toyama Y, Matsumoto H, Nakamura Y. Expression profiles of two types of human knee-joint cartilage. J Hum Genet 2003;48(4):177-82.

31. Wildey GM, McDevitt CA. Matrix protein mRNA levels in canine meniscus cells in vitro. Arch Biochem Biophys 1998;353(1):10-5.

32. Wilson CG. Enzyme-mediated Catabolism of Articular Cartilage and Fibrocartilage Georgia Institute of Technology; 2007.

33. Imler SM, Vanderploeg EJ, Levenston ME. Differential behavior of fibrochondrocytes from distinct regions of the meniscus. Trans. Orthop. Res. Soc. 2005;51:1497.

34. Kavanagh E, Ashhurst DE. Distribution of biglycan and decorin in collateral and cruciate ligaments and menisci of the rabbit knee joint. J Histochem Cytochem 2001;49(7):877-85.

35. Imler SM, Doshi AN, Levenston ME. Combined effects of growth factors and static mechanical compression on meniscus explant biosynthesis. Osteoarthritis Cartilage 2004;12(9):736-44.

36. Vanderploeg EJ, Imler SM, Brodkin KR, Garcia AJ, Levenston ME. Oscillatory tension differentially modulates matrix metabolism and cytoskeletal organization in chondrocytes and fibrochondrocytes. J Biomech 2004;37(12):1941-52.

37. Hunziker EB. Articular cartilage repair: basic science and clinical progress. A review of the current status and prospects. Osteoarthritis Cartilage 2002;10(6):432-63.

38. Control CfD. Update: direct and indirect costs of arthritis and other rheumatic conditions--United States, 1997. MMWR Morb Mortal Wkly Rep 2004;53(18):388-9.

39. Setton LA, Mow VC, Muller FJ, Pita JC, Howell DS. Mechanical properties of canine articular cartilage are significantly altered following transection of the anterior cruciate ligament. J Orthop Res 1994;12(4):451-63.

40. Ratcliffe A, Billingham ME, Saed-Nejad F, Muir H, Hardingham TE. Increased release of matrix components from articular cartilage in experimental canine osteoarthritis. J Orthop Res 1992;10(3):350-8.

41. Guilak F, Ratcliffe A, Lane N, Rosenwasser MP, Mow VC. Mechanical and biochemical changes in the superficial zone of articular cartilage in canine experimental osteoarthritis. J Orthop Res 1994;12(4):474-84.

42. Martin JA, Buckwalter JA. Human chondrocyte senescence and osteoarthritis. Biorheology 2002;39(1-2):145-52.

43. Tran-Khanh N, Hoemann CD, McKee MD, Henderson JE, Buschmann MD. Aged bovine chondrocytes display a diminished capacity to produce a collagen-rich, mechanically functional cartilage extracellular matrix. J Orthop Res 2005;23(6):1354-62.

44. Drosos GI, Pozo JL. The causes and mechanisms of meniscal injuries in the sporting and non-sporting environment in an unselected population. Knee 2004;11(2):143-9.

45. Hede A. Treatment of meniscal lesions in the knee. Epidemiological, clinical and experimental aspects. Dan Med Bull 1993;40(3):317-31.

46. Walker PS, Erkman MJ. The role of the menisci in force transmission across the knee. Clin Orthop Relat Res 1975(109):184-92.

47. Donahue TL, Hull ML, Rashid MM, Jacobs CR. A finite element model of the human knee joint for the study of tibio-femoral contact. J Biomech Eng 2002;124(3):273-80.

48. Hede A, Svalastoga E, Reimann I. Articular cartilage changes following meniscal lesions. Repair and meniscectomy studied in the rabbit knee. Acta Orthop Scand 1991;62(4):319-22.

49. Kurtz S, Mowat F, Ong K, Chan N, Lau E, Halpern M. Prevalence of primary and revision total hip and knee arthroplasty in the United States from 1990 through 2002. J Bone Joint Surg Am 2005;87(7):1487-97.

50. Beiser IH, Kanat IO. Subchondral bone drilling: a treatment for cartilage defects. J Foot Surg 1990;29(6):595-601.

51. Hice G, Freedman D, Lemont H, Khoury S. Scanning and light microscopic study of irrigated and nonirrigated joints following burr surgery performed through a small incision. J Foot Surg 1990;29(4):337-44.

52. Wohl G, Goplen G, Ford J, Novak K, Hurtig M, McPherson R, McGann L, Schachar N, Zernicke RF. Mechanical integrity of subchondral bone in osteochondral autografts and allografts. Can J Surg 1998;41(3):228-33.

53. Hurtig M, Pearce S, Warren S, Kalra M, Miniaci A. Arthroscopic mosaic arthroplasty in the equine third carpal bone. Vet Surg 2001;30(3):228-39.

54. McAndrews PT, Arnoczky SP. Meniscal repair enhancement techniques. Clin Sports Med 1996;15(3):499-510.

55. DeHaven KE, Black KP, Griffiths HJ. Open meniscus repair. Technique and two to nine year results. Am J Sports Med 1989;17(6):788-95.

56. Mouw JK, Case ND, Guldberg RE, Plaas AH, Levenston ME. Variations in matrix composition and GAG fine structure among scaffolds for cartilage tissue engineering. Osteoarthritis Cartilage 2005;13(9):828-36.

57. Bryant SJ, Bender RJ, Durand KL, Anseth KS. Encapsulating chondrocytes in degrading PEG hydrogels with high modulus: engineering gel structural changes to facilitate cartilaginous tissue production. Biotechnol Bioeng 2004;86(7):747-55.

58. Rice MA, Anseth KS. Encapsulating chondrocytes in copolymer gels: bimodal degradation kinetics influence cell phenotype and extracellular matrix development. J Biomed Mater Res A 2004;70(4):560-8.

59. Woodfield TB, Van Blitterswijk CA, De Wijn J, Sims TJ, Hollander AP, Riesle J. Polymer scaffolds fabricated with pore-size gradients as a model for studying the zonal organization within tissue-engineered cartilage constructs. Tissue Eng 2005;11(9-10):1297-311.

60. Sailor LZ, Hewick RM, Morris EA. Recombinant human bone morphogenetic protein-2 maintains the articular chondrocyte phenotype in long-term culture. J Orthop Res 1996;14(6):937-45.

61. Hicks DL, Sage AB, Shelton E, Schumacher BL, Sah RL, Watson D. Effect of bone morphogenetic proteins 2 and 7 on septal chondrocytes in alginate. Otolaryngol Head Neck Surg 2007;136(3):373-9.

62. Loeser RF, Pacione CA, Chubinskaya S. The combination of insulin-like growth factor 1 and osteogenic protein 1 promotes increased survival of and matrix synthesis by normal and osteoarthritic human articular chondrocytes. Arthritis Rheum 2003;48(8):2188-96.

63. Blunk T, Sieminski AL, Gooch KJ, Courter DL, Hollander AP, Nahir AM, Langer R, Vunjak-Novakovic G, Freed LE. Differential effects of growth factors on tissue-engineered cartilage. Tissue Eng 2002;8(1):73-84.

64. Mauck RL, Soltz MA, Wang CC, Wong DD, Chao PH, Valhmu WB, Hung CT, Ateshian GA. Functional tissue engineering of articular cartilage through dynamic loading of chondrocyte-seeded agarose gels. J Biomech Eng 2000;122(3):252-60.

65. Zuk PA, Zhu M, Mizuno H, Huang J, Futrell JW, Katz AJ, Benhaim P, Lorenz HP, Hedrick MH. Multilineage cells from human adipose tissue: implications for cell-based therapies. Tissue Eng 2001;7(2):211-28.

66. Bianco P, Riminucci M, Kuznetsov S, Robey PG. Multipotential cells in the bone marrow stroma: regulation in the context of organ physiology. Crit Rev Eukaryot Gene Expr 1999;9(2):159-73.

67. Kuroda R, Usas A, Kubo S, Corsi K, Peng H, Rose T, Cummins J, Fu FH, Huard J. Cartilage repair using bone morphogenetic protein 4 and muscle-derived stem cells. Arthritis Rheum 2006;54(2):433-42.

68. Miot S, Woodfield T, Daniels AU, Suetterlin R, Peterschmitt I, Heberer M, van Blitterswijk CA, Riesle J, Martin I. Effects of scaffold composition and architecture on human nasal chondrocyte redifferentiation and cartilaginous matrix deposition. Biomaterials 2005;26(15):2479-89.

69. Homicz MR, Chia SH, Schumacher BL, Masuda K, Thonar EJ, Sah RL, Watson D. Human septal chondrocyte redifferentiation in alginate, polyglycolic acid scaffold, and monolayer culture. Laryngoscope 2003;113(1):25-32.

70. Baker BM, Mauck RL. The effect of nanofiber alignment on the maturation of engineered meniscus constructs. Biomaterials 2007;28(11):1967-77.

71. Spalazzi JP, Doty SB, Moffat KL, Levine WN, Lu HH. Development of controlled matrix heterogeneity on a triphasic scaffold for orthopedic interface tissue engineering. Tissue Eng 2006;12(12):3497-508.

72. Majumdar MK, Banks V, Peluso DP, Morris EA. Isolation, characterization, and chondrogenic potential of human bone marrow-derived multipotential stromal cells. J Cell Physiol 2000;185(1):98-106.

73. Caplan AI. Mesenchymal stem cells. J Orthop Res 1991;9(5):641-50.

74. Colter DC, Class R, DiGirolamo CM, Prockop DJ. Rapid expansion of recycling stem cells in cultures of plastic-adherent cells from human bone marrow. Proc Natl Acad Sci U S A 2000;97(7):3213-8.

75. Friedenstein AJ, Gorskaja JF, Kulagina NN. Fibroblast precursors in normal and irradiated mouse hematopoietic organs. Exp Hematol 1976;4(5):267-74.

76. Howlett CR, Cave J, Williamson M, Farmer J, Ali SY, Bab I, Owen ME. Mineralization in in vitro cultures of rabbit marrow stromal cells. Clin Orthop Relat Res 1986(213):251-63.

77. Muraglia A, Cancedda R, Quarto R. Clonal mesenchymal progenitors from human bone marrow differentiate in vitro according to a hierarchical model. J Cell Sci 2000;113 (Pt 7):1161-6.

78. Bosnakovski D, Mizuno M, Kim G, Takagi S, Okumura M, Fujinaga T. Isolation and multilineage differentiation of bovine bone marrow mesenchymal stem cells. Cell Tissue Res 2005;319(2):243-53.

79. Banfi A, Muraglia A, Dozin B, Mastrogiacomo M, Cancedda R, Quarto R. Proliferation kinetics and differentiation potential of ex vivo expanded human bone marrow stromal cells: Implications for their use in cell therapy. Exp Hematol 2000;28(6):707-15.

80. Origuchi N, Ishidou Y, Nagamine T, Onishi T, Matsunaga S, Yoshida H, Sakou T. The spatial and temporal immunolocalization of TGF-beta 1 and bone morphogenetic protein-2/-4 in phallic bone formation in inbred Sprague Dawley male rats. In Vivo 1998;12(5):473-80.

81. Tchetina E, Mwale F, Poole AR. Distinct phases of coordinated early and late gene expression in growth plate chondrocytes in relationship to cell proliferation, matrix assembly, remodeling, and cell differentiation. J Bone Miner Res 2003;18(5):844-51.

82. Johnstone B, Hering TM, Caplan AI, Goldberg VM, Yoo JU. In vitro chondrogenesis of bone marrow-derived mesenchymal progenitor cells. Exp Cell Res 1998;238(1):265-72.

83. Bosnakovski D, Mizuno M, Kim G, Ishiguro T, Okumura M, Iwanaga T, Kadosawa T, Fujinaga T. Chondrogenic differentiation of bovine bone marrow mesenchymal stem cells in pellet cultural system. Exp Hematol 2004;32(5):502-9.

84. Aung T, Miyoshi H, Tun T, Ohshima N. Chondroinduction of mouse mesenchymal stem cells in three-dimensional highly porous matrix scaffolds. J Biomed Mater Res 2002;61(1):75-82.

85. Huang CY, Hagar KL, Frost LE, Sun Y, Cheung HS. Effects of cyclic compressive loading on chondrogenesis of rabbit bone-marrow derived mesenchymal stem cells. Stem Cells 2004;22(3):313-23.

86. Caterson EJ, Nesti LJ, Li WJ, Danielson KG, Albert TJ, Vaccaro AR, Tuan RS. Three-dimensional cartilage formation by bone marrow-derived cells seeded in polylactide/alginate amalgam. J Biomed Mater Res 2001;57(3):394-403.

87. Ma HL, Hung SC, Lin SY, Chen YL, Lo WH. Chondrogenesis of human mesenchymal stem cells encapsulated in alginate beads. J Biomed Mater Res A 2003;64(2):273-81.

88. Diduch DR, Jordan LC, Mierisch CM, Balian G. Marrow stromal cells embedded in alginate for repair of osteochondral defects. Arthroscopy 2000;16(6):571-7.

89. Steinert A, Weber M, Dimmler A, Julius C, Schutze N, Noth U, Cramer H, Eulert J, Zimmermann U, Hendrich C. Chondrogenic differentiation of mesenchymal progenitor cells encapsulated in ultrahigh-viscosity alginate. J Orthop Res 2003;21(6):1090-7.

90. Walsh CJ, Goodman D, Caplan AI, Goldberg VM. Meniscus regeneration in a rabbit partial meniscectomy model. Tissue Eng 1999;5(4):327-37.

91. Murphy JM, Fink DJ, Hunziker EB, Barry FP. Stem cell therapy in a caprine model of osteoarthritis. Arthritis Rheum 2003;48(12):3464-74.

92. Jin M, Frank EH, Quinn TM, Hunziker EB, Grodzinsky AJ. Tissue shear deformation stimulates proteoglycan and protein biosynthesis in bovine cartilage explants. Arch Biochem Biophys 2001;395(1):41-8.

93. Buschmann MD, Gluzband YA, Grodzinsky AJ, Hunziker EB. Mechanical compression modulates matrix biosynthesis in chondrocyte/agarose culture. J Cell Sci 1995;108 (Pt 4):1497-508.

94. Parkkinen JJ, Ikonen J, Lammi MJ, Laakkonen J, Tammi M, Helminen HJ. Effects of cyclic hydrostatic pressure on proteoglycan synthesis in cultured chondrocytes and articular cartilage explants. Arch Biochem Biophys 1993;300(1):458-65.

95. Sah RL, Kim YJ, Doong JY, Grodzinsky AJ, Plaas AH, Sandy JD. Biosynthetic response of cartilage explants to dynamic compression. J Orthop Res 1989;7(5):619-36.

96. Mouw JK, Connelly JT, Wilson CG, Michael KE, Levenston ME. Dynamic compression regulates the expression and synthesis of chondrocyte-specific matrix molecules in bone marrow stromal cells. Stem Cells 2007;25(3):655-63.

97. Mauck RL, Byers BA, Yuan X, Tuan RS. Regulation of cartilaginous ECM gene transcription by chondrocytes and MSCs in 3D culture in response to dynamic loading. Biomech Model Mechanobiol 2007;6(1-2):113-25.

98. Angele P, Yoo JU, Smith C, Mansour J, Jepsen KJ, Nerlich M, Johnstone B. Cyclic hydrostatic pressure enhances the chondrogenic phenotype of human mesenchymal progenitor cells differentiated in vitro. J Orthop Res 2003;21(3):451-7.

99. Connelly JT, Vanderploeg EJ, Levenston ME. The influence of cyclic tension amplitude on chondrocyte matrix synthesis: experimental and finite element analyses. Biorheology 2004;41(3-4):377-87.

100. Honda K, Ohno S, Tanimoto K, Ijuin C, Tanaka N, Doi T, Kato Y, Tanne K. The effects of high magnitude cyclic tensile load on cartilage matrix metabolism in cultured chondrocytes. Eur J Cell Biol 2000;79(9):601-9.

101. Onodera K, Takahashi I, Sasano Y, Bae JW, Mitani H, Kagayama M, Mitani H. Stepwise mechanical stretching inhibits chondrogenesis through cell-matrix adhesion mediated by integrins in embryonic rat limb-bud mesenchymal cells. Eur J Cell Biol 2005;84(1):45-58.

102. Altman GH, Horan RL, Martin I, Farhadi J, Stark PR, Volloch V, Richmond JC, Vunjak-Novakovic G, Kaplan DL. Cell differentiation by mechanical stress. Faseb J 2002;16(2):270-2.

103. Park JS, Chu JS, Cheng C, Chen F, Chen D, Li S. Differential effects of equiaxial and uniaxial strain on mesenchymal stem cells. Biotechnol Bioeng 2004;88(3):359-68.

104. Calderwood DA, Zent R, Grant R, Rees DJ, Hynes RO, Ginsberg MH. The Talin head domain binds to integrin beta subunit cytoplasmic tails and regulates integrin activation. J Biol Chem 1999;274(40):28071-4.

105. Giancotti FG, Ruoslahti E. Integrin signaling. Science 1999;285(5430):1028-32.

106. Critchley DR. Cytoskeletal proteins talin and vinculin in integrin-mediated adhesion. Biochem Soc Trans 2004;32(Pt 5):831-6.

107. Gallant ND, Michael KE, Garcia AJ. Cell adhesion strengthening: contributions of adhesive area, integrin binding, and focal adhesion assembly. Mol Biol Cell 2005;16(9):4329-40.

108. Keselowsky BG, Collard DM, Garcia AJ. Integrin binding specificity regulates biomaterial surface chemistry effects on cell differentiation. Proc Natl Acad Sci U S A 2005;102(17):5953-7.

109. Reyes CD, Garcia AJ. Alpha2beta1 integrin-specific collagen-mimetic surfaces supporting osteoblastic differentiation. J Biomed Mater Res A 2004;69(4):591-600.

110. Thannickal VJ, Lee DY, White ES, Cui Z, Larios JM, Chacon R, Horowitz JC, Day RM, Thomas PE. Myofibroblast differentiation by transforming growth factor-beta1 is dependent on cell adhesion and integrin signaling via focal adhesion kinase. J Biol Chem 2003;278(14):12384-9.

111. Bang OS, Kim EJ, Chung JG, Lee SR, Park TK, Kang SS. Association of focal adhesion kinase with fibronectin and paxillin is required for precartilage condensation of chick mesenchymal cells. Biochem Biophys Res Commun 2000;278(3):522-9.

112. White DG, Hershey HP, Moss JJ, Daniels H, Tuan RS, Bennett VD. Functional analysis of fibronectin isoforms in chondrogenesis: Full-length recombinant mesenchymal fibronectin reduces spreading and promotes condensation and chondrogenesis of limb mesenchymal cells. Differentiation 2003;71(4-5):251-61.

113. Bosnakovski D, Mizuno M, Kim G, Takagi S, Okumura M, Fujinaga T. Chondrogenic differentiation of bovine bone marrow mesenchymal stem cells (MSCs) in different hydrogels: influence of collagen type II extracellular matrix on MSC chondrogenesis. Biotechnol Bioeng 2006;93(6):1152-63.

114. Benya PD, Shaffer JD. Dedifferentiated chondrocytes reexpress the differentiated collagen phenotype when cultured in agarose gels. Cell 1982;30(1):215-24.

115. Pittenger MF, Mackay AM, Beck SC, Jaiswal RK, Douglas R, Mosca JD, Moorman MA, Simonetti DW, Craig S, Marshak DR. Multilineage potential of adult human mesenchymal stem cells. Science 1999;284(5411):143-7.

116. Freed LE, Hollander AP, Martin I, Barry JR, Langer R, Vunjak-Novakovic G. Chondrogenesis in a cell-polymer-bioreactor system. Exp Cell Res 1998;240(1):58-65.

117. Mauck RL, Yuan X, Tuan RS. Chondrogenic differentiation and functional maturation of bovine mesenchymal stem cells in long-term agarose culture. Osteoarthritis Cartilage 2006;14(2):179-89.

118. Miosge N, Flachsbart K, Goetz W, Schultz W, Kresse H, Herken R. Light and electron microscopical immunohistochemical localization of the small proteoglycan core proteins decorin and biglycan in human knee joint cartilage. Histochem J 1994;26(12):939-45.

119. Melrose J, Roughley P, Knox S, Smith S, Lord M, Whitelock J. The structure, location, and function of perlecan, a prominent pericellular proteoglycan of fetal, postnatal, and mature hyaline cartilages. J Biol Chem 2006;281(48):36905-14.

120. Larson CM, Kelley SS, Blackwood AD, Banes AJ, Lee GM. Retention of the native chondrocyte pericellular matrix results in significantly improved matrix production. Matrix Biol 2002;21(4):349-59.

121. Kamiya N, Watanabe H, Habuchi H, Takagi H, Shinomura T, Shimizu K, Kimata K. Versican/PG-M regulates chondrogenesis as an extracellular matrix molecule crucial for mesenchymal condensation. J Biol Chem 2006;281(4):2390-400.

122. Shibata S, Fukada K, Imai H, Abe T, Yamashita Y. In situ hybridization and immunohistochemistry of versican, aggrecan and link protein, and histochemistry of hyaluronan in the developing mouse limb bud cartilage. J Anat 2003;203(4):425-32.

123. Lohmander LS, Neame PJ, Sandy JD. The structure of aggrecan fragments in human synovial fluid. Evidence that aggrecanase mediates cartilage degradation in inflammatory joint disease, joint injury, and osteoarthritis. Arthritis Rheum 1993;36(9):1214-22.

124. Wilson CG, Palmer AW, Zuo F, Eugui E, Wilson S, Mackenzie R, Sandy JD, Levenston ME. Selective and non-selective metalloproteinase inhibitors reduce IL-1-induced cartilage degradation and loss of mechanical properties. Matrix Biol 2006.

125. Sandy JD, Gamett D, Thompson V, Verscharen C. Chondrocyte-mediated catabolism of aggrecan: aggrecanase-dependent cleavage induced by interleukin-1 or retinoic acid can be inhibited by glucosamine. Biochem J 1998;335 (Pt 1):59-66.

126. Wang L, Almqvist KF, Veys EM, Verbruggen G. Control of extracellular matrix homeostasis of normal cartilage by a TGFbeta autocrine pathway. Validation of flow cytometry as a tool to study chondrocyte metabolism in vitro. Osteoarthritis Cartilage 2002;10(3):188-98.

127. Xu C, Oyajobi BO, Frazer A, Kozaci LD, Russell RG, Hollander AP. Effects of growth factors and interleukin-1 alpha on proteoglycan and type II collagen turnover in bovine nasal and articular chondrocyte pellet cultures. Endocrinology 1996;137(8):3557-65.

128. Baddoo M, Hill K, Wilkinson R, Gaupp D, Hughes C, Kopen GC, Phinney DG. Characterization of mesenchymal stem cells isolated from murine bone marrow by negative selection. J Cell Biochem 2003;89(6):1235-49.

129. Farndale RW, Sayers CA, Barrett AJ. A direct spectrophotometric microassay for sulfated glycosaminoglycans in cartilage cultures. Connect Tissue Res 1982;9(4):247-8.

130. Scherer K, Schunke M, Sellckau R, Hassenpflug J, Kurz B. The influence of oxygen and hydrostatic pressure on articular chondrocytes and adherent bone marrow cells in vitro. Biorheology 2004;41(3-4):323-33.

131. Poole CA, Ayad S, Gilbert RT. Chondrons from articular cartilage. V. Immunohistochemical evaluation of type VI collagen organisation in isolated chondrons by light, confocal and electron microscopy. J Cell Sci 1992;103 (Pt 4):1101-10.

132. Reinboth B, Thomas J, Hanssen E, Gibson MA. Beta ig-h3 interacts directly with biglycan and decorin, promotes collagen VI aggregation, and participates in ternary complexing with these macromolecules. J Biol Chem 2006;281(12):7816-24.

133. Graff RD, Kelley SS, Lee GM. Role of pericellular matrix in development of a mechanically functional neocartilage. Biotechnol Bioeng 2003;82(4):457-64.

134. Hildebrand A, Romaris M, Rasmussen LM, Heinegard D, Twardzik DR, Border WA, Ruoslahti E. Interaction of the small interstitial proteoglycans biglycan, decorin and fibromodulin with transforming growth factor beta. Biochem J 1994;302 (Pt 2):527-34.

135. Song RH, Tortorella MD, Malfait AM, Alston JT, Yang Z, Arner EC, Griggs DW. Aggrecan degradation in human articular cartilage explants is mediated by both ADAMTS-4 and ADAMTS-5. Arthritis Rheum 2007;56(2):575-85.

136. Maeda S, Dean DD, Gay I, Schwartz Z, Boyan BD. Activation of latent transforming growth factor beta1 by stromelysin 1 in extracts of growth plate chondrocyte-derived matrix vesicles. J Bone Miner Res 2001;16(7):1281-90.

137. Miyamoto S, Yano K, Sugimoto S, Ishii G, Hasebe T, Endoh Y, Kodama K, Goya M, Chiba T, Ochiai A. Matrix metalloproteinase-7 facilitates insulin-like growth factor bioavailability through its proteinase activity on insulin-like growth factor binding protein 3. Cancer Res 2004;64(2):665-71.

138. Longobardi L, O'Rear L, Aakula S, Johnstone B, Shimer K, Chytil A, Horton WA, Moses HL, Spagnoli A. Effect of IGF-I in the chondrogenesis of bone marrow mesenchymal stem cells in the presence or absence of TGF-beta signaling. J Bone Miner Res 2006;21(4):626-36.

139. Im GI, Jung NH, Tae SK. Chondrogenic differentiation of mesenchymal stem cells isolated from patients in late adulthood: the optimal conditions of growth factors. Tissue Eng 2006;12(3):527-36.

140. Derfoul A, Perkins GL, Hall DJ, Tuan RS. Glucocorticoids promote chondrogenic differentiation of adult human mesenchymal stem cells by enhancing expression of cartilage extracellular matrix genes. Stem Cells 2006;24(6):1487-95.

141. Worster AA, Brower-Toland BD, Fortier LA, Bent SJ, Williams J, Nixon AJ. Chondrocytic differentiation of mesenchymal stem cells sequentially exposed to transforming growth factor-beta1 in monolayer and insulin-like growth factor-I in a three-dimensional matrix. J Orthop Res 2001;19(4):738-49.

142. Angele P, Schumann D, Angele M, Kinner B, Englert C, Hente R, Fuchtmeier B, Nerlich M, Neumann C, Kujat R. Cyclic, mechanical compression enhances chondrogenesis of mesenchymal progenitor cells in tissue engineering scaffolds. Biorheology 2004;41(3-4):335-46.

143. Chomczynski P, Sacchi N. Single-step method of RNA isolation by acid guanidinium thiocyanate-phenol-chloroform extraction. Anal Biochem 1987;162(1):156-9.

144. Farndale RW, Buttle DJ, Barrett AJ. Improved quantitation and discrimination of sulphated glycosaminoglycans by use of dimethylmethylene blue. Biochim Biophys Acta 1986;883(2):173-7.

145. Kim YJ, Sah RL, Doong JY, Grodzinsky AJ. Fluorometric assay of DNA in cartilage explants using Hoechst 33258. Anal Biochem 1988;174(1):168-76.

146. Connelly JT, Garcia AJ, Levenston ME. Inhibition of in vitro chondrogenesis in RGD-modified three-dimensional alginate gels. Biomaterials 2007;28(6):1071-83.

147. Huang CY, Cheung HS, Deitzer MA. Effects of Fibrinolytic Inhibitors on Chondrogenesis of Bone-marrow Derived Mesenchymal Stem Cells in Fibrin Gels. Biomech Model Mechanobiol 2006.

148. Katsumi A, Naoe T, Matsushita T, Kaibuchi K, Schwartz MA. Integrin activation and matrix binding mediate cellular responses to mechanical stretch. J Biol Chem 2005;280(17):16546-9.

149. MacKenna DA, Dolfi F, Vuori K, Ruoslahti E. Extracellular signal-regulated kinase and c-Jun NH2-terminal kinase activation by mechanical stretch is integrin-dependent and matrix-specific in rat cardiac fibroblasts. J Clin Invest 1998;101(2):301-10.

150. Droguett R, Cabello-Verrugio C, Riquelme C, Brandan E. Extracellular proteoglycans modify TGF-beta bio-availability attenuating its signaling during skeletal muscle differentiation. Matrix Biol 2006;25(6):332-41.

151. Tschumperlin DJ, Dai G, Maly IV, Kikuchi T, Laiho LH, McVittie AK, Haley KJ, Lilly CM, So PT, Lauffenburger DA and others. Mechanotransduction through growth-factor shedding into the extracellular space. Nature 2004;429(6987):83-6.

152. Shoemaker SC, Markolf KL. The role of the meniscus in the anterior-posterior stability of the loaded anterior cruciate-deficient knee. Effects of partial versus total excision. J Bone Joint Surg Am 1986;68(1):71-9.

153. Feng Z, Tateishi Y, Nomura Y, Kitajima T, Nakamura T. Construction of fibroblast-collagen gels with orientated fibrils induced by static or dynamic stress: toward the fabrication of small tendon grafts. J Artif Organs 2006;9(4):220-5.

154. Thomopoulos S, Fomovsky GM, Holmes JW. The development of structural and mechanical anisotropy in fibroblast populated collagen gels. J Biomech Eng 2005;127(5):742-50.

155. Tortorella MD, Pratta M, Liu RQ, Austin J, Ross OH, Abbaszade I, Burn T, Arner E. Sites of aggrecan cleavage by recombinant human aggrecanase-1 (ADAMTS-4). J Biol Chem 2000;275(24):18566-73.

156. Kim YJ, Grodzinsky AJ, Plaas AH. Compression of cartilage results in differential effects on biosynthetic pathways for aggrecan, link protein, and hyaluronan. Arch Biochem Biophys 1996;328(2):331-40.

157. Vanderploeg EJ. Mechanotransduction in Engineered Cartilaginous Tissues: In Vitro Oscillatory Tensile Loading. Georgia Institute of Technology Doctoral Dissertation 2006.

158. Rees SG, Flannery CR, Little CB, Hughes CE, Caterson B, Dent CM. Catabolism of aggrecan, decorin and biglycan in tendon. Biochem J 2000;350 Pt 1:181-8.

159. MacLean JJ, Lee CR, Grad S, Ito K, Alini M, Iatridis JC. Effects of immobilization and dynamic compression on intervertebral disc cell gene expression in vivo. Spine 2003;28(10):973-81.

160. Upton ML, Chen J, Guilak F, Setton LA. Differential effects of static and dynamic compression on meniscal cell gene expression. J Orthop Res 2003;21(6):963-9.

161. Fitzgerald JB, Jin M, Dean D, Wood DJ, Zheng MH, Grodzinsky AJ. Mechanical compression of cartilage explants induces multiple time-dependent gene expression patterns and involves intracellular calcium and cyclic AMP. J Biol Chem 2004;279(19):19502-11.

162. Juncosa-Melvin N, Matlin KS, Holdcraft RW, Nirmalanandhan VS, Butler DL. Mechanical Stimulation Increases Collagen Type I and Collagen Type III Gene Expression of Stem Cell-Collagen Sponge Constructs for Patellar Tendon Repair. Tissue Eng 2007.

163. Agarwal S, Long P, Gassner R, Piesco NP, Buckley MJ. Cyclic tensile strain suppresses catabolic effects of interleukin-1beta in fibrochondrocytes from the temporomandibular joint. Arthritis Rheum 2001;44(3):608-17.

164. da Silva Meirelles L, Chagastelles PC, Nardi NB. Mesenchymal stem cells reside in virtually all post-natal organs and tissues. J Cell Sci 2006;119(Pt 11):2204-13.

165. Alsalameh S, Amin R, Gemba T, Lotz M. Identification of mesenchymal progenitor cells in normal and osteoarthritic human articular cartilage. Arthritis Rheum 2004;50(5):1522-32.

166. Chapel A, Bertho JM, Bensidhoum M, Fouillard L, Young RG, Frick J, Demarquay C, Cuvelier F, Mathieu E, Trompier F and others. Mesenchymal stem cells home to injured tissues when co-infused with hematopoietic cells to treat a radiation-induced multi-organ failure syndrome. J Gene Med 2003;5(12):1028-38.

167. Kadiyala S, Young RG, Thiede MA, Bruder SP. Culture expanded canine mesenchymal stem cells possess osteochondrogenic potential in vivo and in vitro. Cell Transplant 1997;6(2):125-34.

168. Hanada K, Dennis JE, Caplan AI. Stimulatory effects of basic fibroblast growth factor and bone morphogenetic protein-2 on osteogenic differentiation of rat bone marrow-derived mesenchymal stem cells. J Bone Miner Res 1997;12(10):1606-14.

169. Chen CW, Tsai YH, Deng WP, Shih SN, Fang CL, Burch JG, Chen WH, Lai WF. Type I and II collagen regulation of chondrogenic differentiation by mesenchymal progenitor cells. J Orthop Res 2005;23(2):446-53.

170. Souchelnytskyi S, Tamaki K, Engstrom U, Wernstedt C, ten Dijke P, Heldin CH. Phosphorylation of Ser465 and Ser467 in the C terminus of Smad2 mediates interaction with Smad4 and is required for transforming growth factor-beta signaling. J Biol Chem 1997;272(44):28107-15.

171. Souchelnytskyi S, ten Dijke P, Miyazono K, Heldin CH. Phosphorylation of Ser165 in TGF-beta type I receptor modulates TGF-beta1-induced cellular responses. Embo J 1996;15(22):6231-40.

172. Wrana JL, Attisano L, Wieser R, Ventura F, Massague J. Mechanism of activation of the TGF-beta receptor. Nature 1994;370(6488):341-7.

173. Heldin CH, Miyazono K, ten Dijke P. TGF-beta signalling from cell membrane to nucleus through SMAD proteins. Nature 1997;390(6659):465-71.

174. Tsuda M, Takahashi S, Takahashi Y, Asahara H. Transcriptional co-activators CREB-binding protein and p300 regulate chondrocyte-specific gene expression via association with Sox9. J Biol Chem 2003;278(29):27224-9.

175. Tuli R, Tuli S, Nandi S, Huang X, Manner PA, Hozack WJ, Danielson KG, Hall DJ, Tuan RS. Transforming growth factor-beta-mediated chondrogenesis of human mesenchymal progenitor cells involves N-cadherin and mitogen-activated protein kinase and Wnt signaling cross-talk. J Biol Chem 2003;278(42):41227-36.

176. Watanabe H, de Caestecker MP, Yamada Y. Transcriptional cross-talk between Smad, ERK1/2, and p38 mitogen-activated protein kinase pathways regulates transforming growth factor-beta-induced aggrecan gene expression in chondrogenic ATDC5 cells. J Biol Chem 2001;276(17):14466-73.

177. Reynolds LE, Conti FJ, Lucas M, Grose R, Robinson S, Stone M, Saunders G, Dickson C, Hynes RO, Lacy-Hulbert A and others. Accelerated re-epithelialization in beta3-integrin-deficient- mice is associated with enhanced TGF-beta1 signaling. Nat Med 2005;11(2):167-74.

178. Dumont N, Bakin AV, Arteaga CL. Autocrine transforming growth factor-beta signaling mediates Smad-independent motility in human cancer cells. J Biol Chem 2003;278(5):3275-85.

179. Muraoka RS, Dumont N, Ritter CA, Dugger TC, Brantley DM, Chen J, Easterly E, Roebuck LR, Ryan S, Gotwals PJ and others. Blockade of TGF-beta inhibits mammary tumor cell viability, migration, and metastases. J Clin Invest 2002;109(12):1551-9.

180. Kim HP, Kim TY, Lee MS, Jong HS, Kim TY, Lee JW, Bang YJ. TGF-beta1-mediated activations of c-Src and Rac1 modulate levels of cyclins and p27(Kip1) CDK inhibitor in hepatoma cells replated on fibronectin. Biochim Biophys Acta 2005;1743(1-2):151-61.

181. Schneiderbauer MM, Dutton CM, Scully SP. Signaling "cross-talk" between TGF-beta1 and ECM signals in chondrocytic cells. Cell Signal 2004;16(10):1133-40.

182. Ruoslahti E, Pierschbacher MD. Arg-Gly-Asp: a versatile cell recognition signal. Cell 1986;44(4):517-8.

183. Redick SD, Settles DL, Briscoe G, Erickson HP. Defining fibronectin's cell adhesion synergy site by site-directed mutagenesis. J Cell Biol 2000;149(2):521-7.

184. Ochsenhirt SE, Kokkoli E, McCarthy JB, Tirrell M. Effect of RGD secondary structure and the synergy site PHSRN on cell adhesion, spreading and specific integrin engagement. Biomaterials 2006;27(20):3863-74.

185. Hersel U, Dahmen C, Kessler H. RGD modified polymers: biomaterials for stimulated cell adhesion and beyond. Biomaterials 2003;24(24):4385-415.

186. Rowley JA, Mooney DJ. Alginate type and RGD density control myoblast phenotype. J Biomed Mater Res 2002;60(2):217-23.

187. Maheshwari G, Brown G, Lauffenburger DA, Wells A, Griffith LG. Cell adhesion and motility depend on nanoscale RGD clustering. J Cell Sci 2000;113 (Pt 10):1677-86.

188. Shin H, Temenoff JS, Bowden GC, Zygourakis K, Farach-Carson MC, Yaszemski MJ, Mikos AG. Osteogenic differentiation of rat bone marrow stromal cells cultured on Arg-Gly-Asp modified hydrogels without dexamethasone and beta-glycerol phosphate. Biomaterials 2005;26(17):3645-54.

189. Genes NG, Rowley JA, Mooney DJ, Bonassar LJ. Effect of substrate mechanics on chondrocyte adhesion to modified alginate surfaces. Arch Biochem Biophys 2004;422(2):161-7.

190. Simmons CA, Alsberg E, Hsiong S, Kim WJ, Mooney DJ. Dual growth factor delivery and controlled scaffold degradation enhance in vivo bone formation by transplanted bone marrow stromal cells. Bone 2004;35(2):562-9.

191. Rowley JA, Madlambayan G, Mooney DJ. Alginate hydrogels as synthetic extracellular matrix materials. Biomaterials 1999;20(1):45-53.

192. Aota S, Nomizu M, Yamada KM. The short amino acid sequence Pro-His-Ser-Arg-Asn in human fibronectin enhances cell-adhesive function. J Biol Chem 1994;269(40):24756-61.

193. Grimmer JF, Gunnlaugsson CB, Alsberg E, Murphy HS, Kong HJ, Mooney DJ, Weatherly RA. Tracheal reconstruction using tissue-engineered cartilage. Arch Otolaryngol Head Neck Surg 2004;130(10):1191-6.

194. Awad HA, Wickham MQ, Leddy HA, Gimble JM, Guilak F. Chondrogenic differentiation of adipose-derived adult stem cells in agarose, alginate, and gelatin scaffolds. Biomaterials 2004;25(16):3211-22.

195. Harbers GM, Healy KE. The effect of ligand type and density on osteoblast adhesion, proliferation, and matrix mineralization. J Biomed Mater Res A 2005;75(4):855-69.

196. Lee KY, Alsberg E, Hsiong SX, Comisar WA, Linderman JJ, Ziff R, Mooney DJ. Nanoscale Adhesion Ligand Organization Regulates Osteoblast Proliferation and Differentiation. Nano Letters 2004;4(8):1501-1506.

197. Hsu SH, Chang SH, Yen HJ, Whu SW, Tsai CL, Chen DC. Evaluation of biodegradable polyesters modified by type II collagen and Arg-Gly-Asp as tissue engineering scaffolding materials for cartilage regeneration. Artif Organs 2006;30(1):42-55.

198. Genes NG, Rowley JA, Mooney DJ, Bonassar LJ. Culture of chondrocytes in RGD-alginate: effects on mechanical and biosynthetic properties. Trans Orthop Res Soc 2000.

199. Meinel L, Hofmann S, Karageorgiou V, Zichner L, Langer R, Kaplan D, Vunjak-Novakovic G. Engineering cartilage-like tissue using human mesenchymal stem cells and silk protein scaffolds. Biotechnol Bioeng 2004;88(3):379-91.

200. Petrie TA, Capadona JR, Reyes CD, Garcia AJ. Integrin specificity and enhanced cellular activities associated with surfaces presenting a recombinant fibronectin fragment compared to RGD supports. Biomaterials 2006;27(31):5459-70.

201. Woodfield TB, Miot S, Martin I, van Blitterswijk CA, Riesle J. The regulation of expanded human nasal chondrocyte re-differentiation capacity by substrate composition and gas plasma surface modification. Biomaterials 2006;27(7):1043-53.

202. Massia SP, Hubbell JA. An RGD spacing of 440 nm is sufficient for integrin alpha V beta 3-mediated fibroblast spreading and 140 nm for focal contact and stress fiber formation. J Cell Biol 1991;114(5):1089-100.

203. Comisar WA, Hsiong SX, Kong HJ, Mooney DJ, Linderman JJ. Multi-scale modeling to predict ligand presentation within RGD nanopatterned hydrogels. Biomaterials 2006;27(10):2322-9.

204. von der Mark K, Gauss V, von der Mark H, Muller P. Relationship between cell shape and type of collagen synthesised as chondrocytes lose their cartilage phenotype in culture. Nature 1977;267(5611):531-2.

205. Newman P, Watt FM. Influence of cytochalasin D-induced changes in cell shape on proteoglycan synthesis by cultured articular chondrocytes. Exp Cell Res 1988;178(2):199-210.

206. Lim YB, Kang SS, Park TK, Lee YS, Chun JS, Sonn JK. Disruption of actin cytoskeleton induces chondrogenesis of mesenchymal cells by activating protein kinase C-alpha signaling. Biochem Biophys Res Commun 2000;273(2):609-13.

207. Woods A, Wang G, Beier F. RhoA/ROCK signaling regulates Sox9 expression and actin organization during chondrogenesis. J Biol Chem 2005;280(12):11626-34.

208. Woods A, Beier F. RhoA/ROCK signaling regulates chondrogenesis in a context-dependent manner. J Biol Chem 2006;281(19):13134-40.

209. Nobes CD, Hall A. Rho, rac, and cdc42 GTPases regulate the assembly of multimolecular focal complexes associated with actin stress fibers, lamellipodia, and filopodia. Cell 1995;81(1):53-62.

210. Amano M, Ito M, Kimura K, Fukata Y, Chihara K, Nakano T, Matsuura Y, Kaibuchi K. Phosphorylation and activation of myosin by Rho-associated kinase (Rho-kinase). J Biol Chem 1996;271(34):20246-9.

211. Leung T, Chen XQ, Manser E, Lim L. The p160 RhoA-binding kinase ROK alpha is a member of a kinase family and is involved in the reorganization of the cytoskeleton. Mol Cell Biol 1996;16(10):5313-27.

212. Ai S, Kuzuya M, Koike T, Asai T, Kanda S, Maeda K, Shibata T, Iguchi A. Rho-Rho kinase is involved in smooth muscle cell migration through myosin light chain phosphorylation-dependent and independent pathways. Atherosclerosis 2001;155(2):321-7.

213. Iwamoto H, Nakamuta M, Tada S, Sugimoto R, Enjoji M, Nawata H. A p160ROCK-specific inhibitor, Y-27632, attenuates rat hepatic stellate cell growth. J Hepatol 2000;32(5):762-70.

214. McBeath R, Pirone DM, Nelson CM, Bhadriraju K, Chen CS. Cell shape, cytoskeletal tension, and RhoA regulate stem cell lineage commitment. Dev Cell 2004;6(4):483-95.

215. Kaartinen V, Haataja L, Nagy A, Heisterkamp N, Groffen J. TGFbeta3-induced activation of RhoA/Rho-kinase pathway is necessary but not sufficient for epithelio-mesenchymal transdifferentiation: implications for palatogenesis. Int J Mol Med 2002;9(6):563-70.

216. Imamura F, Mukai M, Ayaki M, Akedo H. Y-27632, an inhibitor of rho-associated protein kinase, suppresses tumor cell invasion via regulation of focal adhesion and focal adhesion kinase. Jpn J Cancer Res 2000;91(8):811-6.

217. Dodla MC, Bellamkonda RV. Anisotropic scaffolds facilitate enhanced neurite extension in vitro. J Biomed Mater Res A 2006;78(2):213-21.

218. Totsukawa G, Yamakita Y, Yamashiro S, Hartshorne DJ, Sasaki Y, Matsumura F. Distinct roles of ROCK (Rho-kinase) and MLCK in spatial regulation of MLC phosphorylation for assembly of stress fibers and focal adhesions in 3T3 fibroblasts. J Cell Biol 2000;150(4):797-806.

219. Chen S, Crawford M, Day RM, Briones VR, Leader JE, Jose PA, Lechleider RJ. RhoA modulates Smad signaling during transforming growth factor-beta-induced smooth muscle differentiation. J Biol Chem 2006;281(3):1765-70.

220. Amano T, Tanabe K, Eto T, Narumiya S, Mizuno K. LIM-kinase 2 induces formation of stress fibres, focal adhesions and membrane blebs, dependent on its activation by Rho-associated kinase-catalysed phosphorylation at threonine-505. Biochem J 2001;354(Pt 1):149-59.

221. Janji B, Melchior C, Gouon V, Vallar L, Kieffer N. Autocrine TGF-beta-regulated expression of adhesion receptors and integrin-linked kinase in HT-144 melanoma cells correlates with their metastatic phenotype. Int J Cancer 1999;83(2):255-62.

222. Bayless KJ, Salazar R, Davis GE. RGD-dependent vacuolation and lumen formation observed during endothelial cell morphogenesis in three-dimensional fibrin matrices involves the alpha(v)beta(3) and alpha(5)beta(1) integrins. Am J Pathol 2000;156(5):1673-83.

223. Zaman MH, Trapani LM, Sieminski AL, Mackellar D, Gong H, Kamm RD, Wells A, Lauffenburger DA, Matsudaira P. Migration of tumor cells in 3D matrices is governed by matrix stiffness along with cell-matrix adhesion and proteolysis. Proc Natl Acad Sci U S A 2006;103(29):10889-94.

224. Held-Feindt J, Paredes EB, Blomer U, Seidenbecher C, Stark AM, Mehdorn HM, Mentlein R. Matrix-degrading proteases ADAMTS4 and ADAMTS5 (disintegrins and metalloproteinases with thrombospondin motifs 4 and 5) are expressed in human glioblastomas. Int J Cancer 2006;118(1):55-61.

225. Kim SJ, Hwang SG, Kim IC, Chun JS. Actin cytoskeletal architecture regulates nitric oxide-induced apoptosis, dedifferentiation, and cyclooxygenase-2

expression in articular chondrocytes via mitogen-activated protein kinase and protein kinase C pathways. J Biol Chem 2003;278(43):42448-56.

226. Knight MM, Lee DA, Bader DL. The influence of elaborated pericellular matrix on the deformation of isolated articular chondrocytes cultured in agarose. Biochim Biophys Acta 1998;1405(1-3):67-77.

227. Chowdhury TT, Salter DM, Bader DL, Lee DA. Integrin-mediated mechanotransduction processes in TGFbeta-stimulated monolayer-expanded chondrocytes. Biochem Biophys Res Commun 2004;318(4):873-81.

228. Matthews BD, Overby DR, Mannix R, Ingber DE. Cellular adaptation to mechanical stress: role of integrins, Rho, cytoskeletal tension and mechanosensitive ion channels. J Cell Sci 2006;119(Pt 3):508-18.

229. Yang G, Im HJ, Wang JH. Repetitive mechanical stretching modulates IL-1beta induced COX-2, MMP-1 expression, and PGE2 production in human patellar tendon fibroblasts. Gene 2005;363:166-72.

230. Baum O, Hlushchuk R, Forster A, Greiner R, Clezardin P, Zhao Y, Djonov V, Gruber G. Increased invasive potential and up-regulation of MMP-2 in MDA-MB-231 breast cancer cells expressing the beta3 integrin subunit. Int J Oncol 2007;30(2):325-32.

231. Ries C, Egea V, Karow M, Kolb H, Jochum M, Neth P. MMP-2, MT1-MMP, and TIMP-2 are essential for the invasive capacity of human mesenchymal stem cells: differential regulation by inflammatory cytokines. Blood 2007;109(9):4055-63.

232. Ito MM, Kida MY. Morphological and biochemical re-evaluation of the process of cavitation in the rat knee joint: cellular and cell strata alterations in the interzone. J Anat 2000;197 Pt 4:659-79.

233. Mikic B, Johnson TL, Chhabra AB, Schalet BJ, Wong M, Hunziker EB. Differential effects of embryonic immobilization on the development of fibrocartilaginous skeletal elements. J Rehabil Res Dev 2000;37(2):127-33.

234. Merida-Velasco JA, Sanchez-Montesinos I, Espin-Ferra J, Rodriguez-Vazquez JF, Merida-Velasco JR, Jimenez-Collado J. Development of the human knee joint. Anat Rec 1997;248(2):269-78.

235. Robbins JR, Evanko SP, Vogel KG. Mechanical loading and TGF-beta regulate proteoglycan synthesis in tendon. Arch Biochem Biophys 1997;342(2):203-11.

236. Evanko SP, Vogel KG. Ultrastructure and proteoglycan composition in the developing fibrocartilaginous region of bovine tendon. Matrix 1990;10(6):420-36.

237. Dowthwaite GP, Bishop JC, Redman SN, Khan IM, Rooney P, Evans DJ, Haughton L, Bayram Z, Boyer S, Thomson B and others. The surface of articular cartilage contains a progenitor cell population. J Cell Sci 2004;117(Pt 6):889-97.

238. Huebsch ND, Mooney DJ. Fluorescent resonance energy transfer: A tool for probing molecular cell-biomaterial interactions in three dimensions. Biomaterials 2007;28(15):2424-37.

239. Kong HJ, Polte TR, Alsberg E, Mooney DJ. FRET measurements of cell-traction forces and nano-scale clustering of adhesion ligands varied by substrate stiffness. Proc Natl Acad Sci U S A 2005;102(12):4300-5.

240. Ohashi K, Nagata K, Maekawa M, Ishizaki T, Narumiya S, Mizuno K. Rho-associated kinase ROCK activates LIM-kinase 1 by phosphorylation at threonine 508 within the activation loop. J Biol Chem 2000;275(5):3577-82.

241. Sumi T, Matsumoto K, Nakamura T. Specific activation of LIM kinase 2 via phosphorylation of threonine 505 by ROCK, a Rho-dependent protein kinase. J Biol Chem 2001;276(1):670-6.

242. Sotiropoulos A, Gineitis D, Copeland J, Treisman R. Signal-regulated activation of serum response factor is mediated by changes in actin dynamics. Cell 1999;98(2):159-69.

243. Geneste O, Copeland JW, Treisman R. LIM kinase and Diaphanous cooperate to regulate serum response factor and actin dynamics. J Cell Biol 2002;157(5):831-8.

244. de Crombrugghe B, Lefebvre V, Behringer RR, Bi W, Murakami S, Huang W. Transcriptional mechanisms of chondrocyte differentiation. Matrix Biol 2000;19(5):389-94.

245. Lian JB, Stein GS. Runx2/Cbfa1: a multifunctional regulator of bone formation. Curr Pharm Des 2003;9(32):2677-85.

246. Phimphilai M, Zhao Z, Boules H, Roca H, Franceschi RT. BMP signaling is required for RUNX2-dependent induction of the osteoblast phenotype. J Bone Miner Res 2006;21(4):637-46.

247. Zhou G, Zheng Q, Engin F, Munivez E, Chen Y, Sebald E, Krakow D, Lee B. Dominance of SOX9 function over RUNX2 during skeletogenesis. Proc Natl Acad Sci U S A 2006;103(50):19004-9.

248. Day TF, Guo X, Garrett-Beal L, Yang Y. Wnt/beta-catenin signaling in mesenchymal progenitors controls osteoblast and chondrocyte differentiation during vertebrate skeletogenesis. Dev Cell 2005;8(5):739-50.

249. Hill TP, Spater D, Taketo MM, Birchmeier W, Hartmann C. Canonical Wnt/beta-catenin signaling prevents osteoblasts from differentiating into chondrocytes. Dev Cell 2005;8(5):727-38.

250. Akiyama H, Lyons JP, Mori-Akiyama Y, Yang X, Zhang R, Zhang Z, Deng JM, Taketo MM, Nakamura T, Behringer RR and others. Interactions between Sox9 and beta-catenin control chondrocyte differentiation. Genes Dev 2004;18(9):1072-87.

251. Tuan RS. Cellular signaling in developmental chondrogenesis: N-cadherin, Wnts, and BMP-2. J Bone Joint Surg Am 2003;85-A Suppl 2:137-41.

252. Mahmood TA, Miot S, Frank O, Martin I, Riesle J, Langer R, van Blitterswijk CA. Modulation of chondrocyte phenotype for tissue engineering by designing the biologic-polymer carrier interface. Biomacromolecules 2006;7(11):3012-8.

253. Kim YJ, Sah RL, Grodzinsky AJ, Plaas AH, Sandy JD. Mechanical regulation of cartilage biosynthetic behavior: physical stimuli. Arch Biochem Biophys 1994;311(1):1-12.

254. Parkkinen JJ, Lammi MJ, Helminen HJ, Tammi M. Local stimulation of proteoglycan synthesis in articular cartilage explants by dynamic compression in vitro. J Orthop Res 1992;10(5):610-20.

255. Hunter CJ, Levenston ME. The influence of repair tissue maturation on the response to oscillatory compression in a cartilage defect repair model. Biorheology 2002;39(1-2):79-88.

256. Hunter CJ, Imler SM, Malaviya P, Nerem RM, Levenston ME. Mechanical compression alters gene expression and extracellular matrix synthesis by chondrocytes cultured in collagen I gels. Biomaterials 2002;23(4):1249-59.

257. Vanderploeg EJ, Levenston ME. Oscillatory tension modulates chondrocyte biosynthesis and morphology. Trans. Orthop. Res. Soc. 2002;27.

258. Sierra DH, Eberhardt AW, Lemons JE. Failure characteristics of multiple-component fibrin-based adhesives. J Biomed Mater Res 2002;59(1):1-11.

259. Ariens RA, Philippou H, Nagaswami C, Weisel JW, Lane DA, Grant PJ. The factor XIII V34L polymorphism accelerates thrombin activation of factor XIII and affects cross-linked fibrin structure. Blood 2000;96(3):988-95.

260. Fukuda K, Asada S, Kumano F, Saitoh M, Otani K, Tanaka S. Cyclic tensile stretch on bovine articular chondrocytes inhibits protein kinase C activity. J Lab Clin Med 1997;130(2):209-15.

261. Fujisawa T, Hattori T, Takahashi K, Kuboki T, Yamashita A, Takigawa M. Cyclic mechanical stress induces extracellular matrix degradation in cultured

chondrocytes via gene expression of matrix metalloproteinases and interleukin-1. J Biochem (Tokyo) 1999;125(5):966-75.

262. Toyoda T, Saito S, Inokuchi S, Yabe Y. The effects of tensile load on the metabolism of cultured chondrocytes. Clin Orthop 1999(359):221-8.

263. Vanderploeg EJ, Levenston ME. Oscillatory tension induces cytoskeletal reorganization in chondrocytes. Trans. Orthop. Res. Soc. 2003;28.

264. Guilak F, Mow VC. The mechanical environment of the chondrocyte: a biphasic finite element model of cell-matrix interactions in articular cartilage. J Biomech 2000;33(12):1663-73.

265. Kim YJ, Bonassar LJ, Grodzinsky AJ. The role of cartilage streaming potential, fluid flow and pressure in the stimulation of chondrocyte biosynthesis during dynamic compression. J Biomech 1995;28(9):1055-66.

266. Buschmann MD, Kim YJ, Wong M, Frank E, Hunziker EB, Grodzinsky AJ. Stimulation of aggrecan synthesis in cartilage explants by cyclic loading is localized to regions of high interstitial fluid flow. Arch Biochem Biophys 1999;366(1):1-7.

267. Malaviya P, Nerem RM. Fluid-induced shear stress stimulates chondrocyte proliferation partially mediated via TGF-beta1. Tissue Eng 2002;8(4):581-90.

268. Smith RL, Donlon BS, Gupta MK, Mohtai M, Das P, Carter DR, Cooke J, Gibbons G, Hutchinson N, Schurman DJ. Effects of fluid-induced shear on articular chondrocyte morphology and metabolism in vitro. J Orthop Res 1995;13(6):824-31.

269. Mukherjee N, Wayne JS. Load sharing between solid and fluid phases in articular cartilage: II--Comparison of experimental results and u-p finite element predictions. J Biomech Eng 1998;120(5):620-4.

270. Eckstein F, Tieschky M, Faber S, Englmeier KH, Reiser M. Functional analysis of articular cartilage deformation, recovery, and fluid flow following dynamic exercise in vivo. Anat Embryol (Berl) 1999;200(4):419-24.